UNIVERSITÄTSKLINIKUM HAMBURG–EPPENDORF

Klinik und Poliklinik für Neurologie

Direktion:
Prof. Dr. Götz Thomalla
Prof. Dr. Tim Magnus

Interaction of food patterns, vascular brain changes, brain network organization and cognition in a vascular risk population

Dissertation

zur Erlangung des Doktorgrades PhD
an der Medizinischen Fakultät der Universität Hamburg.

vorgelegt von:

Carola Mayer
aus Gronau (Westf.)

Hamburg 2023

Angenommen von der
Medizinischen Fakultät der Universität Hamburg am: **12.09.2023**

Veröffentlicht mit Genehmigung der
Medizinischen Fakultät der Universität Hamburg.

Prüfungsausschuss, der/die Vorsitzende: **Prof. Dr. Götz Thomalla**

Prüfungsausschuss, zweite/r Gutachter/in: **PD Dr. Birgit-Christiane Zyriax**

Table of Contents

1. Synopsis

1.1. Thesis objectives

With an increasing life expectancy worldwide, the prevalence of dementia and cognitive deterioration is also rising continuously. Therefore, identifying and preventing risk factors for cognitive decline is pivotal. Numerous risk factors for cognitive decline are already known, and among those are several which can be modified, such as diabetes mellitus, high blood pressure, increased cholesterol, and obesity[1]. These risk factors are known to be induced by an unhealthy diet[2], but the effect of nutrition on cognitive function and neurological health is not yet fully understood. In this cumulative thesis, we aimed to study the possible interaction of nutrition, vascular brain changes, brain network organization and cognition in healthy individuals with vascular risk factors.

To this end, the thesis covers two main research areas. In the first part (part A), we examined vascular brain changes in association with other imaging markers related to changes in the brain microstructure and cognitive deterioration. With this, we aimed to better define the presumed pathways of cerebrovascular damage, which will be of use for the second part of the thesis. Our approach involved a novel brain magnetic resonance imaging (MRI) analysis to quantify vascular brain damage, assess cortical atrophy, and measure damage beyond the lesioned brain white matter. Two publications resulted from this part of the thesis:

> [1] In the first study, we examined the structural link between white matter hyperintensities (WMH) as a marker of vascular brain damage and cortical atrophy. This study, further referred to as 'study 1', was published in December 2020 in the *Journal Cerebral Blood Flow and Metabolism* entitled "Linking cortical atrophy to white matter hyperintensities of presumed vascular origin"[3].

> [2] In the second study, we focused on the characterization of the direct surrounding white matter of WMH and identified microstructural damage with the novel imaging approach of free–water imaging. This study, referred to as 'study 2', was published in April 2022 in the *Journal of Cerebral Blood Flow and Metabolism* under the title "Free–water diffusion MRI detects structural alterations surrounding white matter hyperintensities in the early stage of cerebral small vessel disease"[4].

In the second part (part B), we evaluated the effect of an unhealthy diet on cognition and vascular brain damage with consideration of the findings from the first part. Using mediation analysis, we considered vascular brain damage and cardiovascular risk factors as mediators in the association between nutrition and cognition. We hypothesize that an unhealthy diet is associated with more pronounced cardiovascular risk factors and vascular as well as structural brain damage, which in turn causes more cognitive deficits. Given the controversial discussion on the association of coffee

consumption with cardiovascular risk, we specifically addressed the potential role of coffee for brain health. In this second part, we performed two separate analyses:

[1] In the first study of the second part, we applied a structural equation modeling approach to examine the direct, indirect, and total effect of an unhealthy diet on cognitive function, possibly mediated by cardiovascular risk factors and brain structure. The manuscript for this study, referred to as 'study 3', is prepared for submission.

[2] The second study of part B analyzed whether regular coffee consumption had beneficial or detrimental effects on the microstructure of the brain, considering cardiovascular risk factors as possible covariates in the association. This study, referred to as 'study 4', was published in January 2023 in the journal *Nutrients* entitled "Association of coffee consumption with brain MRI parameters in the Hamburg City Health Study"[5].

The thesis is structured, to begin with a brief description of the study cohort, including the methodological approach used for assessment and definition of demographic and clinical variables as well as the MRI processing pipeline. This is followed by the description of the studies, separated into parts A and B. Part A comprises a short introduction on the topic of cerebral small vessel disease and microstructural brain damage as well as the description of the results of study 1 and 2. Part B includes a short introduction on nutrition and the definition of dietary patterns, as well as the description of the results of study 3 and 4. Finally, in paragraph 1.5, the results of all four studies are interpreted and discussed in a broader context.

1.2. Methodological approach

1.2.1. Selection of the study sample

All data analyzed in the thesis are from the Hamburg City Health Study (HCHS), which is conducted at the University Medical Center Hamburg–Eppendorf. As described in detail in a previous publication[6], the HCHS is a large, population–based, prospective, single–center cohort study initiated in 2016 with the aim of gaining a deeper understanding of functional health impairments and major chronic diseases in the general population. The study randomly invites 45,000 individuals between the age of 45 and 74 residing in the city of Hamburg, Germany. Although the study design includes a planned follow–up every six years, at the time of the analyses, no longitudinal data were available, which limited all analyses in this thesis to a cross–sectional design. Furthermore, since the studies included in this thesis were published at different time points, different data sets were available, resulting in variations in sample size and covariates. For part A (study 1 and 2), data from the first 1,000 individuals studied by brain MRI were available, while for part B (study 3 and 4), all data from the first 10,000 participants were available, of which 2,652 individuals received a brain MRI.

The HCHS was approved by the local ethics committee of the Landesärztekammer Hamburg (State of Hamburg Chamber of Medical Practitioners, PV5131) and all participants gave written informed consent. The study was registered at ClinicalTrials.gov (NCT03934957). All involved individuals in the study adhered to the ethical principles of the Declaration of Helsinki, Good Clinical Practice and Good Epidemiological Practice.

1.2.2. Assessment of demographic and clinical data

1.2.2.1. Demographic data and cardiovascular risk factors (all studies)

During their visit at the HCHS study center, participants underwent a detailed anamnestic and clinical examination. Their educational status was determined based on years of education and highest degree attained, which was then coded according to the International Standard Classification of Education (ISCED)[7] and grouped into tertiles ranging from 1–3 (low, medium, high). Individuals with diabetes mellitus were identified based on a fasting serum glucose level >126 mg/dl, non–fasting serum glucose level >200 mg/dl, or self–reported prevalence of the condition. Hypertension was defined as an increased blood pressure (≥140/90 mmHg), or the use of antihypertensive medication next to self–report. Smoking status was classified as active or non–smoking, and alcohol consumption was quantified based on the monthly frequency of alcohol intake.

Metabolic syndrome was defined according to the International Diabetes Federation consensus worldwide definition[8] which requires the fulfillment of the abdominal adiposity criterion (waist circumference >94 cm in men and >80 cm in women) and at least two other criteria[8]: high triglycerides (≥150 mg/dl) or the intake of lipid–lowering medication, low high-density lipoprotein cholesterol (men <40 mg/dl and women <50 mg/dl) or the intake of cholesterol–lowering medication, high blood pressure (systolic blood pressure ≥130 mmHg or diastolic blood pressure ≥85 mmHg) or the intake of anti–hypertensive medication, high fasting plasma glucose (≥100 mg/dl) or previously diagnosed diabetes mellitus according to self–report.

1.2.2.2. Nutritional behavior, including coffee consumption (study 3 and 4)

The nutritional behavior of all participants was assessed using a validated food frequency questionnaire (FFQ) containing 102 items, which was specifically developed for the European Prospective Investigation into Cancer and Nutrition Study[9]. The adherence to several dietary patterns was determined based on the FFQ scores, including the Mediterranean diet, the Dietary Approaches to Stop Hypertension (DASH diet) and the Mediterranean–DASH Intervention for Neurodegenerative Delay (MIND diet). The adherence to the Mediterranean diet was calculated with the German version of the original Mediterranean Diet Adherence Screener[10] which assigns a score of 0 or 1 to 14 food items. Therefore, the adherence score ranges from 0 (no adherence) to 14 (maximal adherence). The DASH diet was evaluated according to a previously published scoring scheme[11] which assigns a score of 0, 0.5 or 1 to each of 10 items. Ultimately, this results in an adherence score between 0 (no adherence) and 10 (maximal adherence). Adherence to the MIND diet was calculated as suggested in

the original paper[12] where a score of 0, 0.5 or 1 is assigned to 10 healthy and 5 unhealthy food items. In total, this revealed an adherence score between 0 (no adherence) to 15 (maximal adherence).

Furthermore, the adherence to a fourth dietary pattern representing an anti–inflammatory diet was calculated. As there is standardized definition for this dietary pattern, a data–driven approach was applied to use the scores on all items of the DASH diet, Mediterranean diet, and MIND diet for the definition of the anti–inflammatory diet. To be more precise, all item scores on all three dietary patterns were converted into tertiles to avoid extreme differences in sample size between the groups. Then, all items were correlated with the inflammatory markers CRP and IL–6 by using a Wilcoxon signed–rank test. All items with a significant association with inflammatory markers were selected as items of the anti–inflammatory diet. When multiple items represented the same food group, the item with the higher effect size was selected. When one item represented a specific food of another item with a more general food group, the more general item was selected. This approach resulted in nine items — four items of the DASH diet (vegetables, fruits, total dairy, nuts/seeds/legumes), three items of the MIND diet (red and processed meat, fast fried foods, wine) and two items of the Mediterranean diet (carbonated drinks, tomato sauce). A higher score on the anti–inflammatory diet represents intake of more anti–inflammatory foods and avoiding more pro–inflammatory foods. The anti–inflammatory diet was validated in a χ^2–test showing that the association of the score with several disorders including heart failure, heart insufficiency, arterial fibrillation, cancer, and cognitive function is highly significant.

Coffee consumption was quantified based on the participants' responses to the FFQ which also includes the consumption of espresso, cappuccino, café latte and other preparation types. The frequency of coffee consumption was classified into 5 groups: less than one cup per day (<1 c/d), one to two cups per day (1–2 c/d), three to four cups per day (3–4 c/d), five to six cups per day (5–6 c/d), or more than six cups per day (>6 c/d). One coffee was defined as a cup of 150 milliliters (ml).

1.2.2.3. Cognitive function (study 3)

Cognitive function was assessed using several cognitive tests that cover a variety of cognitive domains. The cognitive screening tests utilized were part of The Consortium to Establish a Registry for Alzheimer's Disease Neuropsychological Assessment Battery (CERAD–NP), in specific the extended German version (CERAD–NP/Plus)[13] which includes tests for cognitive status (Mini–Mental State Exam modified after original version[14]), verbal fluency (CERAD–NP/Plus Subtest Verbal Fluency), verbal learning and verbal memory (CERAD–NP Subtest Word List Memory, CERAD–NP Subtest Word List Recall), processing speed (Trail Making Test Part A as subtest of the CERAD–NP/Plus[15]), executive function (Trail Making Test Part B as subtest of the CERAD–NP/Plus[15]) and general intelligence level (Multiple–Choice Vocabulary Intelligence Test[16]). To ensure the validity of the cognitive test scores, participants were required to have sufficient German language skills and cognitive data were checked for plausibility. Implausible data were subsequently excluded. Table 1 shows the descriptive sample characteristics of the first 10,000 participants in the HCHS to provide an overview of the study sample.

Table 1. Study sample characteristics of 10,000 participants of the Hamburg City Health Study. Categorical variables are reported in number (n) and percentage (%), continuous variables are reported in median and interquartile range (IQR).

Demographic variables	
Age [years], median (IQR)	63 (15)
Female sex, n (%)	5,108 (51)
Education [years], median (IQR)	13 (4)
Education [ISCED[7]]	
Low	466 (4.9)
Medium	4,721 (50)
High	4,232 (45)
Cardiovascular risk factors	
Body mass index, median (IQR)	26.1 (5.7)
Active smokers, n (%)	1,354 (14)
Diabetes mellitus, n (%)	794 (7.9)
Hypertension, n (%)	6,301 (63)
Hypercholesterolemia, n (%)	2,277 (23)
Metabolic syndrome, n (%)	3,540 (35)
Nutritional behavior	
Mediterranean diet, median (IQR)	4 (3)
DASH diet, median (IQR)	4.5 (1.5)
MIND diet, median (IQR)	6.5 (2.5)
Anti–inflammatory diet, median (IQR)	4.5 (1.5)
Coffee consumption [cups per day]	
< 1 cup per day, n (%)	1,766 (18)
1 – 2 cups per day, n (%)	3,933 (39)
3 – 4 cups per day, n (%)	2,333 (23)
5 – 6 cups per day, n (%)	666 (6.7)
> 6 cups per day, n (%)	311 (3.1)
Cognitive function	
Verbal fluency, median (IQR)	25 (10)
Verbal memory, median (IQR)	8 (2)
Processing speed, median (IQR)	37 (17)
Executive function, median (IQR)	80 (42)
General intelligence, median (IQR)	32 (5)

1.2.3. Magnetic resonance imaging

A subgroup of all participants received state–of–the–art brain MRI, either randomly selected from all participants or identified by an increased risk of cardiovascular diseases characterized by a Framingham Risk Score above 7[17].

The brain MRI was performed using a 3 Tesla Siemens Skyra MRI scanner (Siemens, Erlangen, Germany). The imaging protocol included the acquisition of 3D T1–weighted anatomical images using a rapid acquisition gradient–echo sequence with the following sequence parameters: repetition time (TR) = 2,500 ms, echo time (TE) = 2.12 ms, 256 axial slices, slice thickness (ST) = 0.94mm, and in–plane resolution (IPR) = 0.83 × 0.83 mm^2. 3D T2–weighted fluid attenuated inversion recovery (FLAIR)

images were obtained using the following sequence parameters: TR = 4,700 ms, TE = 392 ms, 192 axial slices, ST = 0.9mm and IPR = 0.75 × 0.75mm. For single–shell diffusion weighted imaging (DWI), 75 axial slices covering the entire brain were acquired with gradients (b = 1,000 s/mm^2) applied in 64 noncollinear directions with the following sequence parameters: TR = 8,500 ms, TE = 75 ms, ST = 2mm, IPR = 2 × 2mm^2, anterior–posterior phase–encoding direction. T1-weighted images and DWI underwent quality assurance by deriving measures of image quality from MRIQC[18], Freesurfer[19], and QSI-Prep[20]. Based on these measures, images with outliers in framewise displacement and number of slices with signal dropouts (for DWI) were excluded. The FLAIR images were visually checked for sufficient quality.

1.2.3.1. MRI preprocessing

For study 3 and 4, we implemented an MRI preprocessing protocol according to the latest developments in neuroimaging, as described in detail in a published paper[21] and made openly available in a GitHub repository at: https://github.com/csi-hamburg/CSIframe/wiki. The relevant steps for study 3 and 4 included preprocessing of T1–weighted images and DWI using QSIPrep v.0.14.2[20] based on Nipype v.1.6.1[22]. T1–weighted images were intensity normalized with N4BiasFieldCorrection by using Advanced Normalization Tools v.2.3.1[23]. DWI were further denoised (MRtrix3's denoise[24]) and corrected for Gibbs ringing artefacts (MRtrix3's mrdegibbs[25]) and B1 field inhomogeneity (MRtrix3's dwibiascorrect with N4 algorithm[23]), followed by correction for head motion, eddy currents[26] and susceptibility distortions[27].

For study 1 and 2, preprocessing included only the registration of the structural images (FLAIR and T1–weighted images) on the DWI to overlay the output of one modality on the other. FLAIR and T1–weighted images were resampled to a resolution of 1x1x1mm, as well as DWI. The FLAIR and T1–weighted images were then non–linearly registered on the resampled DWI image with nearest neighbor interpolation.

1.2.3.2. Calculation of brain volume and cortical thickness (study 1, 2, 3 and 4)

The standardized FreeSurfer processing pipeline[28] (v.5.3 for study 1 and 2, v.6.0.1 for study 3 and 4) was applied on the registered T1–weighted images for whole–brain parcellation including segmentation of grey and white matter, ventricles, brainstem, and cerebellum. The brain volume was calculated by summing up the brain tissue without the ventricles. From the white matter masks, the brainstem, cerebellum, and all voxels located at the boundary to the grey matter were subtracted. The white matter masks are needed for the filtering of WMH.

Similarly, the reconstruction of the cortical surface and the calculation of the cortical thickness were conducted on T1–weighted images using the standardized FreeSurfer processing pipeline[19] (v.5.3 for study 1 and 2, v.6.0.1 for study 3 and 4). For study 4, we considered the mean cortical thickness averaged over both hemispheres as input variables. For study 1, we calculated the cortical thickness for each region in the Brainnetome atlas[29].

The measures of brain volume and cortical thickness were checked for quality. Data points with > 2 standard deviations from the mean were defined as outliers and excluded from subsequent analysis.

1.2.3.3. White matter hyperintensities segmentation (study 1, 2 and 4)

To segment WMH, FLAIR and T1–weighted images were utilized. First, two independent raters manually segmented WMH on 100 FLAIR images. The inter–rater overlap of manual segmentations was then used as input for the FSL's Brain Intensity AbNormality Classification Algorithm (BIANCA), a fully automated, supervised k–nearest neighbor (k–NN) algorithm[30]. WMH were then automatically segmented on both T1–weighted and FLAIR images for all participants, as segmentation on multiple image modalities leads to more accurate results. WMH masks were divided into periventricular WMH (pWMH) and deep WMH (dWMH) by defining a 10mm distance threshold to the ventricles, as recommended[31]. Finally, the WMH load was calculated as the ratio of WMH volume to brain tissue volume, excluding the ventricles. This WMH load measurement was used for the calculation of the WMH volume for study 1. The cohort was relatively mildly affected[33,34], with most WMH located in the periventricular white matter.

To overlap the WMH masks on free–water (FW) maps and free–water corrected fractional anisotropy (FA–t) maps in the analyses of study 2, they were registered into DWI–space by applying the warp fields from the structural image registration.

For study 2, the WMH masks were further resized via interpolation and binarized to match the resolution of the original DWI (2x2x2mm). WMH masks containing less than 4 voxels were excluded from subsequent analyses to ensure that all imaging parameters measured within WMH are based on a representative number of voxels. Again, we derived the WMH load from the ratio of WMH volume to brain volume. We further calculated the logarithm of the WMH load to obtain normally distributed data. This measure was used for study 2 and is referred to as 'logarithmic WMH load'. Furthermore, to analyze the non–lesioned, normal–appearing white matter (NAWM) in study 2, several regions of interest (ROIs) were defined by dilating the WMH masks in 3–dimensional space with 1 voxel increments. This step was repeated eight times, creating 8 NAWM masks (each 2mm size, in total a diameter of 16mm surrounding WMH) which indicate the increasing distance to the WMH. The size of the NAWM masks (in total 16mm) was chosen based on previous literature[35,36]. In the final step, the voxels were filtered with a white matter mask (described in paragraph 1.2.3.2), excluding all voxels that are not parcellated as white matter.

For study 4 and the inclusion of the larger MRI dataset (N=2,652), we updated the WMH segmentation by implementing a supervised method called LOCally Adaptive Threshold Estimation[37] for local thresholding of lesion probability maps, which led to significant improvements in the outcome lesion maps. Because the method was published in October 2018, after the first dataset of the HCHS was already processed, we were not able to apply this method in the first dataset (N=1,000). Instead of

using the brain tissue volume, we used the estimated intracranial volume (output from the FreeSurfer processing pipeline[28]) to normalize the WMH volume and retrieve WMH load.

1.2.3.4. Whole–brain tractography (study 1)

To determine the total number of streamlines terminating at the cortex, which was needed for the connectivity analysis in study 1, we applied whole–brain tractography on DWI using anatomically constrained probabilistic streamline tractography[38] by second order integration over fiber orientation distributions[39] with the publicly available MRtrix3 toolbox[40]. Dynamic seeding was applied to improve the biological plausibility of the tractography and consider the uncertainty in the determination of the voxel–wise fiber orientations[41]. From the tractography, four tractograms were derived for all individuals: (1) a tractogram containing all streamlines that terminate at the cortical surface; a tractogram containing all streamlines that pass through at least one such voxel segmented as (2) WMH, (3) periventricular WMH, or (4) deep WMH and then terminate at the cortical surface. Based on the tractograms, the total streamline number and the number of streamlines passing through a WMH were determined, and the proportion of WMH streamlines was calculated, further referred to as the WMH connectivity. This step was repeated for the streamlines passing through periventricular and deep WMH separately, further referred to as the periventricular or deep WMH connectivity. To facilitate the statistical analysis of the data, we translated the cortical thickness and connectivity data from ~320.000 vertices to 210 regions of the connectivity–based Brainnetome atlas[29].

1.2.3.5. Peak width of skeletonized mean diffusivity (study 3 and 4)

Peak width of skeletonized mean diffusivity (PSMD) was initially proposed in a paper published in 2016[42]. PSMD is defined as the difference between the 5th and 95th percentile of mean diffusivity values in the white matter skeleton[42]. Its source code was made openly available in 2019. We estimated diffusion–tensor imaging (DTI) from preprocessed DWI using a least–squares fit[43,44]. The resulting mean diffusivity maps were used for the estimation of PSMD according to the published protocol[42] but adjusted the pipeline by using a non–linear registration with ANTs' SyN registration[45]. We included PSMD as imaging marker of microstructural integrity and vascular brain damage in study 3 and 4.

1.2.3.6. Free–water imaging and free–water corrected fractional anisotropy (study 2)

We also applied free–water imaging by fitting a bi–tensor model optimized for single–shell DWI on the original DWI data[46]. This technique produced FW maps and FW–corrected diffusion tensors of the tissue compartment, which were used to calculate FW–corrected FA–t. WMH and NAWM masks were added to the maps to extract FW and FA–t values for each ROI, the dependent variables of study 2.

This is the end of a detailed description of the methodological approach for this thesis. Moving on, the next paragraph will deal with a brief introduction on the topic of cerebral small vessel disease, which will be followed by a description of the findings from study 1 and study 2.

1.3. Part A

1.3.1. Introduction — Structural brain changes in cerebral small vessel disease and beyond

1.3.1.1. Cerebral small vessel disease

Cerebral small vessel disease (CSVD) is a prevalent brain disorder that affects the small blood vessels in the brain, including the arterioles, capillaries, and venules. The pathogenesis of CSVD ranges from endothelial dysfunction and blood–brain barrier damage over impairment in vasodilatation, stiffening of the vessels and reduced blood flow to demyelination and inflammation[47]. These processes can lead to damage in both grey and white matter[48] as well as the development of stroke[49], cognitive decline and dementia[49]. CSVD can lead to various symptoms, including memory impairments[50,51], mood disorders[52] and gait disturbances[33]. While the underlying causes of CSVD are still not fully understood, certain factors such as high blood pressure[53] or smoking[54] are known to increase an individual's risk of developing CSVD. Treatment options for CSVD include lifestyle modifications, medication for symptom management, and secondary prevention[55(p2)].

Diagnosis of CSVD typically involves a combination of imaging and clinical evaluation. The most observed imaging markers used to diagnose CSVD are: 1) White matter hyperintensities of presumed vascular origin (WMH) are lesions of increased signal intensity on T2–weighted MR sequences in the white matter. WMH can also occur in subcortical grey matter structures or the brainstem but should then be referred to as 'subcortical hyperintensities' instead of WMH[56]; 2) Cerebral microbleeds occur as small hypointense lesions on T2*–weighted gradient–recalled echo or susceptibility–weighted imaging (SWI). Measuring 2mm to 10mm in diameter, they are generally not visible on computer tomography scans, FLAIR, T1–weighted or T2–weighted images[56]; 3) enlarged perivascular spaces, visible as round or linear structures in the same image intensity as cerebrospinal fluid. Generally, perivascular spaces are structures along the walls of cerebral blood vessels which are filled with fluid[57]. They appear linear when viewed parallel to the vessel or round/ovoid when viewed perpendicular to the vessel[56]; 4) Recent small lacunar infarcts occur in the territory of a perforating arteriole. Because of their predominant location in the primary motor and sensory pathways, they often appear clinically as a stroke while other pathologies of CSVD propagate without acute symptoms[48]; 5) Lacunes of presumed vascular origin appear ovoid or round and are fluid–filled cavities in the subcortical brain measuring 3mm to 15mm in diameter. They develop after a recent small lacunar infarct or hemorrhage[56]; 6) brain atrophy refers to a decrease in brain volume, in the context of CSVD not related to a focal brain injury. It encompasses decreases in both gray and white matter volume and an increase in cerebrospinal fluid structures[56].

Among the various imaging markers for CSVD, the most studied pathology is WMH. WMH are an indicator of vascular and age–related brain damage[58], almost ubiquitous with increasing age[59] and more prevalent in individuals with higher cardiovascular risk[60] (including in active smokers[54,59] and in patients with diabetes mellitus[59], overweight[53] or hypertension[59]). In a large multicenter study that

included data from 10 European population cohorts with 1,805 men and women, the prevalence of severe stage WMH increased dramatically with age, from 20.6% in the age group 65–69 years to 31.5% in the age group 70–75 years[61]. The sharp increase is alarming, since individuals with severe WMH have a yearly transition rate to disability or death of 29.5%[62], related to the increased risk of numerous diseases associated with WMH, such as accelerated cognitive decline[63–65], several types of dementia[63], stroke[63], depression[66], and impaired daily functioning[67] (including disturbances in gait[33] and motor function[68]). Extensive WMH burden in the general population has been linked to an 70.8% increased risk of stroke and dementia and 60% increased mortality[49]. WMH are associated with other brain pathologies, including decreased brain volume[69], decreased cortical thickness[70] and lacunes[71] and are more common in patients with subjective memory complaints[50,72–74].

1.3.1.2. Microstructural white matter damage beyond the lesion

Amassing evidence suggests that WMH represent only the most severe form of white matter damage. Although less pronounced, damage can still occur in the non–lesioned, normal–appearing white matter (NAWM) which is not visible to the naked eye but can be quantified with DWI and DTI. The most common DTI–metrics to quantify white matter microstructure are fractional anisotropy (FA) and mean diffusivity (MD). FA reflects the directionality of the movement of water molecules, which usually move along the length of axons and rarely perpendicular to them[75]. Therefore, FA characterizes the microstructural properties and integrity of white matter[76]. Higher FA values indicate that water molecules are more directed in their diffusion, suggesting a preserved microstructure while lower FA reflects neuronal abnormalities[76]. MD reflects the diffusion of water molecules in brain tissue, with a lower magnitude of diffusion (and lower MD) indicates preserved microstructure. FA and MD can be affected by age[77–79] and in various conditions, such as cardiovascular risk factors (i.e., hypertension[79,80] and diabetes mellitus[79,81–83]), systemic inflammation[84,85], gait disturbances[33], kidney dysfunction[86], subjective memory complaints[87], several types of dementia[87–89], amyloid positivity[90], and depression[91,92]. FA and MD are also associated with mortality (especially cardiovascular mortality)[93]. The 5–year prediction of stroke was significantly improved using markers of microstructural white matter integrity beyond the Framingham Stroke Risk Profile[94]. Additionally, both FA and MD are influenced by lifestyle–related factors such as nutrition[95,96], smoking[79,97,98], alcohol consumption[98,99] and physical activity[100,101].

Despite the new discoveries made possible with the development of DTI–metrics, values such as FA and MD can be contaminated by freely diffusing water molecules in the brain[46]. All water molecules that are not hindered in their movement by cellular structures within the diffusion time are considered free water (FW). In the brain, free water is found in the fluid–filled ventricles, around the brain parenchyma or in vasogenic edema, for example occurring due to trauma[102] or tumors[46]. To a lesser degree, FW is also present in the white matter, which is a problem for the estimation of a diffusion tensor[46]. When MRI voxels contain more than one tissue type, partial volume effects alter the diffusion tensor indices as they are no longer tissue–specific but represent the average of all tissue

compartments[103]. In other words, voxels that contain cerebrospinal fluid contaminate the diffusion tensor, causing elevations in MD and decreases in FA without apparent alterations in the white matter microstructure. To correct for this contamination, a method called free–water imaging was developed to calculate a two–tensor model which separates the isotropic free–water compartment from the free–water corrected tissue compartment[46]. Studies have shown that correcting for FW improves the sensitivity and robustness of DTI–metrics, enabling the detection of microstructural alterations in various patient groups that were not noticeable before. For example, radial diffusivity derived from MD was found to be increased in the brain of individuals converting from mild cognitive impairments to Alzheimer's Disease only after correction for FW[104]. Similarly, microstructural brain alterations in women with major depressive disorder were only detectable after FW correction[105].

After initially publishing the method of free–water imaging in 2009[46], subsequent analysis revealed that FW itself — derived from the free–water compartment — is a valid and reliable measure of white matter integrity, as FW highly correlated with age[77], hypertension[106], vascular dementia[89], Alzheimer's Disease[88,89,104] and schizophrenia[107]. Furthermore, FW was superior to conventional and FW–corrected DTI–metrics in the association with cognitive decline[108–111]. In addition, FW imaging has been found to be better at distinguishing patients from healthy controls compared to conventional MRI parameters. For example, hippocampal volumetry — a commonly used marker in the context of cognitive deterioration and Alzheimer's Disease — did not differ between early patients with mild cognitive impairments and healthy controls, but hippocampal FW detected early microstructural differences between the groups[112]. Also, while chronic stroke patients showed only slight differences in FA–t from healthy controls, the differences in FW were substantial and of large magnitude[113]. Additionally, FW was also stronger associated with cognition than several imaging markers of CSVD[114].

Despite the vast amount of research in the context of cerebral small vessel disease, several questions remain. Study 1 and 2 of this thesis deal with unanswered questions in the context of WMH. To be more specific, in study 1, we analyzed the structural connectivity between WMH and cortical thickness by conducting whole–brain tractography in the HCHS. In study 2, we focused more on microstructural properties in the NAWM by applying free–water imaging in the HCHS. In the following paragraph, I will give a short introduction to each of the two studies, describe the aim of the research and the findings. A detailed discussion of the results can be found in paragraph 1.5 together with the findings from the second part of this thesis.

1.3.2. Study 1: Linking cortical atrophy to white matter hyperintensities of presumed vascular origin

1.3.2.1. Background & aims

Several studies showed that WMH and cortical degeneration often occur together[70,115]. Individuals with WMH progression over a three–year period have been shown to have more pronounced cortical thinning compared to those with WMH regression[116(p20)]. Cortical thinning, like WMH, is an imaging marker of CSVD[56]. However, the exact relationship between the two CSVD markers is not yet clear, and there is currently no evidence of a direct structural connection. Research on the connection between stroke lesions and cortical degeneration may provide insight into this topic. In stroke, a subcortical brain lesion causes cortical atrophy[117,118] through the degeneration of the white matter tracts connecting the stroke lesion to the cortex[117]. This tract disturbance and subsequent cortical atrophy can extend to distant gray and white matter regions and even to the contralesional hemisphere[119]. It is hypothesized that similar mechanisms may be present in individuals with CSVD, although this is not yet fully understood. This research question was covered in study 1 entitled "Linking cortical atrophy of white matter hyperintensities of presumed vascular origin"[3]. To investigate the relationship between cortical thinning and WMH, we applied whole–brain tractography to a large population–based cohort with an increased risk of cardiovascular diseases. We expected a decrease in cortical thickness in regions with more WMH streamlines compared to those with fewer WMH streamlines. Moreover, we explored any differences in effect on cortical thickness based on the location of WMH in the periventricular or deep white matter.

1.3.2.2. Methods & results

This paragraph is a summary of a previously published paper[3].

Of the first 1,000 participants in the HCHS, 21 participants were excluded due to missing imaging data (9 without any imaging, 3 without FLAIR, 9 without DWI), 40 participants were excluded due to poor image quality or incomplete sequences (39 DWI, 1 FLAIR) and 9 participants were excluded due to technical problems during image processing. Therefore, data from 930 participants with a median age of 64 (IQR 14) years were included, of which 45.6% were female.

In the first part of the analysis, we projected the streamlines passing through WMH onto the cortical surface in the FreeSurfer average space to analyze the connectivity between WMH and the cortex. The visualization of the connectivity (Figure 1) revealed regional differences with higher WMH connectivity in the occipital and frontal lobes corresponding to the following Brainnetome regions: the cingulate gyrus (Brainnetome atlas labels A32p and A32sg), orbital gyrus (labels A12/47l, A12/47o), inferior frontal gyrus (label A44op), medio–ventral occipital cortex (labels vmPOS, rCunG, cCunG) and superior frontal gyrus (labels A9m, A10m). Consequently, lower connectivity was observed in the parietal and temporal lobes. The pWMH revealed to have a similar connectivity pattern on the cortical

surface with most connections to the frontal and occipital lobes. However, the dWMH connectivity was lower in total and more homogeneously distributed over the cortex.
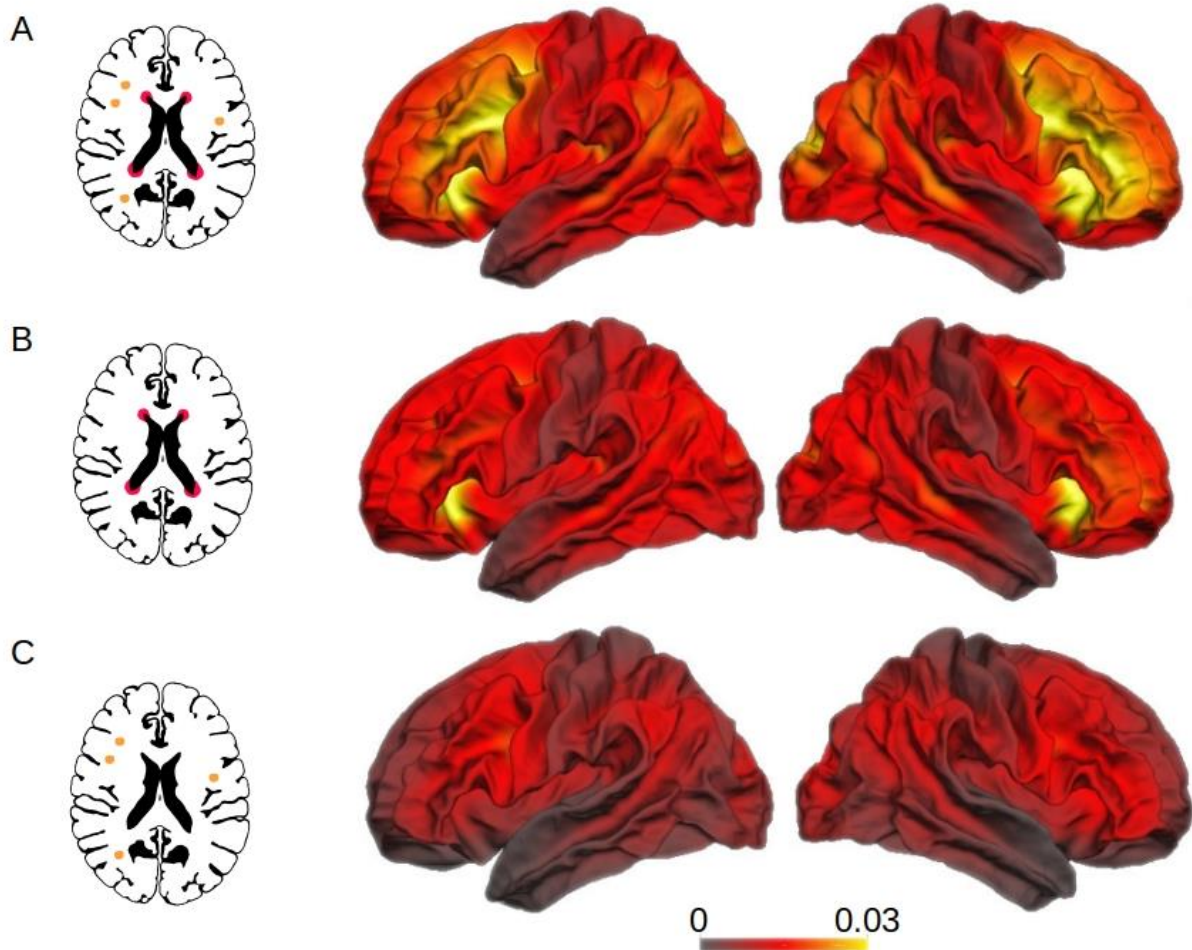

Figure 1[3]. Visualization of the WMH connectivity pattern on the cortical surface. Shown are connectivity patterns of streamlines passing through a WMH (A), a periventricular WMH (B) or a deep WMH (C). Color bars indicate the number of streamlines passing through a WMH relative to all streamlines for each vertex on the cortical surface.

In the second part of the analysis, we investigated the relationship between the thickness of a cortical region and its connectivity to WMH by applying a mixed–effects model. We found that WMH connectivity, as included in Model 1, was significantly negatively associated with cortical thickness ($t(49.12) = -2.71$, $p = 0.009$) after controlling for individual and regional differences in cortical thickness. Additionally, we found lower cortical thickness in male participants ($t(92.22) = 4.64$, $p < 0.001$) and older participants ($t(92.25) = -12.27$, $p < 0.001$) participants, in the left hemisphere ($t(19.24) = 7.89$, $p < 0.001$) and with a higher load of WMH ($t(93.23) = -2.82$, $p = 0.005$). In Model 2, we

replaced the WMH connectivity with pWMH and dWMH connectivity. Only the pWMH connectivity revealed to have a significant negative association with cortical thickness (t(62.33) = -3.38, p = 0.001). Associations with age (t(92.57) = -11.9, p < 0.001), sex (t(92.53) = 4.4, p < 0.001), hemisphere (t(19) = 7.78, p < 0.001) and pWMH load (t(94.45) = -2.72, p = 0.007) were similar to the results in Model 1. Both dWMH connectivity (p = 0.333) and dWMH load (p = 0.495) revealed to have no association with cortical thickness. An overview of the results of the linear mixed–effect models is presented in Table 2 where the estimates, confidence intervals (CI) and p–values are reported.

Table 2. Results of linear mixed–effect models analyzing the association between cortical thickness and WMH connectivity with additional adjustment for age, sex, hemispheric differences, and lesion load. The models also include two random effects to correct for inter–individual and regional differences of cortical thickness.

	Model 1 (WMH)			Model 2 (pWMH and dWMH)		
	Estimate	CI	p–value	Estimate	CI	p–value
Intercept	2.74	2.64 – 2.84	**< 0.001**	2.73	2.63 – 2.84	**< 0.001**
Age	< 0.01	-0.01 – 0.0	**< 0.001**	< 0.01	-0.01 – 0.0	**< 0.001**
Left hemisphere	0.01	0.01 – 0.01	**< 0.001**	0.01	0.01 – 0.01	**< 0.001**
Female sex	0.03	0.02 – 0.04	**< 0.001**	0.03	0.02 – 0.04	**< 0.001**
Connectivity						
WMH	-0.25	-0.43 – 0.07	**0.009**			
dWMH				0.05	-0.05 – 0.16	0.333
pWMH				-0.39	-0.62 – 0.17	**0.001**
Lesion load						
WMH	-6.94	-11.76 – 2.21	**0.005**			
dWMH				5.93	-11.10 – 22.96	0.495
pWMH				-10.24	-17.63 – 2.85	**0.007**

In summary, WMH as an imaging marker of CSVD and vascular brain damage has a significant impact on brain networks. It can be suggested that especially long–ranging white matter tracts with frontal lobe connections are the most affected. Previous studies repeatedly demonstrated a link between frontal lobe dysconnectivity and impaired executive function, a common clinical outcome of CSVD and vascular cognitive impairment[65,120,121]. Additionally, our findings showed that thinner cortices have more connections to WMH, suggesting secondary cortical degeneration following the development of lesioned white matter. Further research advancing the quantification of CSVD markers and the combination of WMH connectivity, brain network measures, and cortical atrophy over time is necessary to fully understand the exact workings of WMH and CSVD on brain network measures and cognitive deterioration.

1.3.3. Study 2: Free–water diffusion MRI detects structural alterations surrounding white matter hyperintensities in the early stage of cerebral small vessel disease

1.3.3.1. Background & aims

The WMH penumbra — or the perilesional zone of white matter surrounding WMH — is prone to lesioning, as revealed with DTI[122]. MD and FA were found to be altered in the WMH penumbra, with a distance–dependent relationship: the lowest integrity (i.e., high MD and low FA) was found closest to the lesion and improved with distance from WMH[35,122,123]. In fact, studies have demonstrated a WMH penumbra up to 9mm from the lesion with impaired white matter integrity[124], even in relatively healthy cohorts of 43 to 56 years of age[125]. Alterations in blood–brain barrier leakage and cerebral blood flow even revealed a WMH penumbra of 10mm[35,126] and 13mm[124] size. This information can be used to determine the time point at which microstructural alterations develop before tissue becomes lesioned. Several studies addressed this topic[127–129], and the WMH penumbra revealed to have altered integrity up to 9 years before the development of WMH[130]. The question remains if the FW–content — as indicator for decreased white matter integrity — is also increased in the penumbra of the WMH and if there is a distance–dependent relationship to WMH itself. This was the research question of the second publication of this thesis entitled "Free–water diffusion MRI detects structural alterations surrounding white matter hyperintensities in the early stage of cerebral small vessel disease"[4]. In this paper, we examined the FW–content and the FA–t in the WMH penumbra and the spatial relationship to WMH. We hypothesized that white matter in the direct surrounding of WMH (less distance) is marked by lower white matter integrity, indicated by increased FW–content, and decreased FA–t. To test this, linear regression models were employed to compare the concentric regions surrounding the WMH, including 8 NAWM regions, in terms of their FW and FA–t values. In addition, we analyzed the relationship between FW content in the NAWM and cerebrovascular risk factors in additional linear regression models. We expected that individuals with more risk factors express higher FW and lower FA–t.

1.3.3.2. Methods & results

This paragraph is a summary of a previously published paper[4].

We used the data set from study 1 including 930 participants for this analysis. We had to exclude additional 30 participants because of technical issues during the DWI processing. Therefore, the final data set contained data from 900 individuals, characterized by a median age of 64 years (IQR = 14) and 412 (45.8%) female participants. We used the WMH segmentations produced for the analysis in study 1 and dilated the masks voxel–wise in three dimensions to create multiple ROIs. This resulted in eight ROIs representing the rims with increasing distance from the lesion. A detailed description of the calculation of FW and FA–t values is described in paragraph 1.2.3.6. To test the hypothesis that FW and FA–t values are different in NAWM depending on the distance to WMH, we compared the concentrically adjacent ROIs including WMH and the 8 NAWM ROIs in their FW and FA–t values with linear regression models. We defined a contrast called 'forward difference coding' to compare

neighboring NAWM ROIs in the statistical analysis. The output of the statistical analysis is reported with standardized coefficients (β) and p–values (p).

Our analysis revealed that FW is significantly higher in the NAWM regions compared to its outer surrounding region in up to 8mm surrounding the WMH. In other words, NAWM ROI 1 (2mm distance to WMH) contained more FW than NAWM with 4mm distance to WMH, which contained significantly more FW than NAWM with 6mm distance to WMH. The outer region with significance was NAWM with 8mm distance to WMH showing significantly more FW than NAWM with 10mm distance to WMH. The relationship between FA–t values was more complex, with the highest FA–t value found in the NAWM 4mm from WMH. Further distant NAWM contained lower FA–t values with significant decreases in up to 14mm distance. A summary of these results is presented in Table 3.

Table 3. Results of multivariate linear mixed–effects regression analyzing FW and FA–t in WMH and adjacent NAWM ROIs.

	Free–water		FA–t	
	β	p–value	β	p–value
Intercept	0.205	**< 0.001**	0.456	**< 0.001**
Age	0.008	**< 0.001**	-0.002	**0.01**
Female sex	0.003	0.051	-0.001	0.35
Logarithmic WMH load	0.007	**< 0.001**	-0.004	**< 0.001**
ROI contrasts				
WMH – 2mm	0.166	**< 0.001**	-0.059	**< 0.001**
2mm – 4mm	0.07	**< 0.001**	-0.008	**< 0.001**
4mm – 6mm	0.015	**< 0.001**	0.019	**< 0.001**
6mm – 8mm	0.006	**< 0.001**	0.015	**< 0.001**
8mm – 10mm	0.002	**0.017**	0.011	**< 0.001**
10mm – 12mm	< -0.001	0.932	0.007	**< 0.001**
12mm – 14mm	-0.001	0.154	0.004	**0.003**
14mm – 16mm	-0.001	0.18	0.002	0.141

The second part of the analysis focused on the association of FW and FA–t with cerebrovascular risk factors including smoking, hypertension, and diabetes mellitus in WMH and in surrounding tissue. For this analysis, ROIs with significantly increased FW were summarized in one WMH–FW–penumbra. This allowed us to examine the effect of cardiovascular risk factors (i.e., diabetes mellitus, hypertension, smoking) on the microstructural integrity as quantified by FW imaging. The results showed higher FW in the WMH–FW–penumbra in active smokers compared to non–smokers (β = 0.006, p = 0.008). There were no significant differences of FW between smokers and non–smokers in WMH (β = 0.001, p = 0.793). There were also no significant differences of FW in individuals with diabetes mellitus (effect in WMH: β = -0.003, p = 0.639; effect in WMH–FW–penumbra: β < -0.001, p = 0.953) or hypertension (effect in WMH: β = < 0.001, p = 0.997; effect in WMH–FW–penumbra: β < 0.002, p = 0.227). For FA–t, the results were similar. Active smokers had significantly lower FA–t values in WMH (β = -0.015, p = 0.008) and WMH–FW–penumbra (β = -0.007, p = 0.003) compared to

19

non–smokers. There was no significant association with diabetes mellitus (effect in WMH: $\beta = 0.007$, p = 0.607; effect in penumbra: $\beta = 0.002$, p = 0.533) or hypertension (effect in WMH: $\beta = 0.002$, p = 0.316; effect in penumbra: $\beta = 0.003$, p = 0.212). See Table 4 for all results.

Table 4. Results of multivariate linear regression models with cerebrovascular disease factors and FW / FA–t in WMH and WMH–FW–penumbra.

	Free–water				FA–t			
	WMH		penumbra		WMH		penumbra	
	β	p	β	p	β	p	β	p
Intercept	0.424	**< 0.001**	0.192	**< 0.001**	0.431	**< 0.001**	0.478	**< 0.001**
Age	0.008	**< 0.001**	0.007	**< 0.001**	0.008	**0.001**	-0.004	**< 0.001**
Sex	-0.008	**0.031**	-0.003	0.084	-0.011	**0.008**	-0.002	0.336
Logarithmic WMH load	0.017	**< 0.001**	0.004	**< 0.001**	0.001	0.775	-0.003	**0.003**
Smoking	0.001	0.793	0.006	**0.008**	-0.015	**0.008**	-0.007	**0.003**
Diabetes mellitus	-0.003	0.639	<-0.001	0.953	0.007	0.607	0.002	0.533
Hypertension	< 0.001	0.997	0.002	0.227	0.002	0.316	0.003	0.212

With supplementary analysis differentiating between WMH in the periventricular and deep white matter, our objective was to investigate the FW in the WMH penumbra independent of the anatomical location of the WMH. The results showed that both the WMH in the periventricular and deep white matter have higher FW in the surrounding tissue with pWMH and dWMH having significantly altered FW in 8mm and 4mm distance, respectively. Also, the standardized effect sizes decreased with increasing distance to white matter. Additionally, we examined differences in FW between the first and last quartile of pWMH volume. The mean volumes for pWMH were 0.08ml (IQR = 0.073) in the lowest quartile and 3.4ml (IQR = 2.55) in the highest quartile. The range of altered FW in the pWMH penumbra is similar for participants in the lowest and highest quartile of pWMH volume, indicating that FW increases in the WMH penumbra represent more than solely the underlying anatomical structure.

Ultimately, FW could not only be superior to conventional DTI–metrics in the prediction of clinical outcomes[108–110] but also in the prediction of longitudinal WMH development. First indications in this direction are given in the literature showing that NAWM contains increased tissue water contents prior to the progression to WMH[131]. However, longitudinal studies are needed that focus on the novel free–water imaging approach. Despite attempts to control for the contamination of conventional DTI–metrics with the development of free–water imaging, confounding of pulsativity cannot be ruled out[132].

This completes the description of the first part of the thesis. A detailed discussion of the results can be found in paragraph 1.5 together with the results of part B. In the following section, I will introduce the relevance of a healthy nutrition, which foods are considered healthy and if regular coffee consumption is beneficial or detrimental for neurological health, followed by the description of study 3 and 4.

1.4. Part B

1.4.1. Introduction — Health benefits of nutrition and regular coffee consumption

In 1960, adult men living in Greece had a 90% lower mortality rate from coronary heart disease compared to their counterparts in the United States[133]. Together with a remarkably high adult life expectancy in Greece and southern Italy, researchers concluded that the food patterns typical in these areas might play a causal role for the particularly good health of their elderly population[133]. This discovery resulted in the creation of the Mediterranean diet, which consists of foods commonly consumed in Greece and southern Italy in the 1960s and is suggested to promote a healthy lifestyle and reduce the risk of nutrition–related chronic diseases. The Mediterranean diet includes the daily consumption of fruits, vegetables, beans, other legumes, nuts, bread, pasta, rice, couscous, polenta, bulgur, other grains, potatoes, olive oil, cheese, yogurt and wine (in moderate amounts), a medium consumption (a few times per week) of fish, poultry, eggs and sweets, and a low consumption (a few times per months) of red meat[133]. The World Health Organization recommends the Mediterranean diet to reduce cognitive decline and dementia[134]. Over the past two decades, there has been an immense amount of literature published in the health outcomes of the Mediterranean diet. Solely summarizing recently published meta–analyses is already beyond the scope of this thesis but briefly describing a selection of those gives an impression on the immense amount of data available on the dietary patterns. A higher adherence to the Mediterranean diet was, according to a selection of meta–analyses published between 2010 and 2022, associated with a reduced risk on the following adverse health outcomes: all–cause mortality[135], cardiovascular diseases (incidence[135] and mortality[135]), stroke[136], depression[136], hypercholesterolemia[137], cognitive deterioration[136,138,139], mild cognitive impairment[135,138], and Alzheimer's Disease[138].

A few years after the Mediterranean diet gained popularity, the DASH diet received public attention following a clinical trial that showed the effective reduction of blood pressure in hypertensive patients after following the DASH diet[140]. Several versions of the DASH diet exist, but generally, the diet promotes a high consumption of vegetables, fruits and low–fat dairy products and a low consumption of saturated fat, total fat, and cholesterol. In contrast to the Mediterranean diet, the DASH diet supports the consumption of more low–fat dairy products, low dietary sodium, and no consumption of alcohol. Because of the strong blood pressure–lowering effects, the DASH diet is recommended as non–pharmacological treatment option of hypertension by the American Heart Association[141]. According to a selection of meta–analyses published between 2010 and 2022, a higher adherence to the DASH diet is linked to reduced risk on all–cause mortality[142–144], cardiovascular diseases[142–145] including coronary heart disease (incidence[145] and mortality[143]), stroke (incidence[145] and mortality[143]) and incident heart failure[145], cancer (incidence[142,144] and mortality[142–144]), hypertension[146,147], diabetes mellitus[142,144], hypercholesterolemia[147], obesity[147,148], systemic inflammation[149], Parkinson's Disease[142,144] and cognitive deterioration[139].

The food components of the Mediterranean and DASH diet that were found to have the strongest correlation with reduced cognitive decline and dementia were summarized in a new dietary pattern, the MIND diet[12]. This new diet aims to promote healthy nutrition for neurological health and is made up of ten healthy components (green leafy vegetables, other vegetables, berries, nuts, olive oil, fish, beans, poultry, and wine) and five unhealthy components (cheese, butter, and margarine, red meat, fast fried foods, and pastries and sweets)[12]. Despite being a recent development, research has shown that the MIND diet is effective in reducing cognitive decline, both in cross–sectional[150,151] and longitudinal analysis[152], and in reducing the risk of dementia[153] and Alzheimer's Disease[153,154]. It was also that the MIND diet was superior in delaying cognitive deterioration compared to, for example, the Mediterranean diet and the DASH diet[12,155,156]. Also, the suggested neuroprotective effects of the MIND diet were detectable on structural brain MRI parameters such as brain volume[153] and white matter integrity[153].

Although the MIND diet was developed to delay neurodegeneration, few studies examined whether adherence to the MIND diet is associated with early microstructural alterations. A higher MIND diet adherence was associated with better outcomes on brain volume in some[153] but not all studies[157,158]. Only one previous study examined the association with microstructural integrity and found a significant relationship with MD but not FA[153]. To this end, we examined the association between the MIND diet, as well as other dietary patterns, with alterations in brain structure and cognitive performance in the HCHS, represented in study 3. Furthermore, as coffee consumption was previously found to reduce the risk of several neurodegenerative diseases longitudinally, we conducted a second study, represented in study 4, to examine the specific effects of coffee on the brain microstructure. A detailed description of the findings of both studies is given below.

1.4.2. Study 3: Association between nutrition, brain structure and cognition and mediating effects of metabolic syndrome — a structural equation modeling approach in the Hamburg City Health Study

1.4.2.1. Background & aims

Although the literature overwhelmingly demonstrated that adhering to a specific dietary pattern, such as the Mediterranean or DASH diet, is linked to numerous health benefits, recent studies have called into question the general concept of dietary patterns due to inconsistent results across populations[159]. For example, the MIND diet was developed based on data from a United States cohort that demonstrated it to be more strongly associated with cognitive decline that other dietary patterns[12]. This finding was replicated in similar studies, also including cohorts from the United States[154,156,160]. However, studies including other populations, such as Canadian and European cohorts[150,161,162], failed to replicate this result, highlighting the challenge of transferring dietary patterns from one country to another. Likewise, the Mediterranean diet recommends foods that are common in Mediterranean regions, to be more specific, foods that *were* common in the 1960's[163]. However, the transferability to other regions is challenging because of limited availability, convenience or affordability[159]. Therefore, it

may be necessary to adapt dietary patterns to local nutritional behavior. In fact, the development of a local dietary pattern based on data from the Swedish population was found to have a stronger correlation with health outcomes in a Swedish cohort than the MIND diet[161]. Similarly, non–inferiority of a Dutch dietary pattern compared to the more popular Mediterranean and MIND diet was found in a Dutch cohort[162,164]. Therefore, while adherence to a specific diet pattern can have significant health benefits, it may be important to consider the local context when developing and promoting dietary guidelines.

Based on the discussion around dietary patterns, we aimed to study not the adherence to a specific dietary pattern, but the general construct nutrition, represented by the adherence to several dietary patterns (Mediterranean diet, DASH diet, MIND diet, anti–inflammatory diet). We analyzed the association of this general construct with the brain microstructure and cognitive function. We measured the brain microstructure with brain volume and the novel imaging marker PSMD, an indicator of early vascular brain damage[42].

1.4.2.2. Methods & results

We conducted two structural equation models (SEM) to examine the association between nutrition, cognition, and brain structure. SEM is a statistical approach which allows the analysis of direct and indirect relationships between variables as well as the total effects in a model, considering additional (mediating) variables. In SEM, measuring multiple manifest variables allows the definition of latent constructs. The constructs represent theoretical concepts that cannot be directly measured. While manifest variables measure observable aspects of a construct, they may not capture the entire depth of the construct. Latent constructs provide a way to account for the underlying dimensions that contribute to the observed patterns.

In our study, the first model included data from 10,000 participants and analyzed the association between the latent constructs nutrition and cognition. The construct nutrition was represented by the manifest variables DASH diet, Mediterranean diet, MIND diet and anti–inflammatory diet (see paragraph 1.2.2.2 for a detailed description of the assessment). The construct cognition represented the performance on four cognitive domains: verbal fluency, verbal memory, processing speed, and executive function. See paragraph 1.2.2.3 for a detailed description of the assessment. Furthermore, we corrected for age, sex, and metabolic syndrome. Metabolic syndrome was added to the model as a mediating factor. The second SEM was conducted in the MRI subsample and additionally contained the construct brain structure, represented by the manifest variables PSMD and normalized brain volume. Missing data points were imputed with full information maximum likelihood.

The first SEM was assessed in the full cohort, which contained 10,000 participants. Figure 2 gives an overview of the SEM with the results. The direct effect and total effect of nutrition on cognition was significant and positive (direct effect: $\beta = 0.308$, $p < 0.001$; total effect: $\beta = 0.14$, $p < 0.001$). There was

a significant indirect effect of nutrition on cognition through metabolic syndrome (β = 0.02, p < 0.001). Table 5 gives a detailed description of all effects.

Table 5. Result of the structural equation model analyzing the association between nutrition and cognition.

|	β	95% CI	p
Direct effects			
nutrition → metabolic syndrome	-0.19	-0.21 – -0.17	**< 0.001**
nutrition → cognition	0.12	0.09 – 0.15	**< 0.001**
age → nutrition	0.09	0.07 – 0.11	**< 0.001**
age → metabolic syndrome	0.23	0.21 – 0.25	**< 0.001**
age → cognition	-0.58	-0.60 – -0.56	**< 0.001**
sex → nutrition	0.41	0.39 – 0.43	**< 0.001**
sex → cognition	0.05	0.03 – 0.08	**< 0.001**
metabolic syndrome → cognition	-0.09	-0.12 – -0.07	**< 0.001**
Indirect effects			
nutrition → metabolic syndrome → cognition	0.02	0.01 – 0.02	**< 0.001**
Total effects			
nutrition → cognition	0.14	0.11 – 0.17	**< 0.001**
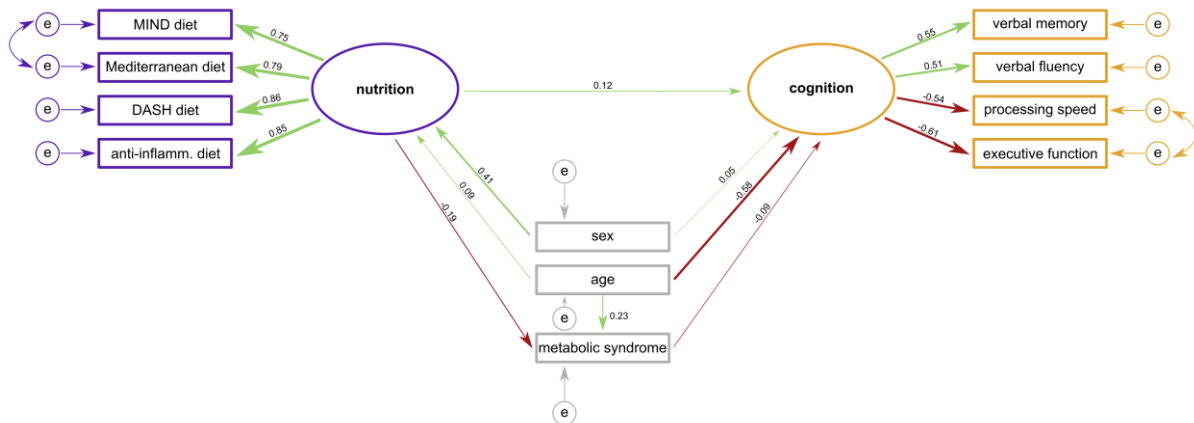
Figure 2. Structural equation model analyzing the association between nutrition and cognition. The numbers show the standardized coefficients. Positive associations are shown in green, negative associations in red.

The MRI subsample contained 2,592 individuals after exclusion of individuals with missing MR sequence (N = 28), pathologies on the MRI (N = 26), insufficient image quality (N = 6), or technical issues during the brain parcellation (N = 53). Figure 3 gives an overview of the SEM with the results from the MRI subsample. Nutrition was significantly and positively associated with cognition, both in the direct and total effect (direct effect: β = 0.1, p < 0.001; total effect: β = 0.12, p < 0.001). In addition, nutrition had a significant indirect effect on cognition through metabolic syndrome and brain structure (β = 0.02, p < 0.001). Nutrition had no direct significant association with brain structure (β = -0.01, p =

0.639) but the association was significant indirectly through metabolic syndrome (β = -0.01, p = 0.03). Table 6 gives a detailed description of all effects in the MRI subsample.

Table 6. Result of the structural equation model analyzing the association between nutrition, brain structure, and cognition.

|	β	95% CI	p
Direct effects			
nutrition → metabolic syndrome	-0.19	-0.23 – -0.15	**< 0.001**
nutrition → brain structure	-0.01	-0.06 – 0.03	0.639
nutrition → cognition	0.1	0.04 – 0.15	**< 0.001**
brain structure → cognition	-0.21	-0.30 – -0.11	**< 0.001**
age → metabolic syndrome	0.2	0.16 – 0.24	**< 0.001**
age → nutrition	0.12	0.09 – 0.16	**< 0.001**
age → brain structure	0.67	0.64 – 0.70	**< 0.001**
age → cognition	-0.43	-0.05 – -0.35	**< 0.001**
sex → nutrition	0.38	0.35 – 0.42	**< 0.001**
sex → brain structure	-0.28	-0.32 – -0.24	**< 0.001**
sex → cognition	-0.01	-0.07 – 0.04	0.639
metabolic syndrome → brain structure	0.05	0.01 – 0.08	**0.025**
metabolic syndrome → cognition	-0.09	-0.14 – -0.03	**0.001**
Indirect effects			
nutrition → metabolic syndrome → brain structure	-0.01	-0.02 – 0	**0.03**
nutrition → metabolic syndrome → brain structure → cognition	0.02	0.01 – 0.03	**< 0.001**
nutrition → brain structure → cognition	0	-0.01 – 0.01	0.641
Total effects			
nutrition → cognition	0.12	0.06 – 0.17	**< 0.001**
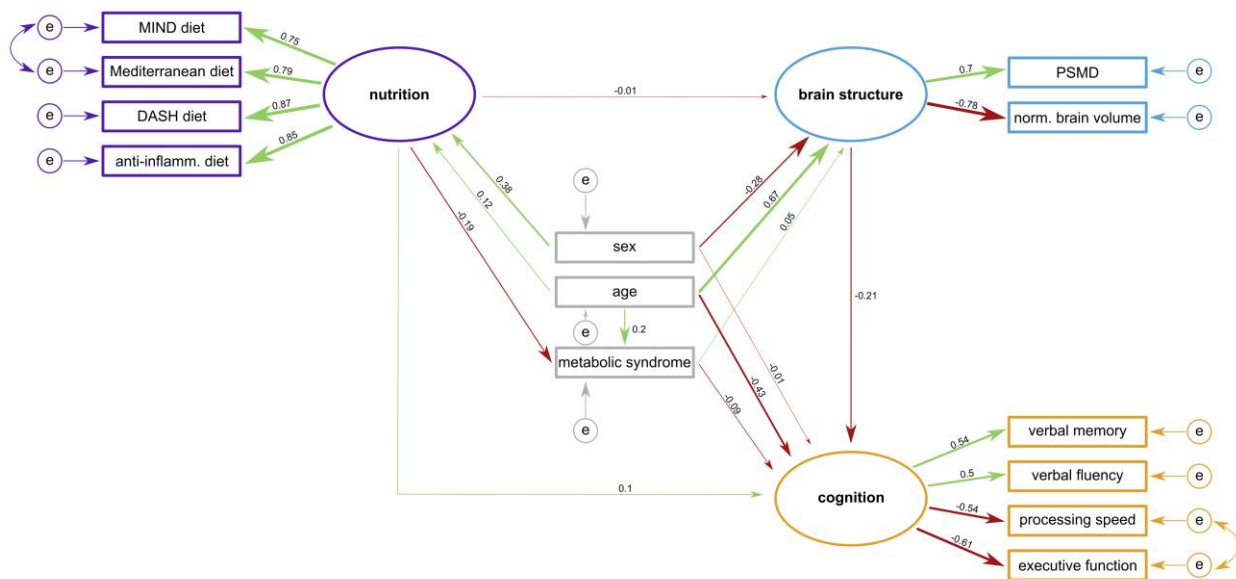
Figure 3. Structural equation model analyzing the association between nutrition, brain structure and cognition. The numbers represent the standardized coefficients. Positive associations are shown in green, negative associations in red.

In conclusion, a healthy diet as proposed by the DASH diet, Mediterranean diet, MIND diet or an anti–inflammatory diet is significantly associated with better cognitive performance. In addition, the nutrition has a significant effect on brain structure by significantly reducing the prevalence of metabolic syndrome. It is important to note that although the effects were significant, the effect size of nutrition to metabolic syndrome, brain structure and cognition were small. Before I will discuss the mechanisms forming a connection between unhealthy nutrition and neurodegeneration in detail in paragraph 1.5.2, I will briefly introduce the topic of coffee consumption in the context of neurodegeneration and present the result of our study in the next paragraph.

1.4.3. Study 4: Association between coffee consumption and brain MRI parameters in the Hamburg City Health Study

1.4.3.1. Background & aims

The consumption of coffee has been shown to have a beneficial impact on several factors that contribute to neurodegeneration and vascular brain damage. These include reducing systemic inflammation levels, inhibiting the deposition of amyloid beta, and mitigating the risk of developing cardiovascular risk factors. Coffee contains anti–inflammatory and antioxidant compounds, such as caffeine, polyphenols, and heterocyclic compounds. A regular coffee consumption can reduce the risk of mortality from inflammatory diseases[165]. Next to its anti–inflammatory mechanisms, coffee consumption has been linked to a reduced amyloid beta deposition[166], a hallmark of neurodegenerative diseases such as dementia. This is due to the high solubility of the coffee

constituent caffeine in lipid and water, which allows caffeine to cross the blood–brain barrier and act as an antagonist to adenosine receptors[167], thereby reducing amyloid beta induced toxicity[168]. Human studies have shown that regular coffee consumption was associated with lower amyloid beta positivity[166] and lower risk of dementia[169]. For example, drinking 3–5 cups per day in midlife was associated with 70% lower risk of incident dementia later in life[170]. The neuroprotective properties of adenosine receptor antagonist have also been shown for brain damage after ischemic stroke[171,172], and in a Parkinson's Disease mice model against the depletion of striatal dopamine levels[173]. A daily coffee consumption of 3 cups has been linked to a lower risk of Parkinson's Disease[174] and 20% lower risk of stroke[175,176] in large meta–analyses. Coffee consumption was also indirectly neuroprotective by reducing cardiovascular risk factors like diabetes mellitus and metabolic syndrome[177,178]. The reduced risk of diabetes mellitus has been found to be one of the most significant health benefits of regular coffee consumption[179].

Given that cardiovascular risk factors are a leading cause of CSVD[53], coffee consumption may help decrease the development and severity of CSVD in individuals with high cardiovascular risk. However, literature on this topic is incongruent with WMH showing either no significant association[166,180,181], significant associations in subgroups[182] or in opposite directions[182,183]. There is also a lack of research for more sensitive imaging markers of brain microstructure. Only one previous study analyzed the microstructural integrity in the context of coffee showed that a moderate–to–high coffee consumption is associated with better microstructural integrity in 145 elderly individuals[184]. Studies considering grey matter volume as outcome variable in the context of coffee consumption had inconsistent results– showing either a positive[185], negative[181,186] or no significant association[187]. Only one previous study considered cortical thickness in predefined regions of interest in the context of coffee consumption[166]. Therefore, with this study, we aimed to investigate whether regular coffee consumption is associated with multiple brain MRI markers of vascular brain damage and neurodegeneration, including WMH, PSMD, and cortical thickness in a large, population–based cohort.

1.4.3.2. Methods and results
This paragraph is a summary of a previously published paper[5].

We considered three brain MRI parameters for the analysis with coffee consumption representing different underlying pathologies. We included cortical thickness as a measure of overall atrophy and WMH as a measure of CSVD and accelerated vascular brain damage. WMH volume was further corrected for intracranial volume and taken the logarithm to assure normal distribution, further referred to as logarithmic WMH load. In addition, we included PSMD, which is also a marker of CSVD but more sensitive to microstructural alterations. We applied three linear regression models with either PSMD, logarithmic WMH load or cortical thickness as dependent variables. Coffee consumption was included as the independent variable, with the reference group consumption of less than one cup per day. Further, the covariates age, sex, education, diabetes mellitus, hypertension, smoking, body mass index, adherence to the Mediterranean diet, and alcohol consumption were added to the model.
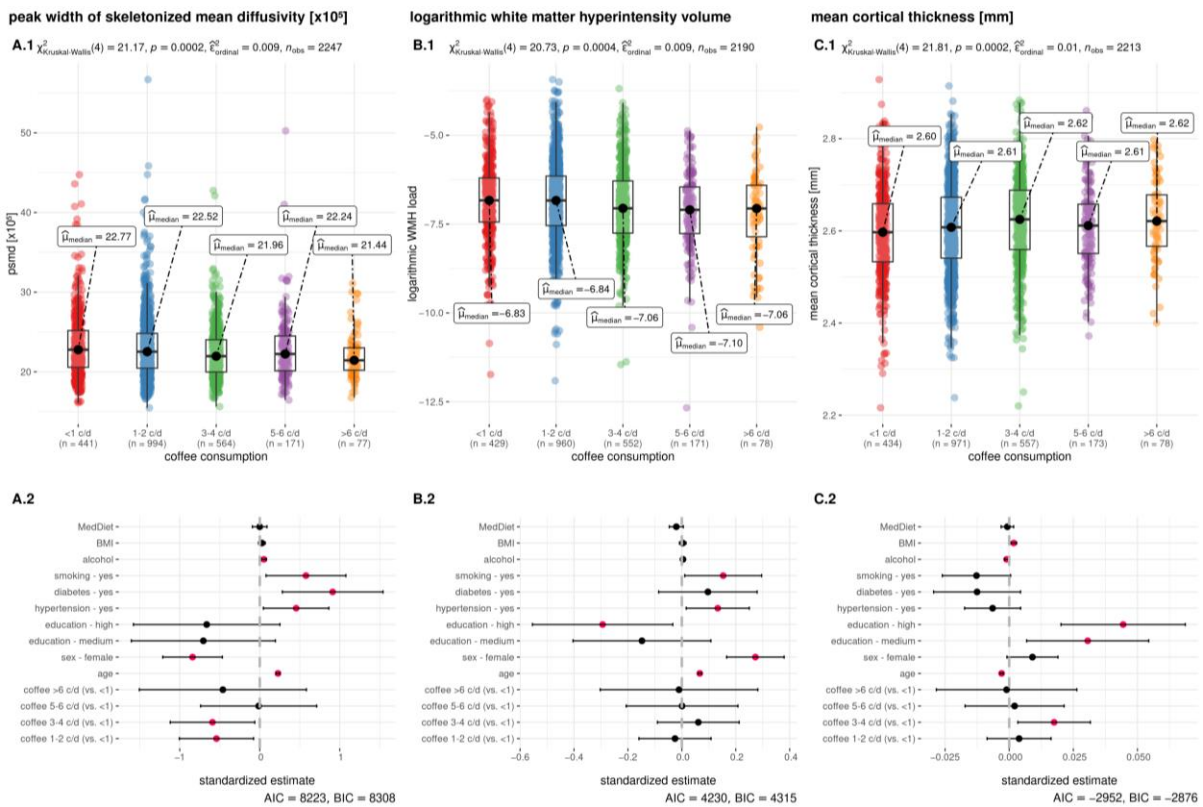
Figure 4. Summary statistics of the association between coffee consumption and the MRI parameters. The upper row shows boxplots with coffee consumption on the x-axis and PSMD (A.1), logarithmic white matter hyperintensity load (logarithmic WMH load, A.2) and mean cortical thickness (A.3) on the y–axis. The inferential test results above the boxplots indicate the output from the non–parametric Kruskal–Wallis test. The bottom row shows the results of the linear regression models. The dependent variable is PSMD (A.2), logarithmic WMH load (B.2) and mean cortical thickness (C.2). Independent variables are presented on the y–axis. The standardized estimates are presented on the x-axis. Pink dots indicate a significant association and black dots a non–significant effect of the independent variable.

In total, 2,316 participants were included in the analysis. 19.8% of all participants consumed less <1 cup of coffee per day, 44% consumed 1–2 cups per day, 25.1% consumed 3–4 cups per day, 7.6% consumed 5–6 cups per day, and 3.5% consumed >6 cups of coffee per day.). The distribution of the MRI parameters across the groups of coffee consumption was visualized in Figure 4. After adjustment for covariates, PSMD and mean cortical thickness were significantly different between the groups of coffee consumption. Drinking 1–2 cups of coffee per day was associated with lower PSMD compared to the reference group (<1 cup per day; β = -0.542, p = 0.022). Also, coffee consumption of 3–4 cups was associated with lower PSMD, compared to the reference group (β = -0.591, p = 0.028). Drinking 5–6 cups per day or >6 cups per day was not associated with a different PSMD compared to the reference group (p > 0.05). In addition, 3–4 cups of coffee were associated with significantly higher

cortical thickness compared to the reference group (β = 0.018, p = 0.015) whereas other groups of coffee consumption did not significantly differ from the reference group (p > 0.05). There was no significant difference in logarithmic WMH load between the groups of coffee consumption. See Table 7 for a detailed description of the results.

Table 7. Results of the linear regression models examining the association between coffee consumption and microstructural brain parameters.

	PSMD [x10^5]		Mean cortical thickness [mm]		logarithmic WMH load	
	β	p	β	p	β	p
Intercept	23.961	**< 0.001**	2.569	**< 0.001**	-6.998	**< 0.001**
Age	1.908	**< 0.001**	-0.025	**< 0.001**	0.557	**< 0.001**
Female sex	-0.888	**< 0.001**	0.008	0.09	0.256	**< 0.001**
Education (medium)	-0.669	0.113	0.031	**0.006**	-0.113	0.35
Education (high)	-0.632	0.141	0.045	**< 0.001**	-0.245	**0.048**
Hypertension	0.41	**0.037**	-0.006	0.264	0.135	**0.017**
Diabetes mellitus	0.928	**0.002**	-0.015	0.071	0.121	0.166
Smoking	0.498	**0.036**	-0.013	**0.048**	0.159	**0.021**
Alcohol consumption	0.283	**0.001**	-0.006	**0.02**	0.012	0.649
Body mass index	0.14	0.112	0.008	**0.002**	0.009	0.734
Coffee (1–2 cups per day)	-0.551	**0.015**	0.008	0.205	-0.034	0.608
Coffee (3–4 cups per day)	-0.597	**0.019**	0.018	**0.008**	0.072	0.331
Coffee (5–6 cups per day)	0.044	0.901	0.003	0.72	0.016	0.87
Coffee (>6 cups per day)	-0.492	0.332	0.002	0.908	-0.057	0.69

To conclude, assessing the pure impact of caffeine on large groups of people can be challenging. In this study, we undertook an initial investigation into the effects of coffee on brain microstructure. Our findings suggest that the potential neurological benefits of coffee may be attributed to caffeine, but further research with a longitudinal design is needed to confirm this hypothesis. Also, the prevalence of decaffeinated coffee consumption was low. Out of the total of 127 participants that reported to drink decaffeinated coffee, only 5.5% reported a daily intake of one or more cups. Moreover, 94.5% of all participants (N = 127) additionally drank caffeinated coffee, leaving only a small group of seven individuals who exclusively drank decaffeinated coffee. This group was too small for meaningful statistical analysis of the effects of decaffeinated coffee. Furthermore, we did not account for other sources of caffeine, such as tea, soft drinks, energy drinks or chocolate, which could have provided a more comprehensive assessment of caffeine intake. It is also worth noting that the study did not differentiate between various types of coffee preparation. For example, coffee consumption may be associated with increased sugar or fat intake if sweeteners or creamers are added. In the end, disentangling this effect is nearly impossible.

1.5. General discussion

1.5.1. Vascular brain damage related to cortical atrophy and microstructural degeneration

The first part of this thesis aimed to evaluate two distinct aspects of vascular brain damage (i.e., WMH): the structural connectivity of vascular brain lesions with cortical grey matter degeneration (study 1), and microstructural alterations in the non–lesioned white matter (study 2). We employed multiple image processing methods including the training of an WMH segmentation algorithm, cortical parcellation, and whole–brain tractography. We also used free–water imaging to examine the FW in the surrounding tissue of WMH in association with the distance to the lesion. Overall, the findings of study 1 and study 2 shed light on the complex structural associations between vascular brain damage, atrophy of the cortical grey matter and microstructural pathologies. In the following paragraphs, I will discuss the findings of study 1 and 2 in the context of related pathological changes (paragraph 1.5.1.1) and the differentiation between pWMH and dWMH (paragraph 1.5.1.2)

1.5.1.1. Association of WMH with cortical atrophy and brain microstructure

The findings of study 1 reveal that the two CSVD imaging markers WMH and cortical atrophy are structurally linked. Disentangling this complex relationship is challenging because WMH and cortical atrophy share numerous similar risk factors, particularly age and cardiovascular risk factors. Generally, three main hypotheses have been proposed to explain the relationship between WMH and cortical atrophy. First, the *disconnection hypothesis* states that WMH cause axonal damage, neuron loss and cognitive deterioration, similar to the mechanisms described in stroke lesions[118,119]. In the case of WMH, impairments in blood flow after cerebral atherosclerosis are considered to lead to WMH[127] through axonal damage and disruption of white matter connections, further damaging neuronal cell bodies and gray matter[47]. A second explanation is the reverse hypothesis, which posits that cortical gray matter damage via amyloid accumulation leads to myelin loss, axonal damage, and the development of WMH, though this hypothesis is debated[188]. The third hypothesis suggests that blood flow impairment causes ischemia leading to both WMH and cortical thinning simultaneously. While cross–sectional analyses found evidence for this type of association[70,116,189], the results of longitudinal studies were mixed with several studies demonstrating a pronounced longitudinal decline in cortical thickness in individuals with a higher WMH burden[64,190,191], while a large cohort study found no longitudinal association[192]. In our study, we showed that WMH were structurally linked to degenerating cortices. A study with a comparable methodological approach analyzing incident subcortical infarcts in a genetic form of CSVD called Cerebral autosomal dominant arteriopathy with subcortical ischemic strokes and leukoencephalopathy (CADASIL)[117] supports our results. The same study also found that the white matter tracts connecting the infarct with the degenerating cortex expressed accelerated damage in their microstructure[117], giving further indication that the *disconnection hypothesis* provides a possible explanation for the association between WMH and cortical degeneration in CSVD. Other studies have analyzed the relationship between white matter integrity in CSVD and cortical thinning over time, but — similar to the findings with WMH — the results have been inconsistent[193,194].

Nevertheless, these studies and our findings support the theory of secondary cortical degeneration following WMH in CSVD.

In study 1, we also found a distinct connectivity pattern of WMH to the cortical surface. This connectivity pattern can be explained by the distribution of hyperintensities in the white matter, which is highest in the occipital and frontal white matter, explaining the increased connectivity to the closely located frontal and occipital cortex[195]. A study that incorporated measures of the brain network along with WMH and cortical thickness analysis revealed a higher WMH load related to lower global efficiency[115]. Since global efficiency is mainly associated with long–ranging white matter tracts, the results indicate that long–ranging white matter fibers are significantly affected by WMH[115]. Findings from another study support this theory, which revealed that the mean tract length of white matter tracts terminating at the cortical surface increased in the frontal, superior parietal and occipital lobes and shorter in the superior temporal and postcentral cortices[196]. The local minima and maxima of the tracts length at the cortical surface are in line with the minimum and maximum WMH connectivity, indicating that cortical regions with receiving longer tracts have a higher connectivity to WMH[196]. An analysis with high-resolution resting–state electroencephalography further confirmed that WMH affected functional connectivity in long–ranging connections, especially in the frontal lobe[197].

In study 2, we examined the microstructural alterations of the white matter in WMH and the surrounding penumbra. Studies that analyzed the penumbra of WMH showed that the surrounding tissue is characterized by altered microstructural characteristics with the strongest alterations in the closest proximity to WMH[122–124,126]. With the development of a new DTI processing method called free–water imaging[46], we analyzed if similar distance–dependent microstructural alterations can be determined by the content of FW. After controlling for age, sex and logarithmic WMH load, the results show that FW was significantly different between WMH and the first four ROIs of NAWM (2mm – 8mm) with the highest FW values in the WMH and lower FW with increasing distance from the WMH. There were no significant differences in FW in adjacent ROIs between 10mm and 16mm. FW is suggested to be an indicator of the microstructural integrity, with increasing values of FW suggesting more unrestricted diffusion of water molecules, which is most probably due to damage of the white matter microstructure. However, the pathological correlates of FW are far from being fully understood. Based on the limited literature available, several mechanisms are suggested to cause an increase in FW. Several authors discussed that FW is an indicator of structural white matter degeneration[89,106]. Analysis of the short and long T2 values representing water in different cellular structures suggests that an increased water content in the NAWM happens due to demyelination of the white matter[198]. Moreover, carotid–femoral pulse wave velocity as a marker of aortic stiffness correlated with increasing FW in white matter[106]. However, histological studies should examine the pathological correlates of increased FW. Currently, increases in FW can only be interpreted as the presence of mechanisms leading to an increase in the extra– or intracellular space[46]. Despite the uncertainty of the pathological mechanisms, we can conclude that the WMH penumbra as defined by alterations in FW

has a size of approximately 8mm. FW imaging has not been conducted in the WMH penumbra previously, highlighting the novelty of this study. Comparable WMH penumbra sizes were determined with studies including conventional DTI–metrics[124].

In addition, only smoking was significantly associated with FW and FA–t, indicating decreased microstructural integrity in active smokers compared to non–smokers in the WMH penumbra. There was no significant difference between active smokers and non–smokers in FW within WMH. Our results are supported by previous findings showing FA differences between smokers and non–smokers exclusively in the penumbra but not in the WMH itself[97]. This association can be explained by the chemical composition of the cigarette smoke can cause neurotoxic brain swelling and plasma fluid leakage into the interstitial space, increasing the extracellular water ratio[98,199]. Diabetes mellitus and hypertension were neither associated with FW and FA–t in WMH nor in the penumbra. Previous literature focusing on uncorrected FA in the brain white matter found a significant association with diabetes mellitus[79,81–83] and hypertension[79,80]. However, significant decreases in white matter integrity were only present in patients with severe hypertension but not in patients with the mild form[79]. No study previously examined the association between the cardiovascular risk factors with FW or free–water corrected DTI–metrics. One study included systolic blood pressure as an indirect marker of hypertension in its analysis, with significant impact on FW[106]. We did not consider additional determinants of WMH severity, such as the disease duration[200] or differentiation between participants with good or bad controlled hypertension[80,200,201] which can be considered a limitation.

1.5.1.2. Differences between periventricular and deep WMH

Typically, pWMH are located within a 10mm distance from the ventricles while dWMH are located further away[31]. With the different locations, the two lesion types differ in several other factors as well. First, there are differences in the anatomical microstructure of the periventricular and deep white matter. The periventricular region has densely packed, long association fibers connecting distant regions, while the deep white matter contains fibers connecting adjacent regions by short U-shaped connections[202]. This had important implications for the methodological approach and the interpretation of the findings of study 1 and 2.

In the context of study 1, differences in the connectivity profile to the cortical surface between pWMH and dWMH can be largely explained by several factors. First, there are differences in the anatomical microstructure of the periventricular and deep white matter. The periventricular region has densely packed, long association fibers connecting distant regions, while the deep white matter contains fibers connecting adjacent regions by short U–shaped connections[202]. The findings of study 1 showed that pWMH had a higher connectivity profile in the frontal and occipital lobes which was significantly associated with cortical thickness and very similar to the connectivity profile of overall WMH. In contrast, dWMH had a more homogeneous connectivity profile on the cortical surface, and its association with cortical thickness was not significant. Previous literature found similar differences with stronger associations for pWMH with cortical thickness than dWMH, with pronounced effects in the

frontal lobe[70], supporting our findings. Also, the pWMH connectivity profile overlaps with the mean tracts length examined in previous studies[196], indicating higher connectivity in cortical regions which receive longer fiber tracts. Second, it was denoted that the two lesion types differ in their genetic correlations[203] and clinical manifestation. pWMH are mainly associated with global brain atrophy[69,204] and cognitive deterioration including general cognitive decline[205], lower mental processing speed[206–208] and development of Alzheimer's Disease[52]. In contrast, dWMH are not associated with cognitive deterioration[205,207] but increase the risk of vascular dementia[209] and depression[51,52]. This differentiation suggests that pWMH and dWMH do not share the same pathophysiology[210]. Alterations in short penetrating microvessels near large arterial blood vessels are suggested causal of pWMH while dWMH occur in white matter where long microvessels with lower blood pressure are located, and probably develop due to hypertension and subsequent hypoperfusion[211,212]. Third, the prevalence of pWMH was in the HCHS significantly higher than that of dWMH, covering 83% of the overall WMH volume Similar distributions can be found in other studies with populations from Australia[195], the Netherlands[206], France[69] and the United States[213]. The discrepancy in the distribution explains why pWMH had a connectivity profile to the cortex very similar to the connectivity profile of the overall WMH, as a large percentage of overall WMH represents pWMH.

As the anatomical microstructure also affects DWI parameters, such that densely packed white matter regions tend to have a higher microstructural integrity, we had to make sure that the findings of study 2 were independent of the anatomical location of WMH. With supplementary analysis differentiating between WMH in the periventricular and deep white matter, our objective was to investigate the FW in the WMH penumbra independent of the anatomical location of the WMH. The results showed that both the WMH in the periventricular and deep white matter have a higher FW in the surrounding tissue, showing that the alterations in FW are independent of the anatomical location.

1.5.1.3. Final remarks

Some additional points need to be considered when interpreting the results of part A. First, despite the usage of advanced segmentation methods for the quantification of WMH, the presence of additional pathologies such as lacunes and enlarged perivascular spaces cannot be excluded. These imaging markers of CSVD are also quite prevalent in population–based cohorts and have a strong correlation with WMH[214] and cortical atrophy[215,216]. Generally, the analyses of such pathologies are very limited because of lacking automated quantification methods. Currently, manual segmentations or visual rating approaches are applied to fill this gap, but both methods are very time–consuming and not feasible for large datasets. This is a major limitation in the field especially because some studies suggest that enlarged perivascular spaces contribute to cognitive deterioration independent of other CSVD imaging markers[217]. Future advancements in the quantification of these imaging markers will help to paint a more complete picture of CSVD.

1.5.2. Nutrition–associated neurodegeneration and possible mechanisms

Both study 1 and 2 were strongly focusing on MRI analysis in CSVD. With study 3 and 4, we applied the imaging methods in a more clinical context. In two separate analyses, we discovered that maintaining a healthy diet and consuming 1–4 cups of coffee per day was associated with improved brain microstructure. It is important to note that the effects of nutrition on the brain are mainly indirect, mediated by cardiovascular risk, as healthy nutrition was associated with reduced metabolic syndrome in study 3. All subcomponents of metabolic syndrome are significant contributors to neurodegenerative disorders and cognitive deterioration. In the following paragraph, I will provide an in–depth discussion of the mechanisms underlying the adverse effects of unhealthy nutrition on the components of metabolic syndrome, and how these further lead to neurodegeneration.

1.5.2.1. Overweight and obesity

The brain (especially the hypothalamus) plays an important role in the maintenance of energy homeostasis, appetite and body weight by processing multiple signals from the body, including the hormone leptin secreted by adipose tissue when energy requirements are met[218,219]. Leptin signals the brain to promote satiety and reducing food intake. However, unhealthy nutrients such as saturated fatty acids and added sugars can promote the accumulation of adipose tissue, leading to increased production of leptin and ultimately, leptin resistance. Various mechanisms have been proposed to explain the development of leptin resistance, including defective transport of leptin across the blood–brain barrier and impaired leptin signaling in the brain[219,220]. Prolonged exposure to high levels of leptin can damage the blood–brain barrier, resulting in reduced leptin transport into the brain[219,220]. Another mechanism is that the brain becomes resistant to prolonged leptin exposure[219,220]. Regardless of which pathway is involved, leptin resistance ultimately causes a distorted regulation of appetite, leading to overconsumption and obesity[218,220]. Studies have shown that regions important for behavioral feeding control exhibit reduced structural integrity[221] and lower gray matter density[222] in overweight individuals. These findings further highlight the importance of leptin signaling in regulating appetite and body weight.

Several studies have shown that overweight is strongly associated with several health issues, including alterations in brain structure and cognitive function. In the United States, overweight was associated with 14% of all deaths and 11% of disability–adjusted life years[223]. Between 1990 and 2010, the disability–adjusted life years due to overweight increased by 45%, indicating a rise in obesity–associated health problems[223]. Research also suggested that higher body weight is associated with various adverse effects on brain health, including WMH[53], reduced white matter integrity[224], lower cerebral blood flow[125], increased brain atrophy[225], lower cortical thickness[225], and decreased performance on several cognitive tasks[225,226]. Obesity alone doubled the risk of developing dementia[227], highlight the need for weight reduction in the general population. Adapting a healthier eating pattern, changing the pattern of food consumption over a day, and reducing the portion size are different aspects of nutrition for successful weight reduction[228]. Lifestyle interventions targeting weight

loss can have additional positive effects on brain health. Individuals with diabetes mellitus and overweight who followed a lifestyle intervention for ten years had 28% smaller WMH volume in the intervention group than the control group[229], suggesting that longitudinal weight loss can be successful in slowing neurodegeneration.

1.5.2.2. Type 2 diabetes mellitus

Maintaining controlled peripheral glucose levels and regulating glucose transport are crucial for proper brain function, as a constant and adequate glucose supply into the brain is essential for cognitive processes. Glucose is transported into the brain via glucose transporters located at the blood–brain barrier which operates at full capacity to facilitate glucose transportation[230]. However, a high intake of sugar can lead to insulin insensitivity and high blood glucose levels, which ultimately result in type 2 diabetes mellitus[231]. This condition can further promote neurodegeneration and cognitive decline. Patients with diabetes mellitus often exhibit greater atrophy[81,232], higher WMH volume[59] and lower white matter integrity[53,79,81,82], the latter was also supported in a large meta–analysis[83].

Although the underlying mechanisms are still not fully understood, several pathways were suggested to play a role in the development of structural brain alterations in diabetic patients. Among others, high plasma glucose can cause endothelial dysfunction and blood–brain barrier damage, oxidative stress, systemic and neuroinflammation[233]. Furthermore, insulin deficiency leads to hyperlipidemia and atherosclerosis, further promoting reduced cerebral blood flow and WMH[233]. In addition, studies congruently showed that diabetic individuals suffer from cognitive deterioration[234], which can be explained by the hippocampus, a brain region crucial for short–term memory which is especially vulnerable to the effects of insulin resistance and hypoglycemia[235,236]. In fact, hippocampal atrophy has been detected in people who have been diagnosed with diabetes mellitus for less than a decade[237]. Additionally, insulin resistance, another characteristic of diabetes mellitus, has been linked to several pathogenic features associated with Alzheimer's Disease[238]. The exact mechanisms of the proposed pathways are not fully understood yet but effective medication of diabetes mellitus can help in the alleviation of CSVD and cognitive deterioration[239]. Next to dietary interventions helpful in weight reduction, choosing plant fat over animal fat, whole grains, fiber, nuts, dairy products, and magnesium are important adaptations in the nutritional behavior to improve insulin sensitivity, reduce blood glucose levels and prevent the development of diabetes mellitus[240,241].

1.5.2.3. Hypertension

The cerebral autoregulation and the neurovascular unit ensure a constant blood supply to the brain, with the former being responsible for a stable blood flow despite varying blood pressure, and the latter responsible for the adequate blood supply to active brain regions[242]. Nutrient imbalances such as high sodium intake[243], red and processed meat consumption[244,245], high sugar intake[246] and alcohol consumption[247] can lead to alterations in blood pressure and blood supply to the brain. A pro–inflammatory diet increased the risk of developing hypertension over a time period of twelve years by 24%[248,249].

Hypertension is considered a major contributor to the development of CSVD[47,48]. Increased blood pressure, i.e., hypertension, is causal for loss of smooth muscle cells, narrowing of the lumen and thickening of the vessel wall[250]. Once hypertension is developed, both the cerebral autoregulation and the neurovascular unit do not work properly, leading to a distorted blood supply (i.e., hypoperfusion) of the brain[251]. Decreased cerebral blood flow can easily cause lesions in the white matter[252]. Arteriolosclerosis, one of two major types of CSVD, is characterized by thickening of arterioles, which is caused by arterial hypertension and therefore also known as "hypertensive small vessel disease"[253]. Longer duration of hypertension was found to be related to more severe WMH manifestations[200]. Detrimental neurological effects of hypertension are also measurable on the microstructural scale. In this thesis, hypertension was not significantly associated with free–water or FA–t in neither lesioned nor non–lesioned white matter (study 2), but previous literature revealed that blood pressure was significantly associated with increased free–water and reduced microstructural integrity in the white matter, mediated by aortic stiffness[106].

Effective treatment of hypertension is essential in reducing the manifestation of WMH in hypertensive individuals, for example in the form of anti–hypertensive medication and lifestyle interventions. Studies have shown that anti–hypertensive medication and a controlled blood pressure significantly decrease the development of WMH in hypertensive individuals[201]. In addition, lifestyle interventions can successfully reduce blood pressure as well. The DASH diet, a dietary pattern which was specifically developed to reduce blood pressure, is similarly effective as anti–hypertensive medication[140], and reduces blood pressure as early as after two weeks of intervention[140]. Especially a reduction in salt intake is crucial for blood pressure control, as a low–salt DASH diet was superior in reducing blood pressure than the "normal" DASH diet[254].

1.5.2.4. Final remarks

In this thesis, we focused on brain structure in the context of nutrition. It is essential to acknowledge that multiple factors can impact our nutritional behavior and mediate the impact of nutrition. For instance, physical activity has been demonstrated to further enhance overall health. Previous clinical trials have demonstrated that physically active participants who also follow a healthy diet have better cognitive function[255,256], lower blood pressure[256], lower amyloid beta levels in the brain[257] and lower incidence of Alzheimer's Disease[258] compared to participants who were physically active *or* followed a healthy diet. Therefore, while our study found a correlation between an unhealthy diet and microstructural brain alterations and lower cognitive performance in a population–based cohort, future research should explore the impact of physical activity and healthy eating on patient cohorts to achieve long–term success in preventing neurodegenerative disorders.

Another important factor to consider is the socioeconomic status. We could not control for income's effect in our study due to the high percentage of missing values in the income variable, and consequently only added the educational level as covariate. However, previous research has shown that income can modify the relationship between nutrition and cognitive function[259]. Specifically, the

MIND diet was found to have a positive impact on cognitive performance only in individuals with higher incomes, while the opposite was observed in the low–income group[259]. This finding suggests food decisions can be influenced by socioeconomic factors. For example, individuals with higher incomes may have better access to less affordable healthy foods (such as nuts, berries, olive oil) and foods of higher quality. Therefore, future research should consider the role of socioeconomic factors in the relationship between nutrition and cognitive function.

1.6. Conclusion

In summary, this thesis aimed to enhance our understanding of the relationship between different imaging markers of CSVD and the potential impact of healthy nutrition and regular coffee consumption on brain health and cognition. Our studies revealed significant associations between WMH and cortical atrophy (study 1), as well as increased free–water content in the surrounding tissue (study 2). These findings were observed in a cohort with relatively low degree of CSVD manifestation[33,34], and the effects may be even more significant in more severely affected populations. Future research is necessary for the validation in other cohorts, including those with genetic forms of CSVD (for example CADASIL), older participants, and in cohorts with a higher diversity. This only mildly affected cohort had a large variance in the microstructural brain health, attributable to age–related alterations and differences in lifestyle. A replication of these analyses in cohorts with a higher prevalence of CSVD might allow a better discrimination between age-associated and disease-associated brain alterations.

Furthermore, our findings from study 3 and 4 suggest that vascular brain health, as measured by the novel imaging marker PSMD, is associated with healthy nutrition and regular coffee consumption. Lifestyle factors, including nutrition, can therefore play a crucial role in the preservation of brain structure. However, a large analysis revealed that the average consumption in nearly all of the considered 195 countries was far below optimal for healthy foods and a far beyond optimal for unhealthy foods[260]. In Europe alone, thirteen countries are considered to follow a Western diet, characterized by a high consumption of ultra–processed foods which are often rich in simple sugar, salt, saturated fatty acids and cholesterol[261]. As a consequence, unhealthy food consumption accounts for a significant proportion of deaths and disability adjusted life years and reduces life quality and life expectancy of billions of people[260]. Therefore, the promotion and implementation of healthy dietary habits is crucial for preventing major chronic diseases affecting the cardiovascular and neurological system. Recognizing that nutritional behavior is within the control and responsibility of each individual person is vital. However, it is important to acknowledge that maintain a healthy nutrition is becoming increasingly challenging due to the current trends towards more (ultra-)processed foods. Addressing this issue should not solely be an individual responsibility but also a shared task for society and governmental institutions. Creating an environment that promotes and supports healthy nutrition is crucial in enabling individuals to make informed choices and improve global health.

2. List of abbreviations

β	(standardized) coefficient
c/d	cup(s) per day
CADASIL	Cerebral Autosomal Dominant Arteriopathy with Subcortical Ischemic strokes and Leukoencephalopathy
CERAD–NP/Plus	Consortium to Establish a Registry for Alzheimer's Disease Neuropsychological Assessment Battery / Extended Version
CI	confidence interval
cm	centimeter
CSVD	cerebral small vessel disease
DASH	Dietary Approaches to Stop Hypertension
DTI	diffusion tensor imaging
DWI	diffusion weighted imaging
dWMH	white matter hyperintensities in the deep white matter
FA	fractional anisotropy
FA–t	free–water corrected fractional anisotropy
FFQ	food frequency questionnaire
FLAIR	fluid–attenuated inversion recovery
FW	free–water
HCHS	Hamburg City Health Study
IPR	in–plane resolution
IQR	interquartile range
ISCED	International Standard Classification of Education
MD	mean diffusivity
mg/dl	milligrams per deciliter
MIND	Mediterranean–DASH Intervention for Neurodegenerative Delay
ml	milliliter
mm	millimeter
mmHg	millimeter of mercury
MRI	magnetic resonance imaging
ms	millisecond(s)
NAWM	normal–appearing white matter
p	p–value
PSMD	peak width of skeletonized mean diffusivity
pWMH	white matter hyperintensities in the periventricular white matter
ROI(s)	region(s) of interest
SEM	structural equation model
ST	slice time
TE	echo time
TR	repetition time
WMH	white matter hyperintensities

3. References

1. Baumgart M, Snyder HM, Carrillo MC, Fazio S, Kim H, Johns H. Summary of the evidence on modifiable risk factors for cognitive decline and dementia: A population-based perspective. *Alzheimers Dement.* 2015;11(6):718-726. doi:10.1016/j.jalz.2015.05.016

2. Kouvari M, D'Cunha NM, Travica N, et al. Metabolic Syndrome, Cognitive Impairment and the Role of Diet: A Narrative Review. *Nutrients.* 2022;14(2):333. doi:10.3390/nu14020333

3. Mayer C, Frey BM, Schlemm E, et al. Linking cortical atrophy to white matter hyperintensities of presumed vascular origin. *J Cereb Blood Flow Metab.* Published online December 2020:0271678X2097417. doi:10.1177/0271678X20974170

4. Mayer C, Naegele FL, Petersen M, et al. Free-water diffusion MRI detects structural alterations surrounding white matter hyperintensities in the early stage of cerebral small vessel disease. *J Cereb Blood Flow Metab.* Published online April 11, 2022:0271678X2210935. doi:10.1177/0271678X221093579

5. Mayer C, Nägele FL, Petersen M, et al. Association between Coffee Consumption and Brain MRI Parameters in the Hamburg City Health Study. *Nutrients.* 2023;15(3):674. doi:10.3390/nu15030674

6. Jagodzinski A, Johansen C, Koch-Gromus U, et al. Rationale and Design of the Hamburg City Health Study. *Eur J Epidemiol.* 2020;35(2):169-181. doi:10.1007/s10654-019-00577-4

7. UNESCO Institute for Statistics. *International Standard Classification of Education (ISCED) 2011.* UNESCO Institute for Statistics; 2012. doi:10.15220/978-92-9189-123-8-en

8. Alberti KGM, Zimmet P, Shaw J. The metabolic syndrome—a new worldwide definition. *The Lancet.* 2005;366(9491):1059-1062. doi:10.1016/S0140-6736(05)67402-8

9. Boeing H, Wahrendorf J, Becker N. EPIC-Germany – A Source for Studies into Diet and Risk of Chronic Diseases. *Ann Nutr Metab.* 1999;43(4):195-204. doi:10.1159/000012786

10. Hebestreit K, Yahiaoui-Doktor M, Engel C, et al. Validation of the German version of the Mediterranean Diet Adherence Screener (MEDAS) questionnaire. *BMC Cancer.* 2017;17(1):341. doi:10.1186/s12885-017-3337-y

11. Folsom AR, Parker ED, Harnack LJ. Degree of concordance with DASH diet guidelines and incidence of hypertension and fatal cardiovascular disease. *Am J Hypertens.* 2007;20(3):225-232. doi:10.1016/j.amjhyper.2006.09.003

12. Morris MC, Tangney CC, Wang Y, et al. MIND diet slows cognitive decline with aging. *Alzheimers Dement*. 2015;11(9):1015-1022. doi:10.1016/j.jalz.2015.04.011

13. Ehrensperger MM, Berres M, Taylor KI, Monsch AU. Early detection of Alzheimer's disease with a total score of the German CERAD. *J Int Neuropsychol Soc*. 2010;16(5):910-920. doi:10.1017/S1355617710000822

14. Folstein MF, Folstein SE, McHugh PR. "Mini-mental state." *J Psychiatr Res*. 1975;12(3):189-198. doi:10.1016/0022-3956(75)90026-6

15. Schmid NS, Ehrensperger MM, Berres M, Beck IR, Monsch AU. The Extension of the German CERAD Neuropsychological Assessment Battery with Tests Assessing Subcortical, Executive and Frontal Functions Improves Accuracy in Dementia Diagnosis. *Dement Geriatr Cogn Disord Extra*. 2014;4(2):322-334. doi:10.1159/000357774

16. Lehrl S. *Manual zum MWT-B: Mehrfachwahl-Wortschatz-Intelligenztest*. 6. Auflage. Spitta GmbH; 2018.

17. D'Agostino RB, Vasan RS, Pencina MJ, et al. General Cardiovascular Risk Profile for Use in Primary Care. *Circulation*. 2008;117(6):743-753. doi:10.1161/CIRCULATIONAHA.107.699579

18. Esteban O, Birman D, Schaer M, Koyejo OO, Poldrack RA, Gorgolewski KJ. MRIQC: Advancing the automatic prediction of image quality in MRI from unseen sites. Bernhardt BC, ed. *PLOS ONE*. 2017;12(9):e0184661. doi:10.1371/journal.pone.0184661

19. Fischl B, Dale AM. Measuring the thickness of the human cerebral cortex from magnetic resonance images. *Proc Natl Acad Sci*. 2000;97(20):11050-11055. doi:10.1073/pnas.200033797

20. Cieslak M, Cook PA, He X, et al. QSIPrep: an integrative platform for preprocessing and reconstructing diffusion MRI data. *Nat Methods*. 2021;18(7):775-778. doi:10.1038/s41592-021-01185-5

21. Petersen M, Nägele FL, Mayer C, et al. *Brain Imaging and Neuropsychological Assessment of Individuals Recovered from a Mild to Moderate SARS-CoV-2 Infection*. Infectious Diseases (except HIV/AIDS); 2022. doi:10.1101/2022.07.08.22277420

22. Gorgolewski K, Burns CD, Madison C, et al. Nipype: A Flexible, Lightweight and Extensible Neuroimaging Data Processing Framework in Python. *Front Neuroinformatics*. 2011;5. doi:10.3389/fninf.2011.00013

23. Tustison NJ, Avants BB, Cook PA, et al. N4ITK: Improved N3 Bias Correction. *IEEE Trans Med Imaging*. 2010;29(6):1310-1320. doi:10.1109/TMI.2010.2046908

24. Veraart J, Novikov DS, Christiaens D, Ades-aron B, Sijbers J, Fieremans E. Denoising of diffusion MRI using random matrix theory. *NeuroImage*. 2016;142:394-406. doi:10.1016/j.neuroimage.2016.08.016

25. Kellner E, Dhital B, Kiselev VG, Reisert M. Gibbs-ringing artifact removal based on local subvoxel-shifts: Gibbs-Ringing Artifact Removal. *Magn Reson Med*. 2016;76(5):1574-1581. doi:10.1002/mrm.26054

26. Andersson JLR, Sotiropoulos SN. An integrated approach to correction for off-resonance effects and subject movement in diffusion MR imaging. *NeuroImage*. 2016;125:1063-1078. doi:10.1016/j.neuroimage.2015.10.019

27. Esteban O, Markiewicz CJ, Blair RW, et al. fMRIPrep: a robust preprocessing pipeline for functional MRI. *Nat Methods*. 2019;16(1):111-116. doi:10.1038/s41592-018-0235-4

28. Fischl B, Salat DH, Busa E, et al. Whole Brain Segmentation: automated labeling of neuroanatomical structures in the human brain. *Neuron*. 2002;33(3):341-355. doi:10.1016/S0896-6273(02)00569-X

29. Fan L, Li H, Zhuo J, et al. The Human Brainnetome Atlas: A New Brain Atlas Based on Connectional Architecture. *Cereb Cortex*. 2016;26(8):3508-3526. doi:10.1093/cercor/bhw157

30. Griffanti L, Zamboni G, Khan A, et al. BIANCA (Brain Intensity AbNormality Classification Algorithm): A new tool for automated segmentation of white matter hyperintensities. *NeuroImage*. 2016;141:191-205. doi:10.1016/j.neuroimage.2016.07.018

31. Griffanti L, Jenkinson M, Suri S, et al. Classification and characterization of periventricular and deep white matter hyperintensities on MRI: A study in older adults. *NeuroImage*. 2018;170:174-181. doi:10.1016/j.neuroimage.2017.03.024

32. Petersen M, Frey BM, Schlemm E, et al. Network Localisation of White Matter Damage in Cerebral Small Vessel Disease. *Sci Rep*. 2020;10(1):9210. doi:10.1038/s41598-020-66013-w

33. de Laat KF, Tuladhar AM, van Norden AGW, Norris DG, Zwiers MP, de Leeuw FE. Loss of white matter integrity is associated with gait disorders in cerebral small vessel disease. *Brain J Neurol*. 2011;134(Pt 1):73-83. doi:10.1093/brain/awq343

34. Tuladhar AM, van Dijk E, Zwiers MP, et al. Structural network connectivity and cognition in cerebral small vessel disease. *Hum Brain Mapp*. 2016;37(1):300-310. doi:10.1002/hbm.23032

35. Wu X, Ge X, Du J, et al. Characterizing the Penumbras of White Matter Hyperintensities and Their Associations With Cognitive Function in Patients With Subcortical Vascular Mild Cognitive Impairment. *Front Neurol.* 2019;10. doi:10.3389/fneur.2019.00348

36. Promjunyakul N, Lahna D, Kaye JA, et al. Characterizing the white matter hyperintensity penumbra with cerebral blood flow measures. *NeuroImage Clin.* 2015;8:224-229. doi:10.1016/j.nicl.2015.04.012

37. Sundaresan V, Zamboni G, Le Heron C, et al. *Automated Lesion Segmentation with BIANCA: Impact of Population-Level Features, Classification Algorithm and Locally Adaptive Thresholding.* Neuroscience; 2018. doi:10.1101/437608

38. Smith RE, Tournier JD, Calamante F, Connelly A. Anatomically-constrained tractography: Improved diffusion MRI streamlines tractography through effective use of anatomical information. *NeuroImage.* 2012;62(3):1924-1938. doi:10.1016/j.neuroimage.2012.06.005

39. Tournier JD, Calamante F, Connelly A. Improved probabilistic streamlines tractography by 2nd order integration over fibre orientation distributions. *Proc Int Soc Magn Reson Med.* Published online 2010:1670.

40. Tournier JD, Smith RE, Raffelt D, et al. MRtrix3: A fast, flexible and open software framework for medical image processing and visualisation. *bioRxiv.* Published online February 2019:551739. doi:10.1101/551739

41. Smith RE, Tournier JD, Calamante F, Connelly A. SIFT2: Enabling dense quantitative assessment of brain white matter connectivity using streamlines tractography. *NeuroImage.* 2015;119:338-351. doi:10.1016/j.neuroimage.2015.06.092

42. Baykara E, Gesierich B, Adam R, et al. A Novel Imaging Marker for Small Vessel Disease Based on Skeletonization of White Matter Tracts and Diffusion Histograms: Novel SVD Imaging Marker. *Ann Neurol.* 2016;80(4):581-592. doi:10.1002/ana.24758

43. Basser PJ, Mattiello J, LeBihan D. MR diffusion tensor spectroscopy and imaging. *Biophys J.* 1994;66(1):259-267. doi:10.1016/S0006-3495(94)80775-1

44. Basser PJ, Pierpaoli C. Microstructural and Physiological Features of Tissues Elucidated by Quantitative-Diffusion-Tensor MRI. *J Magn Reson B.* 1996;111(3):209-219. doi:10.1006/jmrb.1996.0086

45. Avants B, Tustison NJ, Song G. Advanced Normalization Tools: V1.0. *Insight J.* Published online July 29, 2009. doi:10.54294/uvnhin

46. Pasternak O, Sochen N, Gur Y, Intrator N, Assaf Y. Free water elimination and mapping from diffusion MRI. *Magn Reson Med.* 2009;62(3):717-730. doi:10.1002/mrm.22055

47. Wardlaw JM, Smith C, Dichgans M. Small vessel disease: mechanisms and clinical implications. *Lancet Neurol.* 2019;18(7):684-696. doi:10.1016/S1474-4422(19)30079-1

48. Wardlaw JM, Smith C, Dichgans M. Mechanisms of sporadic cerebral small vessel disease: insights from neuroimaging. *Lancet Neurol.* 2013;12(5):483-497. doi:10.1016/S1474-4422(13)70060-7

49. Debette S, Schilling S, Duperron MG, Larsson SC, Markus HS. Clinical Significance of Magnetic Resonance Imaging Markers of Vascular Brain Injury: A Systematic Review and Meta-analysis. *JAMA Neurol.* 2019;76(1):81. doi:10.1001/jamaneurol.2018.3122

50. Haley AP, Hoth KF, Gunstad J, et al. Subjective cognitive complaints relate to white matter hyperintensities and future cognitive decline in patients with cardiovascular disease. *Am J Geriatr Psychiatry Off J Am Assoc Geriatr Psychiatry.* 2009;17(11):976-985. doi:10.1097/JGP.0b013e3181b208ef

51. de Groot JC, de Leeuw FE, Oudkerk M, Hofman A, Jolles J, Breteler MMB. Cerebral White Matter Lesions and Depressive Symptoms in Elderly Adults. *Arch Gen Psychiatry.* 2000;57(11):1071. doi:10.1001/archpsyc.57.11.1071

52. O'Brien J, Desmond P, Ames D, Schweitzer I, Harrigan S, Tress B. A Magnetic Resonance Imaging Study of White Matter Lesions in Depression and Alzheimer's Disease. *Br J Psychiatry.* 1996;168(4):477-485. doi:10.1192/bjp.168.4.477

53. Taylor-Bateman V, Gill D, Georgakis MK, et al. Cardiovascular Risk Factors and MRI Markers of Cerebral Small Vessel Disease: A Mendelian Randomization Study. *Neurology.* 2022;98(4):e343-e351. doi:10.1212/WNL.0000000000013120

54. Power MC, Deal JA, Sharrett AR, et al. Smoking and white matter hyperintensity progression: The ARIC-MRI Study. *Neurology.* 2015;84(8):841-848. doi:10.1212/WNL.0000000000001283

55. Gao Y, Li D, Lin J, et al. Cerebral small vessel disease: Pathological mechanisms and potential therapeutic targets. *Front Aging Neurosci.* 2022;14:961661. doi:10.3389/fnagi.2022.961661

56. Wardlaw JM, Smith EE, Biessels GJ, et al. Neuroimaging standards for research into small vessel disease and its contribution to ageing and neurodegeneration. *Lancet Neurol.* 2013;12(8):822-838. doi:10.1016/S1474-4422(13)70124-8

57. Bown CW, Carare RO, Schrag MS, Jefferson AL. Physiology and Clinical Relevance of Enlarged Perivascular Spaces in the Aging Brain. *Neurology.* 2022;98(3):107-117. doi:10.1212/WNL.0000000000013077

58. Jäger HR, Gomez-Anson B. Small Vessel Disease: Imaging and Clinical Aspects. In: Barkhof F, Jäger HR, Thurnher MM, Rovira À, eds. *Clinical Neuroradiology.* Springer International Publishing; 2019:167-201. doi:10.1007/978-3-319-68536-6_22

59. Zhuang FJ, Chen Y, He WB, Cai ZY. Prevalence of white matter hyperintensities increases with age. *Neural Regen Res.* 2018;13(12):2141. doi:10.4103/1673-5374.241465

60. Cai M, Jacob MA, van Loenen MR, et al. Determinants and Temporal Dynamics of Cerebral Small Vessel Disease: 14-Year Follow-Up. *Stroke.* Published online May 4, 2022:10.1161/STROKEAHA.121.038099. doi:10.1161/STROKEAHA.121.038099

61. Launer LJ, Berger K, Breteler MMB, et al. Regional variability in the prevalence of cerebral white matter lesions: An MRI study in 9 European countries (CASCADE). *Neuroepidemiology.* 2005;26(1):23-29. doi:10.1159/000089233

62. Inzitari D, Pracucci G, Poggesi A, et al. Changes in white matter as determinant of global functional decline in older independent outpatients: three year follow-up of LADIS (leukoaraiosis and disability) study cohort. *BMJ.* 2009;339(jul06 1):b2477-b2477. doi:10.1136/bmj.b2477

63. Debette S, Markus HS. The clinical importance of white matter hyperintensities on brain magnetic resonance imaging: Systematic review and meta-analysis. *BMJ Online.* 2010;341(7767):288. doi:10.1136/bmj.c3666

64. Ritchie SJ, Dickie DA, Cox SR, et al. Brain volumetric changes and cognitive ageing during the eighth decade of life. *Hum Brain Mapp.* 2015;36(12):4910-4925. doi:10.1002/hbm.22959

65. Kloppenborg RP, Nederkoorn PJ, Geerlings MI, van den Berg E. Presence and progression of white matter hyperintensities and cognition: A meta-analysis. *Neurology.* 2014;82(23):2127-2138. doi:10.1212/WNL.0000000000000505

66. Taylor WD, Steffens DC, MacFall JR, et al. White Matter Hyperintensity Progression and Late-Life Depression Outcomes. *Arch Gen Psychiatry.* 2003;60(11):1090. doi:10.1001/archpsyc.60.11.1090

67. Inzitari D. Risk of Rapid Global Functional Decline in Elderly Patients With Severe Cerebral Age-Related White Matter Changes. *Arch Intern Med.* 2007;167(1):81. doi:10.1001/archinte.167.1.81

68. Silbert LC, Nelson C, Howieson DB, Moore MM, Kaye JA. Impact of white matter hyperintensity volume progression on rate of cognitive and motor decline. *Neurology*. 2008;71(2):108-113. doi:10.1212/01.wnl.0000316799.86917.37

69. Godin O, Maillard P, Crivello F, et al. Association of White-Matter Lesions with Brain Atrophy Markers: The Three-City Dijon MRI Study. *Cerebrovasc Dis*. 2009;28(2):177-184. doi:10.1159/000226117

70. Seo SW, Lee JM, Im K, et al. Cortical thinning related to periventricular and deep white matter hyperintensities. *Neurobiol Aging*. 2012;33(7):1156-1167.e1. doi:10.1016/j.neurobiolaging.2010.12.003

71. Ghaznawi R, Geerlings MI, Jaarsma-Coes MG, et al. The association between lacunes and white matter hyperintensity features on MRI: The SMART-MR study. *J Cereb Blood Flow Metab*. 2019;39(12):2486-2496. doi:10.1177/0271678X18800463

72. Minett TSC, Dean JL, Firbank M, English P, O'Brien JT. Subjective memory complaints, white-matter lesions, depressive symptoms, and cognition in elderly patients. *Am J Geriatr Psychiatry Off J Am Assoc Geriatr Psychiatry*. 2005;13(8):665-671. doi:10.1176/appi.ajgp.13.8.665

73. Dhana A, DeCarli C, Dhana K, et al. Association of Subjective Memory Complaints With White Matter Hyperintensities and Cognitive Decline Among Older Adults in Chicago, Illinois. *JAMA Netw Open*. 2022;5(4):e227512. doi:10.1001/jamanetworkopen.2022.7512

74. Stewart R, Dufouil C, Godin O, et al. Neuroimaging correlates of subjective memory deficits in a community population. *Neurology*. 2008;70(18):1601-1607. doi:10.1212/01.wnl.0000310982.99438.54

75. Beaulieu C. The Biological Basis of Diffusion Anisotropy. In: *Diffusion MRI*. Elsevier; 2014:155-183. doi:10.1016/B978-0-12-396460-1.00008-1

76. Nucifora PGP, Verma R, Lee SK, Melhem ER. Diffusion-Tensor MR Imaging and Tractography: Exploring Brain Microstructure and Connectivity. *Radiology*. 2007;245(2):367-384. doi:10.1148/radiol.2452060445

77. Chad JA, Pasternak O, Salat DH, Chen JJ. Re-examining age-related differences in white matter microstructure with free-water corrected diffusion tensor imaging. *Neurobiol Aging*. 2018;71:161-170. doi:10.1016/j.neurobiolaging.2018.07.018

78. Sexton CE, Walhovd KB, Storsve AB, et al. Accelerated Changes in White Matter Microstructure during Aging: A Longitudinal Diffusion Tensor Imaging Study. *J Neurosci*. 2014;34(46):15425-15436. doi:10.1523/JNEUROSCI.0203-14.2014

79. de Groot M, Ikram MA, Akoudad S, et al. Tract-specific white matter degeneration in aging: The Rotterdam Study. *Alzheimers Dement*. 2015;11(3):321-330. doi:10.1016/j.jalz.2014.06.011

80. Gons RAR, van Oudheusden LJB, de Laat KF, et al. Hypertension is Related to the Microstructure of the Corpus Callosum: The RUN DMC Study. de la Torre J, ed. *J Alzheimers Dis*. 2012;32(3):623-631. doi:10.3233/JAD-2012-121006

81. Falvey CM, Rosano C, Simonsick EM, et al. Macro- and Microstructural Magnetic Resonance Imaging Indices Associated With Diabetes Among Community-Dwelling Older Adults. *Diabetes Care*. 2013;36(3):677-682. doi:10.2337/dc12-0814

82. Hsu JL, Chen YL, Leu JG, et al. Microstructural white matter abnormalities in type 2 diabetes mellitus: A diffusion tensor imaging study. *NeuroImage*. 2012;59(2):1098-1105. doi:10.1016/j.neuroimage.2011.09.041

83. Huang L, Zhang Q, Tang T, et al. Abnormalities of Brain White Matter in Type 2 Diabetes Mellitus: A Meta-Analysis of Diffusion Tensor Imaging. *Front Aging Neurosci*. 2021;13:693890. doi:10.3389/fnagi.2021.693890

84. Wersching H, Duning T, Lohmann H, et al. Serum C-reactive protein is linked to cerebral microstructural integrity and cognitive function. *Neurology*. 2010;74(13):1022-1029. doi:10.1212/WNL.0b013e3181d7b45b

85. Walker KA, Power MC, Hoogeveen RC, et al. Midlife systemic inflammation, late-life white matter integrity, and cerebral small vessel disease the atherosclerosis risk in communities study. *Stroke*. 2017;48(12):3196-3202. doi:10.1161/STROKEAHA.117.018675

86. Sedaghat S, Cremers LGM, de Groot M, et al. Kidney function and microstructural integrity of brain white matter. *Neurology*. 2015;85(2):154-161. doi:10.1212/WNL.0000000000001741

87. Li XY, Tang ZC, Sun Y, Tian J, Liu ZY, Han Y. White matter degeneration in subjective cognitive decline: a diffusion tensor imaging study. *Oncotarget*. 2016;7(34):54405-54414. doi:10.18632/oncotarget.10091

88. Bergamino M, Walsh RR, Stokes AM. Free-water diffusion tensor imaging improves the accuracy and sensitivity of white matter analysis in Alzheimer's disease. *Sci Rep*. 2021;11(1):6990. doi:10.1038/s41598-021-86505-7

89. Ji F, Pasternak O, Liu S, et al. Distinct white matter microstructural abnormalities and extracellular water increases relate to cognitive impairment in Alzheimer's disease with and without cerebrovascular disease. *Alzheimers Res Ther*. 2017;9(1):63. doi:10.1186/s13195-017-0292-4

90. Collij LE, Ingala S, Top H, et al. White matter microstructure disruption in early stage amyloid pathology. *Alzheimers Dement Diagn Assess Dis Monit.* 2021;13(1). doi:10.1002/dad2.12124

91. Jiang J, Zhao YJ, Hu XY, et al. Microstructural brain abnormalities in medication-free patients with major depressive disorder: a systematic review and meta-analysis of diffusion tensor imaging. *J Psychiatry Neurosci.* 2017;42(3):150-163. doi:10.1503/jpn.150341

92. Abe O, Yamasue H, Kasai K, et al. Voxel-based analyses of gray/white matter volume and diffusion tensor data in major depression. *Psychiatry Res Neuroimaging.* 2010;181(1):64-70. doi:10.1016/j.pscychresns.2009.07.007

93. Sedaghat S, Cremers LGM, de Groot M, et al. Lower microstructural integrity of brain white matter is related to higher mortality. *Neurology.* 2016;87(9):927-934. doi:10.1212/WNL.0000000000003032

94. Evans TE, O'Sullivan MJ, de Groot M, et al. White Matter Microstructure Improves Stroke Risk Prediction in the General Population. *Stroke.* 2016;47(11):2756-2762. doi:10.1161/STROKEAHA.116.014651

95. Pelletier A, Barul C, Féart C, et al. Mediterranean diet and preserved brain structural connectivity in older subjects. *Alzheimers Dement.* 2015;11(9):1023-1031. doi:10.1016/j.jalz.2015.06.1888

96. Gu Y, Vorburger RS, Gazes Y, et al. White matter integrity as a mediator in the relationship between dietary nutrients and cognition in the elderly. *Ann Neurol.* 2016;79(6):1014-1025. doi:10.1002/ana.24674

97. Gons RAR, van Norden AGW, de Laat KF, et al. Cigarette smoking is associated with reduced microstructural integrity of cerebral white matter. *Brain.* 2011;134(7):2116-2124. doi:10.1093/brain/awr145

98. Gazdzinski S, Durazzo TC, Mon A, Yeh PH, Meyerhoff DJ. Cerebral white matter recovery in abstinent alcoholics—a multimodality magnetic resonance study. *Brain.* 2010;133(4):1043-1053. doi:10.1093/brain/awp343

99. Daviet R, Aydogan G, Jagannathan K, et al. Associations between alcohol consumption and gray and white matter volumes in the UK Biobank. *Nat Commun.* 2022;13(1):1175. doi:10.1038/s41467-022-28735-5

100. Tian Q, Erickson KI, Simonsick EM, et al. Physical Activity Predicts Microstructural Integrity in Memory-Related Networks in Very Old Adults. *J Gerontol A Biol Sci Med Sci.* 2014;69(10):1284-1290. doi:10.1093/gerona/glt287

101. Chen F, Erickson KI, Huang H, Chang Y. The association between physical fitness parameters and white matter microstructure in older adults: A diffusion tensor imaging study. *Psychophysiology.* 2020;57(5). doi:10.1111/psyp.13539

102. Unterberg AW, Stover J, Kress B, Kiening KL. Edema and brain trauma. *Neuroscience.* 2004;129(4):1019-1027. doi:10.1016/j.neuroscience.2004.06.046

103. Pierpaoli C, Jezzard P, Basser PJ, Barnett A, Di Chiro G. Diffusion tensor MR imaging of the human brain. *Radiology.* 1996;201(3):637-648. doi:10.1148/radiology.201.3.8939209

104. Maier-Hein KH, Westin CF, Shenton ME, et al. Widespread white matter degeneration preceding the onset of dementia. *Alzheimers Dement J Alzheimers Assoc.* 2015;11(5):485-493.e2. doi:10.1016/j.jalz.2014.04.518

105. Bergamino M, Pasternak O, Farmer M, Shenton ME, Paul Hamilton J. Applying a free-water correction to diffusion imaging data uncovers stress-related neural pathology in depression. *NeuroImage Clin.* 2016;10:336-342. doi:10.1016/j.nicl.2015.11.020

106. Maillard P, Mitchell GF, Himali JJ, et al. Aortic Stiffness, Increased White Matter Free Water, and Altered Microstructural Integrity. *Stroke.* 2017;48(6):1567-1573. doi:10.1161/STROKEAHA.116.016321

107. Oestreich LKL, Pasternak O, Shenton ME, et al. Abnormal white matter microstructure and increased extracellular free-water in the cingulum bundle associated with delusions in chronic schizophrenia. *NeuroImage Clin.* 2016;12:405-414. doi:10.1016/j.nicl.2016.08.004

108. Gullett JM, O'Shea A, Lamb DG, et al. The association of white matter free water with cognition in older adults. *NeuroImage.* 2020;219:117040. doi:10.1016/j.neuroimage.2020.117040

109. Duering M, Finsterwalder S, Baykara E, et al. Free water determines diffusion alterations and clinical status in cerebral small vessel disease. *Alzheimers Dement.* 2018;14(6):764-774. doi:10.1016/j.jalz.2017.12.007

110. Maillard P, Fletcher E, Singh B, et al. Cerebral white matter free water: A sensitive biomarker of cognition and function. *Neurology.* 2019;92(19):e2221-e2231. doi:10.1212/WNL.0000000000007449

111. Edde M, Theaud G, Rheault F, et al. Free water: A marker of age-related modifications of the cingulum white matter and its association with cognitive decline. *PloS One.* 2020;15(11):e0242696. doi:10.1371/journal.pone.0242696

112. Ofori E, DeKosky ST, Febo M, et al. Free-water imaging of the hippocampus is a sensitive marker of Alzheimer's disease. *NeuroImage Clin.* 2019;24:101985. doi:10.1016/j.nicl.2019.101985

113. Archer DB, Patten C, Coombes SA. Free-water and free-water corrected fractional anisotropy in primary and premotor corticospinal tracts in chronic stroke. *Hum Brain Mapp.* 2017;38(9):4546-4562. doi:10.1002/hbm.23681

114. Huang P, Zhang R, Jiaerken Y, et al. White Matter Free Water is a Composite Marker of Cerebral Small Vessel Degeneration. *Transl Stroke Res.* Published online February 2021. doi:10.1007/s12975-021-00899-0

115. Tuladhar AM, Reid AT, Shumskaya E, et al. Relationship Between White Matter Hyperintensities, Cortical Thickness, and Cognition. *Stroke.* 2015;46(2):425-432. doi:10.1161/STROKEAHA.114.007146

116. Kim SJ, Lee DK, Jang YK, et al. The Effects of Longitudinal White Matter Hyperintensity Change on Cognitive Decline and Cortical Thinning over Three Years. *J Clin Med.* 2020;9(8):2663. doi:10.3390/jcm9082663

117. Duering M, Righart R, Wollenweber FA, Zietemann V, Gesierich B, Dichgans M. Acute infarcts cause focal thinning in remote cortex via degeneration of connecting fiber tracts. *Neurology.* 2015;84(16):1685-1692. doi:10.1212/WNL.0000000000001502

118. Cheng B, Schulz R, Bönstrup M, et al. Structural Plasticity of Remote Cortical Brain Regions is Determined by Connectivity to the Primary Lesion in Subcortical Stroke. *J Cereb Blood Flow Metab.* 2015;35(9):1507-1514. doi:10.1038/jcbfm.2015.74

119. Cheng B, Dietzmann P, Schulz R, et al. Cortical atrophy and transcallosal diaschisis following isolated subcortical stroke. *J Cereb Blood Flow Metab.* 2020;40(3):611-621. doi:10.1177/0271678X19831583

120. Boutzoukas EM, O'Shea A, Albizu A, et al. Frontal White Matter Hyperintensities and Executive Functioning Performance in Older Adults. *Front Aging Neurosci.* 2021;13:672535. doi:10.3389/fnagi.2021.672535

121. Smith EE, Salat DH, Jeng J, et al. Correlations between MRI white matter lesion location and executive function and episodic memory. *Neurology.* 2011;76(17):1492-1499. doi:10.1212/WNL.0b013e318217e7c8

122. Maillard P, Fletcher E, Harvey D, et al. White Matter Hyperintensity Penumbra. *Stroke.* 2011;42(7):1917-1922. doi:10.1161/STROKEAHA.110.609768

123. Muñoz Maniega S, Valdés Hernández MC, Clayden JD, et al. White matter hyperintensities and normal-appearing white matter integrity in the aging brain. *Neurobiol Aging*. 2015;36(2):909-918. doi:10.1016/j.neurobiolaging.2014.07.048

124. Promjunyakul N, Lahna DL, Kaye JA, et al. Comparison of cerebral blood flow and structural penumbras in relation to white matter hyperintensities: A multi-modal magnetic resonance imaging study. *J Cereb Blood Flow Metab*. 2016;36(9):1528-1536. doi:10.1177/0271678X16651268

125. Nasrallah IM, Hsieh MK, Erus G, et al. White Matter Lesion Penumbra Shows Abnormalities on Structural and Physiologic MRIs in the Coronary Artery Risk Development in Young Adults Cohort. *Am J Neuroradiol*. 2019;40(8):1291-1298. doi:10.3174/ajnr.A6119

126. Wardlaw JM, Makin SJ, Valdés Hernández MC, et al. Blood-brain barrier failure as a core mechanism in cerebral small vessel disease and dementia: evidence from a cohort study. *Alzheimers Dement*. 2017;13(6):634-643. doi:10.1016/j.jalz.2016.09.006

127. Promjunyakul N on, Dodge HH, Lahna D, et al. Baseline NAWM structural integrity and CBF predict periventricular WMH expansion over time. *Neurology*. 2018;90(24):e2119-e2126. doi:10.1212/WNL.0000000000005684

128. de Groot M, Verhaaren BFJ, de Boer R, et al. Changes in Normal-Appearing White Matter Precede Development of White Matter Lesions. *Stroke*. 2013;44(4):1037-1042. doi:10.1161/STROKEAHA.112.680223

129. Maillard P, Carmichael O, Harvey D, et al. FLAIR and Diffusion MRI Signals Are Independent Predictors of White Matter Hyperintensities. *Am J Neuroradiol*. 2013;34(1):54-61. doi:10.3174/ajnr.A3146

130. van Leijsen EMC, Bergkamp MI, van Uden IWM, et al. Progression of White Matter Hyperintensities Preceded by Heterogeneous Decline of Microstructural Integrity. *Stroke*. 2018;49(6):1386-1393. doi:10.1161/STROKEAHA.118.020980

131. Khan W, Khlif MS, Mito R, Dhollander T, Brodtmann A. Investigating the microstructural properties of normal-appearing white matter (NAWM) preceding conversion to white matter hyperintensities (WMHs) in stroke survivors. *NeuroImage*. Published online February 2021:117839. doi:10.1016/j.neuroimage.2021.117839

132. Rydhög AS, Szczepankiewicz F, Wirestam R, et al. Separating blood and water: Perfusion and free water elimination from diffusion MRI in the human brain. *NeuroImage*. 2017;156:423-434. doi:10.1016/j.neuroimage.2017.04.023

133. Willett WC, Sacks F, Trichopoulou A, et al. Mediterranean diet pyramid: a cultural model for healthy eating. Intergovernmental Panel on Climate Change, ed. *Am J Clin Nutr*. 1995;61(6):1402S-1406S. doi:10.1093/ajcn/61.6.1402S

134. World Health Organization. *Risk Reduction of Cognitive Decline and Dementia: WHO Guidelines*. World Health Organization; 2019. Accessed January 4, 2023. https://apps.who.int/iris/handle/10665/312180

135. Sofi F, Abbate R, Gensini GF, Casini A. Accruing evidence on benefits of adherence to the Mediterranean diet on health: an updated systematic review and meta-analysis. *Am J Clin Nutr*. 2010;92(5):1189-1196. doi:10.3945/ajcn.2010.29673

136. Psaltopoulou T, Sergentanis TN, Panagiotakos DB, Sergentanis IN, Kosti R, Scarmeas N. Mediterranean diet, stroke, cognitive impairment, and depression: A meta-analysis. *Ann Neurol*. 2013;74(4):580-591. doi:10.1002/ana.23944

137. Bakaloudi DR, Chrysoula L, Kotzakioulafi E, Theodoridis X, Chourdakis M. Impact of the Level of Adherence to Mediterranean Diet on the Parameters of Metabolic Syndrome: A Systematic Review and Meta-Analysis of Observational Studies. *Nutrients*. 2021;13(5):1514. doi:10.3390/nu13051514

138. Singh B, Parsaik AK, Mielke MM, et al. Association of Mediterranean Diet with Mild Cognitive Impairment and Alzheimer's Disease: A Systematic Review and Meta-Analysis. *J Alzheimers Dis*. 2014;39(2):271-282. doi:10.3233/JAD-130830

139. McBean L, O'Reilly S. Diet quality interventions to prevent neurocognitive decline: a systematic review and meta-analysis. *Eur J Clin Nutr*. 2022;76(8):1060-1072. doi:10.1038/s41430-021-01032-y

140. Appel LJ, Moore TJ, Obarzanek E, et al. A Clinical Trial of the Effects of Dietary Patterns on Blood Pressure. *N Engl J Med*. 1997;336(16):1117-1124. doi:10.1056/NEJM199704173361601

141. Van Horn L, Carson JAS, Appel LJ, et al. Recommended Dietary Pattern to Achieve Adherence to the American Heart Association/American College of Cardiology (AHA/ACC) Guidelines: A Scientific Statement From the American Heart Association. *Circulation*. 2016;134(22). doi:10.1161/CIR.0000000000000462

142. Schwingshackl L, Hoffmann G. Diet Quality as Assessed by the Healthy Eating Index, the Alternate Healthy Eating Index, the Dietary Approaches to Stop Hypertension Score, and Health Outcomes: A Systematic Review and Meta-Analysis of Cohort Studies. *J Acad Nutr Diet*. 2015;115(5):780-800.e5. doi:10.1016/j.jand.2014.12.009

143. Soltani S, Arablou T, Jayedi A, Salehi-Abargouei A. Adherence to the dietary approaches to stop hypertension (DASH) diet in relation to all-cause and cause-specific mortality: a systematic review and dose-response meta-analysis of prospective cohort studies. *Nutr J*. 2020;19(1):37. doi:10.1186/s12937-020-00554-8

144. Schwingshackl L, Bogensberger B, Hoffmann G. Diet Quality as Assessed by the Healthy Eating Index, Alternate Healthy Eating Index, Dietary Approaches to Stop Hypertension Score, and Health Outcomes: An Updated Systematic Review and Meta-Analysis of Cohort Studies. *J Acad Nutr Diet*. 2018;118(1):74-100.e11. doi:10.1016/j.jand.2017.08.024

145. Salehi-Abargouei A, Maghsoudi Z, Shirani F, Azadbakht L. Effects of Dietary Approaches to Stop Hypertension (DASH)-style diet on fatal or nonfatal cardiovascular diseases—Incidence: A systematic review and meta-analysis on observational prospective studies. *Nutrition*. 2013;29(4):611-618. doi:10.1016/j.nut.2012.12.018

146. Filippou CD, Tsioufis CP, Thomopoulos CG, et al. Dietary Approaches to Stop Hypertension (DASH) Diet and Blood Pressure Reduction in Adults with and without Hypertension: A Systematic Review and Meta-Analysis of Randomized Controlled Trials. *Adv Nutr*. 2020;11(5):1150-1160. doi:10.1093/advances/nmaa041

147. Lari A, Sohouli MH, Fatahi S, et al. The effects of the Dietary Approaches to Stop Hypertension (DASH) diet on metabolic risk factors in patients with chronic disease: A systematic review and meta-analysis of randomized controlled trials. *Nutr Metab Cardiovasc Dis*. 2021;31(10):2766-2778. doi:10.1016/j.numecd.2021.05.030

148. Soltani S, Shirani F, Chitsazi MJ, Salehi-Abargouei A. The effect of dietary approaches to stop hypertension (DASH) diet on weight and body composition in adults: a systematic review and meta-analysis of randomized controlled clinical trials: Effect of DASH diet on weight and body composition. *Obes Rev*. 2016;17(5):442-454. doi:10.1111/obr.12391

149. Soltani S, Chitsazi MJ, Salehi-Abargouei A. The effect of dietary approaches to stop hypertension (DASH) on serum inflammatory markers: A systematic review and meta-analysis of randomized trials. *Clin Nutr*. 2018;37(2):542-550. doi:10.1016/j.clnu.2017.02.018

150. Wesselman LMP, van Lent DM, Schröder A, et al. Dietary patterns are related to cognitive functioning in elderly enriched with individuals at increased risk for Alzheimer's disease. *Eur J Nutr*. 2021;60(2):849-860. doi:10.1007/s00394-020-02257-6

151. McEvoy CT, Guyer H, Langa KM, Yaffe K. Neuroprotective Diets Are Associated with Better Cognitive Function: The Health and Retirement Study. *J Am Geriatr Soc*. 2017;65(8):1857-1862. doi:10.1111/jgs.14922

152. Berendsen AM, Kang JH, Feskens EJM, de Groot CPGM, Grodstein F, van de Rest O. Association of long-term adherence to the mind diet with cognitive function and cognitive decline in American women. *J Nutr Health Aging*. 2018;22(2):222-229. doi:10.1007/s12603-017-0909-0

153. Thomas A, Lefèvre-Arbogast S, Féart C, et al. Association of a MIND Diet with Brain Structure and Dementia in a French Population. *J Prev Alzheimers Dis*. Published online 2022. doi:10.14283/jpad.2022.67

154. Morris MC, Tangney CC, Wang Y, Sacks FM, Bennett DA, Aggarwal NT. MIND diet associated with reduced incidence of Alzheimer's disease. *Alzheimers Dement*. 2015;11(9):1007-1014. doi:10.1016/j.jalz.2014.11.009

155. Hosking DE, Eramudugolla R, Cherbuin N, Anstey KJ. MIND not Mediterranean diet related to 12-year incidence of cognitive impairment in an Australian longitudinal cohort study. *Alzheimers Dement*. 2019;15(4):581-589. doi:10.1016/j.jalz.2018.12.011

156. Cherian L, Wang Y, Fakuda K, Leurgans S, Aggarwal N, Morris M. Mediterranean-Dash Intervention for Neurodegenerative Delay (MIND) Diet Slows Cognitive Decline After Stroke. *J Prev Alzheimers Dis*. 2019;6(4):267-273. doi:10.14283/jpad.2019.28

157. Arjmand G, Abbas-Zadeh M, Eftekhari MH. Effect of MIND diet intervention on cognitive performance and brain structure in healthy obese women: a randomized controlled trial. *Sci Rep*. 2022;12(1):2871. doi:10.1038/s41598-021-04258-9

158. Arjmand G, Abbas-Zadeh M, Fardaei M, Eftekhari MH. The Effect of Short-Term Mediterranean-DASH Intervention for Neurodegenerative Delay (MIND) Diet on Hunger Hormones, Anthropometric Parameters, and Brain Structures in Middle-Aged Overweight and Obese Women: A Randomized Controlled Trial. *Iran J Med Sci*. 2022;47(5). doi:10.30476/ijms.2021.90829.2180

159. Duplantier SC, Gardner CD. A Critical Review of the Study of Neuroprotective Diets to Reduce Cognitive Decline. *Nutrients*. 2021;13(7):2264. doi:10.3390/nu13072264

160. Cherian L, Wang Y, Holland T, Agarwal P, Aggarwal N, Morris MC. DASH and Mediterranean-Dash Intervention for Neurodegenerative Delay (MIND) Diets Are Associated With Fewer Depressive Symptoms Over Time. Newman A, ed. *J Gerontol Ser A*. 2021;76(1):151-156. doi:10.1093/gerona/glaa044

161. Shakersain B, Rizzuto D, Larsson S, Faxén-Irving G, Fratiglioni L, Xu WL. The Nordic Prudent Diet Reduces Risk of Cognitive Decline in the Swedish Older Adults: A Population-Based Cohort Study. *Nutrients*. 2018;10(2):229. doi:10.3390/nu10020229

162. de Crom TOE, Mooldijk SS, Ikram MK, Ikram MA, Voortman T. MIND diet and the risk of dementia: a population-based study. *Alzheimers Res Ther*. 2022;14(1):8. doi:10.1186/s13195-022-00957-1

163. Trichopoulou A, Costacou T, Bamia C, Trichopoulos D. Adherence to a Mediterranean Diet and Survival in a Greek Population. *N Engl J Med*. 2003;348(26):2599-2608. doi:10.1056/NEJMoa025039

164. Croll PH, Voortman T, Ikram MA, et al. Better diet quality relates to larger brain tissue volumes. *Neurology*. 2018;90(24):e2166-e2173. doi:10.1212/WNL.0000000000005691

165. Andersen LF, Jacobs DR, Carlsen MH, Blomhoff R. Consumption of coffee is associated with reduced risk of death attributed to inflammatory and cardiovascular diseases in the Iowa Women's Health Study. *Am J Clin Nutr*. 2006;83(5):1039-1046. doi:10.1093/ajcn/83.5.1039

166. Kim JW, Byun MS, Yi D, et al. Coffee intake and decreased amyloid pathology in human brain. *Transl Psychiatry*. 2019;9(1):270. doi:10.1038/s41398-019-0604-5

167. Fredholm BB, Bättig K, Holmén J, Nehlig A, Zvartau EE. Actions of caffeine in the brain with special reference to factors that contribute to its widespread use. *Pharmacol Rev*. 1999;51(1):83-133.

168. Dall'Igna OP, Porciúncula LO, Souza DO, Cunha RA, Lara DR. Neuroprotection by caffeine and adenosine A 2A receptor blockade of β -amyloid neurotoxicity. *Br J Pharmacol*. 2003;138(7):1207-1209. doi:10.1038/sj.bjp.0705185

169. Driscoll I, Shumaker SA, Snively BM, et al. Relationships Between Caffeine Intake and Risk for Probable Dementia or Global Cognitive Impairment: The Women's Health Initiative Memory Study. *J Gerontol A Biol Sci Med Sci*. 2016;71(12):1596-1602. doi:10.1093/gerona/glw078

170. Eskelinen MH, Ngandu T, Tuomilehto J, Soininen H, Kivipelto M. Midlife Coffee and Tea Drinking and the Risk of Late-Life Dementia: A Population-Based CAIDE Study. *J Alzheimers Dis*. 2009;16(1):85-91. doi:10.3233/JAD-2009-0920

171. Monopoli A, Lozza G, Forlani A, Mattavelli A, Ongini E. Blockade of adenosine A2A receptors by SCH 58261 results in neuroprotective effects in cerebral ischaemia in rats: *NeuroReport*. 1998;9(17):3955-3958. doi:10.1097/00001756-199812010-00034

172. Behan WMH, Stone TW. Enhanced neuronal damage by co-administration of quinolinic acid and free radicals, and protection by adenosine A 2A receptor antagonists: Quinolinate and free radicals. *Br J Pharmacol*. 2002;135(6):1435-1442. doi:10.1038/sj.bjp.0704613

173. Chen JF, Xu K, Petzer JP, et al. Neuroprotection by Caffeine and A $_{2A}$ Adenosine Receptor Inactivation in a Model of Parkinson's Disease. *J Neurosci*. 2001;21(10):RC143-RC143. doi:10.1523/JNEUROSCI.21-10-j0001.2001

174. Qi H, Li S. Dose-response meta-analysis on coffee, tea and caffeine consumption with risk of Parkinson's disease. *Geriatr Gerontol Int*. 2014;14(2):430-439. doi:10.1111/ggi.12123

175. Ding M, Bhupathiraju SN, Satija A, van Dam RM, Hu FB. Long-Term Coffee Consumption and Risk of Cardiovascular Disease: A Systematic Review and a Dose–Response Meta-Analysis of Prospective Cohort Studies. *Circulation*. 2014;129(6):643-659. doi:10.1161/CIRCULATIONAHA.113.005925

176. Liebeskind DS, Sanossian N, Fu KA, Wang HJ, Arab L. The coffee paradox in stroke: Increased consumption linked with fewer strokes. *Nutr Neurosci*. 2016;19(9):406-413. doi:10.1179/1476830515Y.0000000035

177. Shang F, Li X, Jiang X. Coffee consumption and risk of the metabolic syndrome: A meta-analysis. *Diabetes Metab*. 2016;42(2):80-87. doi:10.1016/j.diabet.2015.09.001

178. Ding M, Bhupathiraju SN, Chen M, van Dam RM, Hu FB. Caffeinated and decaffeinated coffee consumption and risk of type 2 diabetes: a systematic review and a dose-response meta-analysis. *Diabetes Care*. 2014;37(2):569-586. doi:10.2337/dc13-1203

179. Poole R, Kennedy OJ, Roderick P, Fallowfield JA, Hayes PC, Parkes J. Coffee consumption and health: umbrella review of meta-analyses of multiple health outcomes. *BMJ*. Published online November 22, 2017:j5024. doi:10.1136/bmj.j5024

180. Araújo LF, Mirza SS, Bos D, et al. Association of Coffee Consumption with MRI Markers and Cognitive Function: A Population-Based Study. *J Alzheimers Dis JAD*. 2016;53(2):451-461. doi:10.3233/JAD-160116

181. Pham K, Mulugeta A, Zhou A, O'Brien JT, Llewellyn DJ, Hyppönen E. High coffee consumption, brain volume and risk of dementia and stroke. *Nutr Neurosci*. Published online June 24, 2021:1-12. doi:10.1080/1028415X.2021.1945858

182. Ritchie K, Artero S, Portet F, et al. Caffeine, cognitive functioning, and white matter lesions in the elderly: Establishing causality from epidemiological evidence. In: *Journal of Alzheimer's Disease*. Vol 20. Inserm; 2010:S161. doi:10.3233/JAD-2010-1387

183. Park J, Han JW, Lee JR, et al. Association between lifetime coffee consumption and late life cerebral white matter hyperintensities in cognitively normal elderly individuals. *Sci Rep*. 2020;10(1):421. doi:10.1038/s41598-019-57381-z

184. Haller S, Montandon ML, Rodriguez C, Herrmann FR, Giannakopoulos P. Impact of coffee, wine, and chocolate consumption on cognitive outcome and MRI parameters in old age. *Nutrients*. 2018;10(10):1391. doi:10.3390/nu10101391

185. West RK, Ravona-Springer R, Livny A, et al. Age modulates the association of caffeine intake with cognition and with gray matter in elderly diabetics. *J Gerontol - Ser Biol Sci Med Sci*. 2019;74(5):683-688. doi:10.1093/gerona/gly090

186. Kang J, Jia T, Jiao Z, et al. Increased brain volume from higher cereal and lower coffee intake: shared genetic determinants and impacts on cognition and metabolism. *Cereb Cortex*. Published online February 7, 2022:bhac005. doi:10.1093/cercor/bhac005

187. Perlaki G, Orsi G, Kovacs N, et al. Coffee consumption may influence hippocampal volume in young women. *Brain Imaging Behav*. 2011;5(4):274-284. doi:10.1007/s11682-011-9131-6

188. Schmidt R, Ropele S, Enzinger C, et al. White matter lesion progression, brain atrophy, and cognitive decline: The Austrian stroke prevention study. *Ann Neurol*. 2005;58(4):610-616. doi:10.1002/ana.20630

189. Habes M, Sotiras A, Erus G, et al. White matter lesions. *Neurology*. 2018;91(10):e964-e975. doi:10.1212/WNL.0000000000006116

190. Rizvi B, Lao PJ, Chesebro AG, et al. Association of Regional White Matter Hyperintensities With Longitudinal Alzheimer-Like Pattern of Neurodegeneration in Older Adults. *JAMA Netw Open*. 2021;4(10):e2125166. doi:10.1001/jamanetworkopen.2021.25166

191. Raz N, Rodrigue KM, Kennedy KM, Acker JD. Vascular health and longitudinal changes in brain and cognition in middle-aged and older adults. *Neuropsychology*. 2007;21(2):149-157. doi:10.1037/0894-4105.21.2.149

192. Dickie DA, Karama S, Ritchie SJ, et al. Progression of White Matter Disease and Cortical Thinning Are Not Related in Older Community-Dwelling Subjects. *Stroke*. 2016;47(2):410-416. doi:10.1161/STROKEAHA.115.011229

193. Reijmer YD, Fotiadis P, Charidimou A, et al. Relationship between white matter connectivity loss and cortical thinning in cerebral amyloid angiopathy: Connectivity and Cortical Thinning in CAA. *Hum Brain Mapp*. Published online April 2017. doi:10.1002/hbm.23629

194. Storsve AB, Fjell AM, Yendiki A, Walhovd KB. Longitudinal Changes in White Matter Tract Integrity across the Adult Lifespan and Its Relation to Cortical Thinning. Ebmeier K, ed. *PLOS ONE*. 2016;11(6):e0156770. doi:10.1371/journal.pone.0156770

195. Wen W, Sachdev P. The topography of white matter hyperintensities on brain MRI in healthy 60-to 64-year-old individuals. *NeuroImage*. 2004;22(1):144-154. doi:10.1016/j.neuroimage.2003.12.027

196. Padula MC, Schaer M, Scariati E, et al. Quantifying indices of short- and long-range white matter connectivity at each cortical vertex. Huang H, ed. *PLoS ONE*. 2017;12(11):e0187493. doi:10.1371/journal.pone.0187493

197. Quandt F, Fischer F, Schröder J, et al. Higher white matter hyperintensity lesion load is associated with reduced long-range functional connectivity. *Brain Commun*. 2020;2(2):fcaa111. doi:10.1093/braincomms/fcaa111

198. Papadaki E, Kavroulakis E, Kalaitzakis G, et al. Age-related deep white matter changes in myelin and water content: A T $_2$ relaxometry study. *J Magn Reson Imaging*. 2019;50(5):1393-1404. doi:10.1002/jmri.26707

199. Wang X, Huang X, Gao Z, Jiang H, Lu X. Vasogenic cerebral edema associated with the disability in activities of daily living in patients with chronic obstructive pulmonary disease. *Brain Behav*. 2018;8(8):e01065. doi:10.1002/brb3.1065

200. de Leeuw F -E., de Groot JC, Oudkerk M, et al. Hypertension and cerebral white matter lesions in a prospective cohort study. *Brain*. 2002;125(4):765-772. doi:10.1093/brain/awf077

201. Dufouil C, De Kersaint-Gilly A, Besançon V, et al. Longitudinal study of blood pressure and white matter hyperintensities: The EVA MRI cohort. *Neurology*. 2001;56(7):921-926. doi:10.1212/WNL.56.7.921

202. Haines DE, Mihailoff GA, eds. *Fundamental Neuroscience for Basic and Clinical Applications*. Fifth edition. Elsevier; 2018.

203. Armstrong NJ, Mather KA, Sargurupremraj M, et al. Common Genetic Variation Indicates Separate Causes for Periventricular and Deep White Matter Hyperintensities. *Stroke*. 2020;51(7):2111-2121. doi:10.1161/STROKEAHA.119.027544

204. Kloppenborg RP, Nederkoorn PJ, Grool AM, et al. Cerebral small-vessel disease and progression of brain atrophy : The SMART-MR study. *Neurology*. 2012;79(20):2029-2036. doi:10.1212/WNL.0b013e3182749f02

205. De Groot JC, De Leeuw FE, Oudkerk M, et al. Periventricular cerebral white matter lesions predict rate of cognitive decline. *Ann Neurol*. 2002;52(3):335-341. doi:10.1002/ana.10294

206. Van Den Heuvel DMJ, Ten Dam VH, De Craen AJM, et al. Increase in periventricular white matter hyperintensities parallels decline in mental processing speed in a non-demented elderly population. *J Neurol Neurosurg Psychiatry*. 2006;77(2):149-153. doi:10.1136/jnnp.2005.070193

207. Söderlund H, Nilsson LG, Berger K, et al. Cerebral changes on MRI and cognitive function: The CASCADE study. *Neurobiol Aging*. 2006;27(1):16-23. doi:10.1016/j.neurobiolaging.2004.12.008

208. Jiménez-Balado J, Corlier F, Habeck C, Stern Y, Eich T. Effects of white matter hyperintensities distribution and clustering on late-life cognitive impairment. *Sci Rep*. 2022;12(1):1955. doi:10.1038/s41598-022-06019-8

209. Smith CD, Johnson ES, Van Eldik LJ, et al. Peripheral (deep) but not periventricular MRI white matter hyperintensities are increased in clinical vascular dementia compared to Alzheimer's disease. *Brain Behav*. 2016;6(3):1-11. doi:10.1002/brb3.438

210. Fazekas F, Kleinert R, Offenbacher H, et al. Pathologic correlates of incidental MRI white matter signal hyperintensities. *Neurology*. 1993;43(9):1683-1683. doi:10.1212/WNL.43.9.1683

211. Fernando MS, Simpson JE, Matthews F, et al. White Matter Lesions in an Unselected Cohort of the Elderly: Molecular Pathology Suggests Origin From Chronic Hypoperfusion Injury. *Stroke*. 2006;37(6):1391-1398. doi:10.1161/01.STR.0000221308.94473.14

212. Blanco PJ, Müller LO, Spence JD. Blood pressure gradients in cerebral arteries: a clue to pathogenesis of cerebral small vessel disease. *Stroke Vasc Neurol*. 2017;2(3):108-117. doi:10.1136/svn-2017-000087

213. DeCarli C, Fletcher E, Ramey V, Harvey D, Jagust WJ. Anatomical Mapping of White Matter Hyperintensities (WMH). *Stroke*. 2004;36(1):50-55. doi:10.1161/01.str.0000150668.58689.f2

214. Li Y, Kalpouzos G, Laukka EJ, et al. Progression of neuroimaging markers of cerebral small vessel disease in older adults: A 6-year follow-up study. *Neurobiol Aging*. 2022;112:204-211. doi:10.1016/j.neurobiolaging.2022.01.006

215. Thong JYJ, Hilal S, Wang Y, et al. Association of silent lacunar infarct with brain atrophy and cognitive impairment. *J Neurol Neurosurg Psychiatry*. 2013;84(11):1219-1225. doi:10.1136/jnnp-2013-305310

216. Zhang X, Ding L, Yang L, et al. Brain Atrophy Correlates with Severe Enlarged Perivascular Spaces in Basal Ganglia among Lacunar Stroke Patients. Baron JC, ed. *PLOS ONE*. 2016;11(2):e0149593. doi:10.1371/journal.pone.0149593

217. Passiak BS, Liu D, Kresge HA, et al. Perivascular spaces contribute to cognition beyond other small vessel disease markers. *Neurology*. 2019;92(12):e1309-e1321. doi:10.1212/WNL.0000000000007124

218. Friedman JM. Leptin and the Regulation of Body Weigh. *Keio J Med*. 2011;60(1):1-9. doi:10.2302/kjm.60.1

219. Obradovic M, Sudar-Milovanovic E, Soskic S, et al. Leptin and Obesity: Role and Clinical Implication. *Front Endocrinol*. 2021;12:585887. doi:10.3389/fendo.2021.585887

220. Münzberg H, Björnholm M, Bates SH, Myers MG. Leptin receptor action and mechanisms of leptin resistance. *Cell Mol Life Sci*. 2005;62(6):642. doi:10.1007/s00018-004-4432-1

221. Cazettes F, Cohen JI, Yau PL, Talbot H, Convit A. Obesity-mediated inflammation may damage the brain circuit that regulates food intake. *Brain Res*. 2011;1373:101-109. doi:10.1016/j.brainres.2010.12.008

222. Pannacciulli N, Del Parigi A, Chen K, Le DSNT, Reiman EM, Tataranni PA. Brain abnormalities in human obesity: A voxel-based morphometric study. *NeuroImage*. 2006;31(4):1419-1425. doi:10.1016/j.neuroimage.2006.01.047

223. Murray CJL. The State of US Health, 1990-2010. *JAMA*. 2013;310(6):591. doi:10.1001/jama.2013.13805

224. Bettcher BM, Yaffe K, Boudreau RM, et al. Declines in inflammation predict greater white matter microstructure in older adults. *Neurobiol Aging*. 2015;36(2):948-954. doi:10.1016/j.neurobiolaging.2014.11.004

225. Isaac V, Sim S, Zheng H, Zagorodnov V, Tai ES, Chee M. Adverse Associations between Visceral Adiposity, Brain Structure, and Cognitive Performance in Healthy Elderly. *Front Aging Neurosci*. 2011;3. doi:10.3389/fnagi.2011.00012

226. Coppin G, Nolan-Poupart S, Jones-Gotman M, Small DM. Working memory and reward association learning impairments in obesity. *Neuropsychologia*. 2014;65:146-155. doi:10.1016/j.neuropsychologia.2014.10.004

227. Kivipelto M, Ngandu T, Fratiglioni L, et al. Obesity and Vascular Risk Factors at Midlife and the Risk of Dementia and Alzheimer Disease. *Arch Neurol*. 2005;62(10). doi:10.1001/archneur.62.10.1556

228. Smethers AD, Rolls BJ. Dietary Management of Obesity. *Med Clin North Am*. 2018;102(1):107-124. doi:10.1016/j.mcna.2017.08.009

229. Espeland MA, Erickson K, Neiberg RH, et al. Brain and White Matter Hyperintensity Volumes After 10 Years of Random Assignment to Lifestyle Intervention. *Diabetes Care*. 2016;39(5):764-771. doi:10.2337/dc15-2230

230. Simpson IA, Carruthers A, Vannucci SJ. Supply and Demand in Cerebral Energy Metabolism: The Role of Nutrient Transporters. *J Cereb Blood Flow Metab*. 2007;27(11):1766-1791. doi:10.1038/sj.jcbfm.9600521

231. Imamura F, O'Connor L, Ye Z, et al. Consumption of sugar sweetened beverages, artificially sweetened beverages, and fruit juice and incidence of type 2 diabetes: systematic review, meta-analysis, and estimation of population attributable fraction. *BMJ*. Published online July 21, 2015:h3576. doi:10.1136/bmj.h3576

232. Manschot SM, Brands AMA, van der Grond J, et al. Brain Magnetic Resonance Imaging Correlates of Impaired Cognition in Patients With Type 2 Diabetes. *Diabetes*. 2006;55(4):1106-1113. doi:10.2337/diabetes.55.04.06.db05-1323

233. Sun J, Xu B, Zhang X, et al. The Mechanisms of Type 2 Diabetes-Related White Matter Intensities: A Review. *Front Public Health*. 2020;8:498056. doi:10.3389/fpubh.2020.498056

234. Tsai CK, Kao TW, Lee JT, et al. Increased risk of cognitive impairment in patients with components of metabolic syndrome. *Medicine (Baltimore)*. 2016;95(36):e4791. doi:10.1097/MD.0000000000004791

235. Korf ESC, White LR, Scheltens P, Launer LJ. Brain Aging in Very Old Men With Type 2 Diabetes. *Diabetes Care*. 2006;29(10):2268-2274. doi:10.2337/dc06-0243

236. den Heijer T, Vermeer SE, van Dijk EJ, et al. Type 2 diabetes and atrophy of medial temporal lobe structures on brain MRI. *Diabetologia*. 2003;46(12):1604-1610. doi:10.1007/s00125-003-1235-0

237. Gold SM, Dziobek I, Sweat V, et al. Hippocampal damage and memory impairments as possible early brain complications of type 2 diabetes. *Diabetologia*. 2007;50(4):711-719. doi:10.1007/s00125-007-0602-7

238. Ho L, Qin W, Pompl PN, et al. Diet-induced insulin resistance promotes amyloidosis in a transgenic mouse model of Alzheimer's disease. *FASEB J*. 2004;18(7):902-904. doi:10.1096/fj.03-0978fje

239. Teng Z, Feng J, Qi Q, et al. Long-Term Use of Metformin Is Associated With Reduced Risk of Cognitive Impairment With Alleviation of Cerebral Small Vessel Disease Burden in Patients With Type 2 Diabetes. *Front Aging Neurosci*. 2021;13:773797. doi:10.3389/fnagi.2021.773797

240. Ley SH, Hamdy O, Mohan V, Hu FB. Prevention and management of type 2 diabetes: dietary components and nutritional strategies. *The Lancet*. 2014;383(9933):1999-2007. doi:10.1016/S0140-6736(14)60613-9

241. Toi PL, Anothaisintawee T, Chaikledkaew U, Briones JR, Reutrakul S, Thakkinstian A. Preventive Role of Diet Interventions and Dietary Factors in Type 2 Diabetes Mellitus: An Umbrella Review. *Nutrients*. 2020;12(9):2722. doi:10.3390/nu12092722

242. Evans LE, Taylor JL, Smith CJ, Pritchard HAT, Greenstein AS, Allan SM. Cardiovascular comorbidities, inflammation, and cerebral small vessel disease. *Cardiovasc Res*. Published online September 9, 2021:cvab284. doi:10.1093/cvr/cvab284

243. Aaron KJ, Sanders PW. Role of Dietary Salt and Potassium Intake in Cardiovascular Health and Disease: A Review of the Evidence. *Mayo Clin Proc*. 2013;88(9):987-995. doi:10.1016/j.mayocp.2013.06.005

244. Steffen LM, Kroenke CH, Yu X, et al. Associations of plant food, dairy product, and meat intakes with 15-y incidence of elevated blood pressure in young black and white adults: the Coronary Artery Risk Development in Young Adults (CARDIA) Study. *Am J Clin Nutr*. 2005;82(6):1169-1177. doi:10.1093/ajcn/82.6.1169

245. van Dam RM, Grievink L, Ocké MC, Feskens EJ. Patterns of food consumption and risk factors for cardiovascular disease in the general Dutch population,,. *Am J Clin Nutr*. 2003;77(5):1156-1163. doi:10.1093/ajcn/77.5.1156

246. Kim Y, Je Y. Prospective association of sugar-sweetened and artificially sweetened beverage intake with risk of hypertension. *Arch Cardiovasc Dis*. 2016;109(4):242-253. doi:10.1016/j.acvd.2015.10.005

247. Kaplan NormanM. Alcohol and hypertension. *The Lancet*. 1995;345(8965):1588-1589. doi:10.1016/S0140-6736(95)90110-8

248. Vissers LET, Waller M, van der Schouw YT, et al. A pro-inflammatory diet is associated with increased risk of developing hypertension among middle-aged women. *Nutr Metab Cardiovasc Dis*. 2017;27(6):564-570. doi:10.1016/j.numecd.2017.03.005

249. Neufcourt L, Assmann KE, Fezeu LK, et al. Prospective association between the dietary inflammatory index and metabolic syndrome: Findings from the SU.VI.MAX study. *Nutr Metab Cardiovasc Dis*. 2015;25(11):988-996. doi:10.1016/j.numecd.2015.09.002

250. Touyz RM, Alves-Lopes R, Rios FJ, et al. Vascular smooth muscle contraction in hypertension. *Cardiovasc Res*. 2018;114(4):529-539. doi:10.1093/cvr/cvy023

251. van Beek AH, Claassen JA, Rikkert MGO, Jansen RW. Cerebral Autoregulation: An Overview of Current Concepts and Methodology with Special Focus on the Elderly. *J Cereb Blood Flow Metab*. 2008;28(6):1071-1085. doi:10.1038/jcbfm.2008.13

252. Pantoni L, Garcia JH. Pathogenesis of Leukoaraiosis: A Review. *Stroke*. 1997;28(3):652-659. doi:10.1161/01.STR.28.3.652

253. Pantoni L. Cerebral small vessel disease: from pathogenesis and clinical characteristics to therapeutic challenges. *Lancet Neurol*. 2010;9(7):689-701. doi:10.1016/S1474-4422(10)70104-6

254. Al-Solaiman Y, Jesri A, Zhao Y, Morrow JD, Egan BM. Low-sodium DASH reduces oxidative stress and improves vascular function in salt-sensitive humans. *J Hum Hypertens*. 2009;23(12):826-835. doi:10.1038/jhh.2009.32

255. Blumenthal JA, Smith PJ, Mabe S, et al. Lifestyle and Neurocognition in Older Adults With Cardiovascular Risk Factors and Cognitive Impairment. *Psychosom Med*. 2017;79(6):719-727. doi:10.1097/PSY.0000000000000474

256. Smith PJ, Blumenthal JA, Babyak MA, et al. Effects of the Dietary Approaches to Stop Hypertension Diet, Exercise, and Caloric Restriction on Neurocognition in Overweight Adults With High Blood Pressure. *Hypertension*. 2010;55(6):1331-1338. doi:10.1161/HYPERTENSIONAHA.109.146795

257. Matthews DC, Davies M, Murray J, et al. Physical Activity, Mediterranean Diet and Biomarkers-Assessed Risk of Alzheimer's: A Multi-Modality Brain Imaging Study. *Adv Mol Imaging*. 2014;04(04):43-57. doi:10.4236/ami.2014.44006

258. Scarmeas N, Luchsinger JA, Schupf N, et al. Physical activity, diet, and risk of Alzheimer disease. *JAMA*. 2009;302(6):627-637. doi:10.1001/jama.2009.1144

259. Ferreira NV, Lotufo PA, Marchioni DML, et al. Association Between Adherence to the MIND Diet and Cognitive Performance is Affected by Income: The ELSA-Brasil Study. *Alzheimer Dis Assoc Disord*. Published online January 28, 2022. doi:10.1097/WAD.0000000000000491

260. Afshin A, Sur PJ, Fay KA, et al. Health effects of dietary risks in 195 countries, 1990–2017: a systematic analysis for the Global Burden of Disease Study 2017. *The Lancet*. 2019;393(10184):1958-1972. doi:10.1016/S0140-6736(19)30041-8

261. Azzam A. Is the world converging to a 'Western diet'? *Public Health Nutr*. 2021;24(2):309-317. doi:10.1017/S136898002000350X

4. List of publications & contributing work

Mayer C, Frey BM, Schlemm E, et al. Linking cortical atrophy to white matter hyperintensities of presumed vascular origin. *J Cereb Blood Flow Metab*. Published online December 2020:0271678X2097417. doi:10.1177/0271678X20974170

I shared the first authorship on this paper with a colleague (BMF), therefore we were equally responsible for the conception of the work, the analysis and interpretation of the data, and drafting of the manuscript. More specifically, we were responsible for the processing of the MR images including the development of a processing pipeline and the quality assurance of the output. BMF and I conducted the statistical analysis and wrote the first draft of the manuscript.

Mayer C, Naegele FL, Petersen M, et al. Free-water diffusion MRI detects structural alterations surrounding white matter hyperintensities in the early stage of cerebral small vessel disease. *J Cereb Blood Flow Metab*. Published online April 11, 2022:0271678X2210935. doi:10.1177/0271678X221093579

As first author, I was responsible for the conception of the work, the analysis and interpretation of the data, and drafting of the manuscript. More specifically, together with colleagues, I was responsible for the processing of the MR images including the development of a processing pipeline and the quality assurance of the output. I conducted the statistical analysis and wrote the first draft of the manuscript.

Mayer C, Nägele FL, Petersen M, et al. Association between Coffee Consumption and Brain MRI Parameters in the Hamburg City Health Study. *Nutrients*. 2023;15(3):674. doi:10.3390/nu15030674

As first author, I was responsible for the conception of the work, the analysis and interpretation of the data, and drafting of the manuscript. More specifically, together with colleagues, I was responsible for the processing of the MR images including the development of a processing pipeline and the quality assurance of the output. In addition, I conducted the statistical analysis, and wrote the initial draft of the paper.

Mayer C, Nägele FL, Petersen M, et al. Association between Nutrition, Brain Structure and Cognition and mediating effects of Metabolic Syndrome – a Structural Equation Modeling Approach in the Hamburg City Health Study. *In preparation*.

As first author, I was responsible for the conception of the work, the analysis and interpretation of the data, and drafting of the manuscript. More specifically, together with colleagues, I was responsible for the processing of the MR images including the development of a processing pipeline and the quality assurance of the output. In addition, I wrote the initial draft of the paper.

5. Summary

Cerebral small vessel disease (CSVD) contributes to cognitive deterioration and functional impairment among the elderly population. CSVD is characterized by several imaging markers, including white matter hyperintensities (WMH) and cortical thickness. Given that a majority of older individuals exhibit signs of CSVD on brain MRI, it becomes imperative to identify risk factors and implement preventive mechanisms to promote successful aging. This thesis focused on the investigation of WMH as imaging marker of CSVD in order to gain insights into the disease. The research involved the data analysis from a large, population-based cohort to quantify CSVD markers and assess microstructural brain damage.

The first part of the thesis revealed several important findings regarding the association between the prevalence and location of WMH and other imaging characteristics. The findings from study 1 revealed that cortical regions with a higher proportion of connections to WMH demonstrated reduced thickness, suggesting a direct structural link between WMH burden and cortical thinning. In study 2, the white matter surrounding WMH exhibited an increase in free-water, indicating compromised microstructural integrity. Notably, the damage to the white matter was most pronounced in the closest proximity to the WMH, emphasizing that WMH is the end stage of a gradually deteriorating white matter. These findings shed light on the intricate relationship between WMH, cortical thinning and microstructural abnormalities in CSVD and contribute to our understanding of the disease's underlying mechanisms.

The second part of the thesis delved into the clinical aspects of CSVD and microstructural brain damage, with specific focus on the role of nutrition and coffee consumption. A food-frequency questionnaire was utilized to assess adherence to different dietary patterns, and nutritional behavior was then associated with imaging markers of brain structure and cognition. The findings of study 3 unveiled the associations between nutritional behavior, brain structure and cognitive function. One notable result was the link between healthy nutrition and a reduced risk of metabolic syndrome, which, in turn, contributed to the preservation of brain structure. Similarly, the cognitive performance was significantly better in individuals with a healthier diet. In study 4, it was demonstrated that a moderate coffee consumption was associated with preserved white matter structure and higher cortical thickness. The findings of studies 3 and 4 emphasize the significance of nutrition in maintaining brain health and suggest that adopting a healthy diet may serve a protective factor against CSVD-related deterioration.

6. Zusammenfassung

Die zerebrale Mikroangiopathie beeinträchtigt die kognitive Funktion und die Funktionsfähigkeit im Alter. Diese Erkrankung zeigt sich durch typische Merkmale in der MRT-Bildgebung, wie etwa Hyperintensitäten in der weißen Substanz (WMH) und eine Veränderung der kortikalen Dicke. Da bei einem Großteil der älteren Bevölkerungsgruppe Anzeichen der zerebralen Mikroangiopathie im MRT-Bild nachgewiesen werden können, ist die Identifizierung von Risikofaktoren und Implementierung von präventiven Maßnahmen entscheidend für ein erfolgreiches Altern. Diese Dissertation untersucht WMH als Bildgebungsmarker von zerebraler Mikroangiopathie, um Erkenntnisse über diese Erkrankung zu gewinnen. Für die Analyse wurden Daten aus einer populations-basierten Studie ausgewertet, um Marker von zerebraler Mikroangiopathie zu quantifizieren und mikrostrukturelle Hirnschäden zu beurteilen.

Der erste Teil der Dissertation lieferte wichtige Erkenntnisse über den Zusammenhang zwischen der Prävalenz und Lokalisation von WMH sowie anderen bildgebenden Markern. Die Ergebnisse der ersten Studie zeigten, dass kortikale Regionen, die eine höhere Konnektivität zu WMH hatten, eine geringere kortikale Dicke aufwiesen. Dies suggeriert eine direkte strukturelle Verbindung zwischen WMH und kortikaler Verdünnung. In der zweiten Studie wurde festgestellt, dass die scheinbar unbeeinträchtigte weiße Substanz in unmittelbarer Nähe der WMH eine Zunahme an freiem Wasser auswies, was auf eine beeinträchtigte mikrostrukturelle Integrität hinweist. Insbesondere die weiße Substanz, die sich am nächsten zu den WMH befand, zeigte die stärkste Schädigung. Dies unterstreicht, dass WMH das Endstadium der graduellen Verschlechterung der weißen Substanz darstellen. Insgesamt liefern die Ergebnisse wichtige Erkenntnisse über die komplexe Beziehung zwischen WMH, kortikale Dicke und mikrostrukturelle Veränderungen bei zerebraler Mikroangiopathie und tragen zu unserem Verständnis der zugrunde liegenden Mechanismen von CSVD bei.

Der zweite Teil der Dissertation untersuchte die klinischen Aspekte der zerebralen Mikroangiopathie und mikrostrukturellen Schädigungen, insbesondere den Einfluss von Ernährung und Kaffeekonsum. Mit Hilfe eines Fragebogens zum Lebensmittelkonsum wurden verschiedene Diätmuster bewertet, um die Verbindung mit bildgebenden Markern der Hirnstruktur und Kognition zu untersuchen. Die Ergebnisse der dritten Studie zeigten signifikante Zusammenhänge zwischen Ernährungsverhalten, Hirnstruktur und kognitiver Funktion. Besonders erwähnenswert war die Beziehung zwischen der gesunden Ernährung und dem geringeren Risiko für das metabolischen Syndroms, das wiederum mit einer verbesserten Hirnstruktur assoziiert war. Darüber hinaus zeigten Personen mit einer gesünderen Ernährung eine bessere kognitive Leistungsfähigkeit, teilweise bedingt durch das reduzierte Risiko für das metabolische Syndrom. Die vierte Studie zeigte, dass moderater Kaffeekonsum mit einer besseren Erhaltung der weißen Substanz und einer höheren kortikalen Dicke assoziiert war. Die Ergebnisse der dritten und vierten Studie betonen die Bedeutung einer gesunden Ernährung für die Erhaltung der Hirngesundheit und empfehlen, dass eine gesunde Ernährung Schutz vor Schädigungen durch zerebrale Mikroangiopathie bieten kann.

7. Acknowledgements

8. Curriculum Vitae

-- this paragraph was intentionally left blank --

9. Declaration on Oath (Eidesstattliche Versicherung)

Ich versichere ausdrücklich, dass ich die Arbeit selbständig und ohne fremde Hilfe verfasst, andere als die von mir angegebenen Quellen und Hilfsmittel nicht benutzt und die aus den benutzten Werken wörtlich oder inhaltlich entnommenen Stellen einzeln nach Ausgabe (Auflage und Jahr des Erscheinens), Band und Seite des benutzten Werkes kenntlich gemacht habe.

Ferner versichere ich, dass ich die Dissertation bisher nicht einem Fachvertreter an einer anderen Hochschule zur Überprüfung vorgelegt oder mich anderweitig um Zulassung zur Promotion beworben habe.

Ich erkläre mich einverstanden, dass meine Dissertation vom Dekanat der Medizinischen Fakultät mit einer gängigen Software zur Erkennung von Plagiaten überprüft werden kann.

Unterschrift: ....

Linking cortical atrophy to white matter hyperintensities of presumed vascular origin

Carola Mayer[1],*, Benedikt M Frey[1],*, Eckhard Schlemm[1] ,
Marvin Petersen[1] , Kristin Engelke[2], Uta Hanning[2],
Annika Jagodzinski[3,4], Katrin Borof[3], Jens Fiehler[2],
Christian Gerloff[1], Götz Thomalla[1] and Bastian Cheng[1]

Abstract

We examined the relationship between white matter hyperintensities (WMH) and cortical neurodegeneration in cerebral small vessel disease (CSVD) by investigating whether cortical thickness is a remote effect of WMH through structural fiber tract connectivity in a population at increased risk of CSVD. We measured cortical thickness on T1-weighted images and segmented WMH on FLAIR images in 930 participants of a population-based cohort study at baseline. DWI-derived whole-brain probabilistic tractography was used to define WMH connectivity to cortical regions. Linear mixed-effects models were applied to analyze the relationship between cortical thickness and connectivity to WMH. Factors associated with cortical thickness (age, sex, hemisphere, region, individual differences in cortical thickness) were added as covariates. Median age was 64 [IQR 46–76] years. Visual inspection of surface maps revealed distinct connectivity patterns of cortical regions to WMH. WMH connectivity to the cortex was associated with reduced cortical thickness ($p = 0.009$) after controlling for covariates. This association was found for periventricular WMH ($p = 0.001$) only. Our results indicate an association between WMH and cortical thickness via connecting fiber tracts. The results imply a mechanism of secondary neurodegeneration in cortical regions distant, yet connected to subcortical vascular lesions, which appears to be driven by periventricular WMH.

Introduction

White matter hyperintensities of presumed vascular origin (WMH) are the most common radiological marker of cerebral small vessel disease (CSVD).[1] WMH are associated with various clinical sequelae like dementia, cognitive impairment, mood disorders, mortality, an increased risk of stroke, and worsened recovery from stroke.[2–4] Supporting the hypothesis of damage to small perforating arteries in CSVD, major contributors for the development of WMH are atherosclerosis and cardiovascular risk factors like age, hypertension and smoking.[3,5,6]

Global cortical atrophy is another recurring pathology in CSVD and found to be associated with the

[1]Department of Neurology, University Medical Center Hamburg-Eppendorf, Hamburg, Germany
[2]Department of Diagnostic and Interventional Neuroradiology, University Medical Center Hamburg-Eppendorf, Hamburg, Germany
[3]Epidemiological Study Center, University Medical Center Hamburg-Eppendorf, Hamburg, Germany
[4]Department of General and Interventional Cardiology, University Heart and Vascular Center Hamburg, Hamburg, Germany

*These authors contributed equally to this work.

Corresponding author:
Carola Mayer, Martinistraße 52, Hamburg 20246, Germany.
Email: c.mayer@uke.de

extent of WMH in whole-brain and region-specific analyses.[7–9] This association appears to contain a location-dependent component, since spatial patterns of cortical thinning were identified for WMH located either in periventricular (pWMH) or deep white matter (dWMH).[8,10]

The hypothesis of secondary cortical degeneration through damaged white matter tracts indicates a direct pathophysiological link between WMH and cortical thickness.[11–13] In subcortical stroke and CADASIL patients, cortical thinning occurred in brain regions distant, yet connected to subcortical lesions through degenerated white matter tracts.[14–16] Based on these observations, we investigate the impact of WMH on cortical thickness through white matter connectivity in a population at increased risk for cardiovascular diseases. We hypothesize that a higher connectivity between WMH and cortical regions is associated with reduced grey matter thickness in these areas after adjusting for the overall connectivity and lesion load. We further distinguished between pWMH and dWMH connectivity on the cortex to underpin possible location dependent effects of WMH on cortical thickness.

Material and methods

Study design and participants

Data from participants of the Hamburg City Health Study (HCHS) was selected for this analysis. HCHS is a single center, prospective, epidemiologic cohort study with emphasis on imaging to improve the identification of individuals at increased risk for major chronic diseases and to improve early diagnosis and survival. A detailed description of the overall study design was published separately.[17] In brief, 45,000 citizens of the city of Hamburg, Germany, between 45 and 74 years are invited to an extensive baseline evaluation. A subgroup of participants with increased risk for cardiovascular diseases undergoes a standardized MRI brain imaging protocol. Specifically, this subgroup is selected based on the presence of cardiovascular risk factors using the Framingham Risk Score.[18] For this study, we analyzed the first 1,000 brain MRI datasets from participants of the HCHS at the time of baseline visit. Imaging data of insufficient quality for white matter segmentation and reconstruction of white matter fibers were excluded.

The local ethics committee of the Landesärztekammer Hamburg (State of Hamburg Chamber of Medical Practitioners, PV5131) approved the HCHS, and written informed consent was obtained from all participants. The study has been registered at ClinicalTrial.gov (NCT03934957). The HCHS design ensures that all involved individuals abide by the ethical principles described in the current revision of the Declaration of Helsinki, by Good Clinical Practice (GCP) and by Good Epidemiological Practice (GEP).

Magnetic resonance imaging

Images were acquired using a 3 T Siemens Skyra MRI scanner (Siemens, Erlangen, Germany). For single-shell diffusion weighted imaging (DWI), 75 axial slices were obtained covering the whole brain with gradients ($b = 1,000 \, s/mm^2$) applied along 64 noncollinear directions with the following sequence parameters: repetition time (TR) = 8500 ms, echo time (TE) = 75 ms, slice thickness (ST) = 2 mm, in-plane resolution (IPR) = $2 \times 2 \, mm^2$, anterior-posterior phase-encoding direction. For 3 D T1-weighted anatomical images, rapid acquisition gradient-echo sequence (MPRAGE) was used with the following sequence parameters: TR = 2500 ms, TE = 2.12 ms, 256 axial slices, ST = 0.94 mm, and IPR = $0.83 \times 0.83 \, mm^2$. 3 D T2-weighted fluid attenuated inversion recovery (FLAIR) images were acquired with the following sequence parameters: TR = 4700 ms, TE = 392 ms, 192 axial slices, ST = 0.9 mm and IPR = 0.75×0.75 mm.

WMH segmentation

For segmentation of WMH, we used FSL's Brain Intensity AbNormality Classification Algorithm (BIANCA), a fully automated, supervised k-nearest neighbor (k-NN) algorithm.[19] The training dataset comprised WMH masks for the first 100 participants generated by selecting only voxels that had been marked by two experienced investigators (CM and MP) independently with manual segmentation. Mean Dice Similarity Index for manual WMH segmentations of the training data was 0.63. Derived masks of WMH were divided into periventricular (pWMH) and deep (dWMH) by defining a 10 mm distance threshold to the ventricles.[20,21] WMH load was calculated as the fraction of whole brain tissue volume (excluding ventricle volume). The algorithm was trained on multiple modalities by including both T1-weighted and FLAIR images to the algorithm. Additionally, spatial information of each voxel was implemented in the algorithm after linear registration to MNI space.

Probabilistic tractography

Whole-brain streamlines were reconstructed using anatomically constrained probabilistic streamlines tractography (ACT) by second order integration over fiber orientation distributions (iFOD2) using the publicly available MRtrix 3 toolbox.[22–24] Dynamic seeding was applied.[25] This approach addresses the uncertainty

in the calculation of the fiber orientations in each voxel and is constrained to anatomical priors to improve the biological plausibility of the tractography. Specifically, white matter fibers were reconstructed by starting probabilistic streamlines strategically in the white matter, producing streamline bundles that match the distribution of modelled fiber directions in every voxel. In addition, the reconstructed streamline densities were matched and adjusted with fiber density estimated from the diffusion model for each voxel.

Analysis of cortical thickness and connectivity to WMH

Figure 1 illustrates the methodological approach of our study. Cortical surface areas were defined, and cortical thickness was measured on T1-weighted imaging data using the standardized Freesurfer processing pipeline (Version 5.3).[26] Three steps were applied to calculate connectivity of WMH with the cortical surface: (1) an individual tractogram containing all streamlines was reconstructed based on the whole-brain tractography as described above. At their cortical terminations, all streamlines were counted at each cortical vertex; the number of terminating streamlines was taken as a measure of connectivity at corresponding cortical areas (Figure 1(a)); (2) WMH segmentations generated previously used to filter only the streamlines passing through at least one voxel with WMH. Analogous to step 1, the number of filtered streamlines was used as a measure of connectivity to WMH, calculated at each

cortical vertex and normalized with respect to whole-brain connectivity to account for physiological disparities in regional connectivity of the cerebral cortex (Figure 1(b)). For simplicity, this connectivity to hyperintensities proportional to the overall connectivity is simply referred to as WMH connectivity; (3) the second step was repeated for previously generated masks of deep and periventricular WMH separately. The extracted connectivity from these masks is further referred to as dWMH and pWMH connectivity (Figure 1(c)). Of note, "dWMH and pWMH connectivity" in our study is not applied as a surrogate marker of structural white matter integrity since these measures do not relate to specific, predefined white matter tracts. They rather characterize the connectivity profile of cortical brain areas, specifically in relation to the probability of connectivity to WMH. To facilitate subsequent statistical analysis and anatomical mapping, vertex-vise connectivity was summarized with regard to 210 distinct brain regions of the connectivity-based Brainnetome atlas.[27] To assess regional patterns of connectivity to the different types of WMH, the regions were sorted in descending order according to their median connectivity to WMH, pWMH and dWMH.

Statistical analysis

Demographic data of all participants was recorded, and the median of demographic and imaging data was calculated together with the interquartile range.
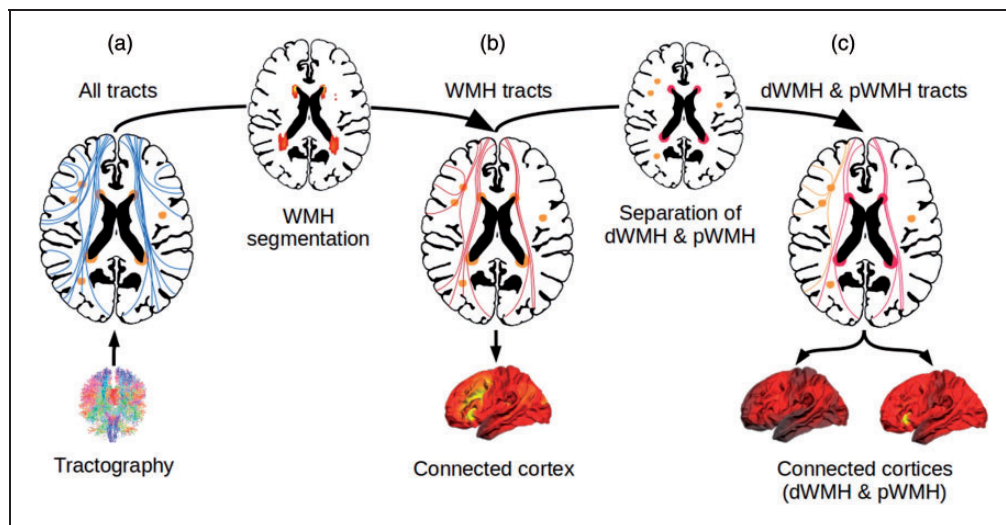
Figure 1. Methodological approach of the generation of a WMH connectivity pattern to the cortical surface. Whole-brain tractograms were calculated for all individuals using anatomically constrained probabilistic tractography (a). All WMH were automatically segmented with a k-nearest neighbor algorithm and the segmentation was used to select only the streamlines passing through at least one voxel with WMH, visualized in (b). Derived masks of WMH were divided into pWMH and dWMH by a 10mm distance threshold to the ventricles. These masks were used to further select streamlines crossing dWMH and streamlines crossing pWMH, shown in (c). Abbreviations: dWMH = deep white matter hyperintensities, mm = millimeter, pWMH = periventricular white matter hyperintensities, WMH = white matter hyperintensities.

For the primary analysis, two linear mixed-effects models were fitted both including cortical thickness as the dependent variable and fixed effects age, sex (female, male) and hemisphere (right or left) to control for their known association with cortical thickness. In addition, random effects for participants and cortical region were introduced to control for inter-individual and regional variability in cortical thickness.[28–30] For the first model ("Model 1") analyzing the impact of WMH connectivity on cortical thickness, values of WMH connectivity was included as an independent variable together with modelling of random slopes for a hypothesized region-specific effect size of the WMH connectivity and lesion load. The second model ("Model 2") analyzed the impact of deep and periventricular WMH connectivity on cortical thickness and therefore included dWMH and pWMH connectivity as independent variables with modelling of random slopes for an assumed region-specific effect of dWMH and pWMH connectivity and lesion load. All statistical analysis was carried out using R (Version 3.5.1).[31]

Results

Study sample characteristics

We considered MRI data from the first 1000 participants of HCHS for inclusion in this study. Of those, 21 participants were excluded due to missing imaging data (9 no imaging data at all, 3 FLAIR, 9 DWI), 40 participants were excluded due to poor quality or incompleteness of imaging data (39 DWI, 1 FLAIR) and in 9 participants, image processing was unsuccessful for technical reasons. The final sample for this study comprised 930 participants (424 females; 45.6%) with a median age of 64 (IQR = 14, range 46–76) years. Median brain volume was 1,484 ml (203), median WMH 0.6 ml (1.4), median pWMH 0.5 ml (1.1) and median dWMH 0.1 ml (0.2). Demographic and imaging data are summarized in Table 1.

Distribution of cortical connectivity to WMH

Connectivity to WMH was averaged over all participants and visualized as a projection on the cortical surface in Freesurfer average space for all WMH as well as pWMH and dWMH, separately. As illustrated in Figure 2, distinct patterns with regional differences in connectivity to WMH can be observed. In general, WMH demonstrated high connectivity with cortical regions of the frontal and occipital lobes with lesser and more sparse connectivity to parietal and temporal lobes (Figure 2(a)). In reference to the Brainnetome anatomical atlas, cortical regions with the highest connectivity were almost exclusively located in the frontal,

Table 1. Sample characteristics and image analysis results.

Female sex [n, (%)]	424 (45.6%)
Age [years], median (IQR)	64 (14)
Vascular risk factors	
Current smoking [n, (%)]	167 (18.0%)
Hypertension* [n, (%)]	637 (68.5%)
Diabetes** [n, (%)]	74 (8.0%)
BMI, median (IQR)	26.36 (5.62)
Conventional MRI measures	
Brain volume [ml], median (IQR)	1483.7 (203.1)
WMH volume [ml], median (IQR)	0.6 (1.4)
pWMH volume [ml], median (IQR)	0.5 (1.1)
dWMH volume [ml], median (IQR)	0.1 (0.2)
WMH load [%], median (IQR)	0.04 (0.098)
pWMH load [%], median (IQR)	0.035 (0.081)
dWMH load [%], median (IQR)	0.006 (0.015)
Cortical thickness [mm], median (IQR)	2.4 (0.6)
Connectivity measures	
WMH connectivity [%], median (IQR)	0.5 (<0.1)
dWMH connectivity [%], median (IQR)	0.03 (<0.1)
pWMH connectivity [%], median (IQR)	0.4 (<0.1)

Abbreviations: dWMH = deep white matter hyperintensities, IQR = interquartile range, ml = milliliter, mm = millimeter, pWMH = periventricular white matter hyperintensities, WMH = white matter hyperintensities.
*Presence of hypertension was defined as blood pressure >= 140/90 mm/Hg, intake of antihypertensive medication or a self-reported prevalence of hypertension.
**Presence of diabetes was defined as blood glucose level > 126 mg/dl or a self-reported prevalence of diabetes.

occipital, limbic and insular cortex with less connectivity to cortical areas at the parietal and temporal lobes. Cortical areas with the highest connectivity to WMH were located at the cingulate gyrus (Brainnetome atlas region A32p and A32sg), orbital gyrus (A12/47l, A12/47o), inferior frontal gyrus (A44op), medio-ventral occipital cortex (vmPOS, rCunG, cCunG) and superior frontal gyrus (A9m, A10m). WMH connectivity to periventricular WMH demonstrated a similar pattern with highest connectivity observed in the frontal and occipital lobes and lesser connectivity located at the parietal and temporal cortices (Figure 2(b)). In contrast, deep WMH connectivity analysis resulted in a different cortical pattern. As illustrated in Figure 2(c), connectivity of dWMH was generally lower compared to pWMH and demonstrated a more homogeneous distribution over the cortical surface. In respect to the Brainnetome atlas, cortical regions with the highest dWMH connectivity were distributed without a preference for a specific lobe.

Connectivity to WMH and cortical thickness

Results from mixed-effect linear models including connectivity of all WMH (Model 1) or pWMH and
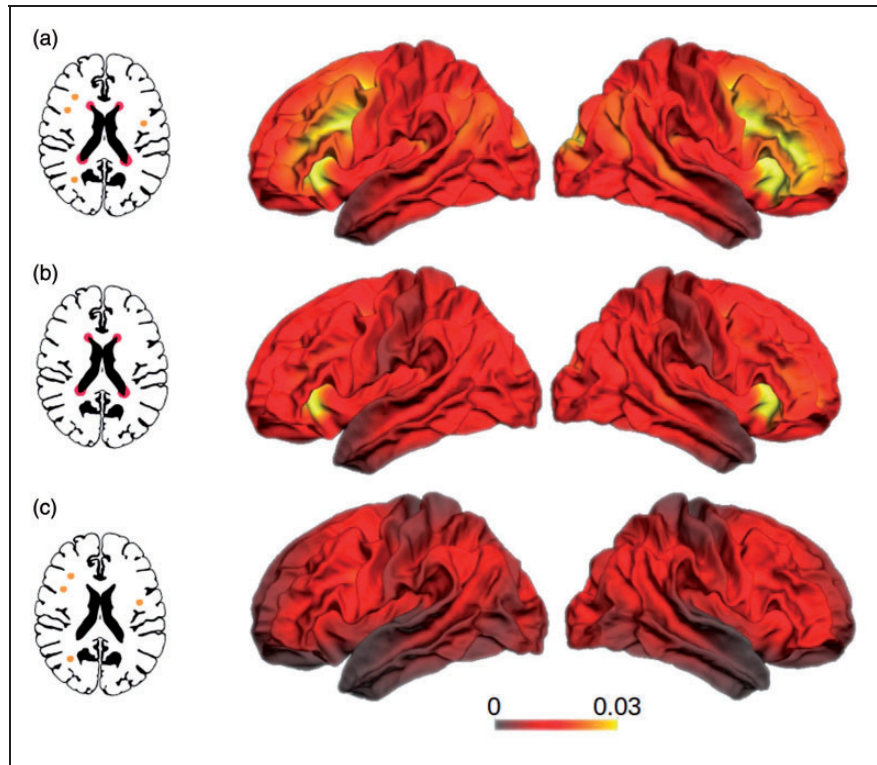
Figure 2. WMH cortical connectivity pattern grouped by WMH location. Frequency of cortical terminations of white matter tracts reconstructed by probabilistic tractography passing through white matter hyperintensities relative to all streamlines terminating in the respective vertex. Shown are connectivity patterns for white matter tracts passing through (a) all WMH as well as (b) periventricular white matter hyperintensities and (c) deep white matter hyperintensities. Color bars indicate the proportion of streamlines passing through a WMH on vertex level. This vertex-wise connectivity was only used for visualization, the statistical model includes the WMH connectivity summarized in 210 cortical regions. Please see Figure 1 for the methodological approach.

dWMH separately (Model 2) are shown in Table 2. In detail, Model 1 revealed a negative association between WMH connectivity and cortical thickness controlled for age, sex, hemisphere, region and participant ($t(49.12) = -2.71$, p = 0.009). Further factors associated with decreased cortical thickness were male sex ($t(92.62) = 4.64$, p < 0.001), left hemisphere ($t(19.24) = 7.89$, p < 0.001), higher age ($t(92.65) = -12.27$, p < 0.001), and higher lesion load ($t(93.33) = -2.82$, p = 0.005).

For Model 2, the linear mixed-effects model including the connectivity to the deep and periventricular WMH as independent variables, the pWMH revealed to have a negative association with cortical thickness ($t(62.33) = -3.38$, p = 0.001). Both the connectivity of dWMH (p = 0.333) and lesion load of dWMH (p = 0.495) were not significant associated with cortical thickness. All other effects were associated with a decreased cortical thickness in male participants, in the left hemisphere, with higher age and with higher periventricular lesion load (sex: $t(92.53) = 4.4$, p < 0.001; hemisphere: $t(19) = 7.78$, p < 0.001;

age: $t(92.57) = -11.9$, p < 0.001; periventricular lesion load: $t(94.45) = -2.72$, p = 0.007).

Discussion

Our study of topographical associations between white matter hyperintensity connectivity and cortical thickness provides two major results. First, WMH demonstrated a distinct pattern of connectivity to cortical regions with stronger connections to occipital and frontal brain areas with specific connectivity patterns for deep and periventricular WMH. Second, higher probability of connectivity between WMH and the cerebral cortex was associated with lower cortical thickness suggesting a direct relationship between the white matter lesions and cortical atrophy. This association was specifically found for periventricular lesions after adjusting for global connectivity, WMH lesion volume, and demographic factors.

In our study, we found thinner cortical regions associated with higher connectivity to WMH. These findings are in line with a previous report of cortical

Table 2. Results of linear mixed-effect models controlled for random effects.

Predictors of cortical thickness (DV)	Model 1*			Model 2**		
	Estimates	CI	p-Value	Estimates	CI	p-Value
Intercept	2.74	2.64–2.84	**<0.001**	2.73	2.63–2.84	**<0.001**
age	0.00	–0.01–0.00	**<0.001**	0.00	–0.01–0.00	**<0.001**
hemisphere (right)	0.01	0.01–0.01	**<0.001**	0.01	0.01–0.01	**<0.001**
sex (female)	0.03	0.02–0.04	**<0.001**	0.03	0.02–0.04	**<0.001**
Connectivity						
WMH	–0.25	–0.43––0.07	**0.009**	–	–	–
dWMH	–	–	–	0.05	–0.05–0.16	.333
pWMH	–	–	–	–0.39	–0.62––0.17	**0.001**
Lesion load						
WMH	–6.94	–11.76–2.12	**0.005**	–	–	–
dWMH	–	–	–	5.93	–11.10–22.96	.495
pWMH	–	–	–	–10.24	–17.63–2.85	**0.007**

Cortical thickness values were used as dependent variable. Both models included random effects of inter-individual and regional variability in cortical thickness and random slopes of region-specific effect size of WMH connectivity and WMH lesion load.
P-values < 0.05 are indicated in bold. Abbreviations: CI = 95% confidence interval, DV = dependent variable, dWMH = deep white matter hyperintensities, pWMH = periventricular white matter hyperintensities, WMH = white matter hyperintensities.
*Model 1 includes connectivity and lesion load of WMH.
**Model 2 includes connectivity and lesion load of pWMH and dWMH.

thinning and white matter connectivity to subcortical white matter lesions in CADASIL, a genetic disorder with autosomal dominant hereditary transmission characterized by cerebral arteriopathy with subcortical infarcts and leukoencephalopathy.[15] In this work, cortical atrophy was shown to be specifically prominent in regions with a higher probability of connectivity to subcortical infarcts compared to unconnected cortical areas. Similar remote effects of isolated stroke lesions on distant, yet connected cortical areas were found in stroke patients, where cortical thinning occurred as a result of secondary degeneration of inter- and intrahemispheric white matter tracts.[16] However, studies on the longitudinal association of WMH burden and cortical thickness are contradictory. Several studies demonstrated a pronounced longitudinal decline in cortical thickness related to higher burden of WMH volume, whilst a cohort study found no longitudinal effect of WMH on cortical atrophy in a large group of elder community-dwelling subjects.[32–34]

We further studied distinct connectivity profiles of periventricular and deep WMH and observed differences in the association with cortical thickness according to the topological classification of WMH. Cortical thickness was significantly lower with stronger connectivity to pWMH while the connectivity to dWMH had no impact on cortical thickness. In line with this, the lesion load of pWMH had a significant impact on cortical thickness, while the lesion load of dWMH did not. The distinction between periventricular and deep white matter hyperintensities is of great importance when

analyzing the effect of WMH on cortical thickness since pWMH and dWMH are known to differ both in the effect on cortical thickness and in their clinical manifestation. While pWMH are known to mainly affect cognitive functioning including general cognitive decline and mental processing speed, dWMH had no effect on cognition but increases the risk of developing depressive symptoms, late-onset depression and vascular dementia.[35–38] Additionally, previous literature found that a higher pWMH volume was related to cortical thinning in a clinical sample with cognitively impaired patients, showing that pWMH was related to frontal lobe thinning while dWMH had no effect.[8] Moreover, our results are in line with reports of a longitudinal relationship between pWMH volume and decline in cortical thickness in a patient population with symptomatic atherosclerotic disease, while dWMH again showed no significance.[34]

Visualization of WMH cortical connectivity patterns in our study revealed distinct characteristics in topology and cortical connectivity profiles. All types of WMH (overall, deep and periventricular) were found to primarily connect to brain regions in the frontal and occipital lobes with less connectivity to areas in anterior temporal lobe and pre- and postcentral gyri. This visual impression was confirmed by applying a standardized anatomical atlas demonstrating the rank order of brain regions with highest connectivity to subcortical WMH.

Furthermore, there was a striking disparity in prevalence and connectivity to cortical surfaces for

periventricular and deep WMH. First, pWMH were found to be much more prevalent than dWMH. This distribution of WMH is comparable to normal aging participants from other studies with more hyperintensities in the periventricular white matter and few lesions in the deep white matter.[20,39] Moreover, pWMH showed a connectivity pattern similar to overall WMH with strongly connected regions located in the frontal, occipital, limbic and insular lobe. In contrast, dWMH connectivity was overall lower and followed a different pattern that was more evenly distributed across all cortical brain regions. These distinctive connectivity profiles are most likely explained by the characteristic anatomical locations of dWMH and pWMH in relation to specific types of white matter fiber tracts. In detail, dWMH and pWMH could be associated with disruption of short and long association fibers, respectively. Short association fibers consist of arcuate U-shaped fibers directly underlying the cortex, mainly located in the parietal and temporal lobe.[40,41] They connect adjacent gyri and are primarily prone to disruption by dWMH. On the other hand, long association fibers connect distant brain regions with each other, run in close proximity to the periventricular white matter and are therefore often affected by periventricular WMH.[40,42] Moreover, previous studies suggested that white matter tracts terminating at the frontal and occipital cortex have a long tract length on average while the postcentral and superior temporal gyri are primarily connected to white matter tracts with a rather short tract length.[43]

This study was aimed at unraveling the relationship between WMH resulting from CSVD and cortical thickness in a large cohort of 930 participants at elevated risk for cardiovascular diseases. Compared with previous studies on CSVD, our sample was rather mildly affected as suggested by a lower median WMH volume.[44–46] Nonetheless, we were able to detect a relevant association between higher probability of connectivity between WMH and the cerebral cortex and cortical thickness in our participants. This indicates that distant grey matter degeneration is linked to WMH and observable already in the early stages of CSVD.

While the large number of participants and advanced methodological approaches are strengths of our study, we focused on associations of imaging findings and potential pathophysiological mechanisms in CSVD and did not analyze cognitive functioning in this paper. This can therefore be considered a limitation of our study. Since the assumed effects of WMH connectivity (especially the differentiation between pWMH and dWMH connectivity) on cognitive dysfunctions were not extensively investigated previously, further research is necessary to address this topic.

Moreover, although the Hamburg City Health Study is a longitudinal cohort study, only cross-sectional data are currently available.

In conclusion, we reveal a direct relationship between WMH and cortical atrophy through profiles and degree of underlying white matter connectivity. Our results indicate that reduced cortical thickness in participants with cardiovascular risk factors is associated with a higher connection probability to underlying to WMH. Further studies are needed to analyze the effect of the connectivity and secondary cortical neurodegeneration on cognitive performance.

Busch, Chia-Jung
Büchel, Christian
Debus, Eike Sebastian
Fiehler, Jens
Gallinat, Jürgen
Gellißen, Simone
Gerloff, Christian
Girdauskas, Evaldas
Gosau, Martin
Härter, Martin
Harth, Volker
Heydecke, Guido
Huber, Tobias
Jagodzinski, Annika
Johansen, Christoffer
Koch-Gromus, Uwe
Konnopka, Alexander
König, Hans-Helmut
Kromer, Robert
Kubisch, Christian
Kühn, Simone
Löwe, Bernd
Lund, Gunnar
Meyer, Christian
Nienhaus, Albert
Pantel, Klaus
Püschel, Klaus
Reichenspurner, Hermann,
Sauter, Guido
Scherer, Martin
Schnabel, Renate
Schulz, Holger
Smeets, Ralf
Spitzer, Martin S.
Terschüren, Claudia
Thomalla, Götz
von dem Knesebeck, Olaf
Waschki, Benjamin
Wegscheider, Karl
Zeller, Tanja
Zyriax, Birgit-Christiane
Steering board:
Augustin, Matthias
Blankenberg, Stefan
Gallinat, Jürgen
Gerloff, Christian
Härter, Martin
Jagodzinski, Annika
Johansen, Christoffer
Koch-Gromus, Uwe
Sauter, Guido
Zeller, Tanja
Wegscheider, Karl
Betz, Christian/Heydecke, Guido/Gosau, Martin
Research consortium:
Aarabi, Ghazal
Andrees, Valerie
Behrendt, Christian Brassen, Stefanie
Brekenfeld, Caspar

Brünahl, Christian
Busch, Chia-Jung
Freitag, Janina
Gallinat, Jürgen
Gellißen, Susanne
Girdauskas, Evaldas
Heidemann, Christoph
Hussein, Yassin
Klein, Verena
Kofahl, Christopher
Kohlmann, Sebastian
Konnopka, Alexander
Kühn, Simone
Lühmann, Dagmar
Lund, Gunnar
Magnussen, Christina
Meyer, Christian
Nagel, Lina
Petersen, Elina
Scherschel, Katharina
Schiffner, Ulrich
Schnabel, Renate
Schulz, Holger
Seedorf, Udo
Smeets, Ralf
Terschüren, Claudia
Thomalla, Götz
Waschki, Benjamin
Zeller, Tanja
Zyriax, Birgit-Christiane

Declaration of conflicting interests

Authors' contributions

CM and BMF designed and conceptualized the study, analyzed and interpreted the data, and made major contribution in revising the manuscript. ES analyzed and interpreted the

data and made contribution in revising the manuscript. MP analyzed and interpreted the data. KE, UH, AJ, KB and JF participated in the data acquisition. CG drafted and revised the manuscript. GT and BC made major contributions in supervising and coordinating the study and in drafting and revising the manuscript.

ORCID iDs

Eckhard Schlemm https://orcid.org/0000-0002-5729-2935
Marvin Petersen https://orcid.org/0000-0001-6426-7167

References

1. Wardlaw JM, Smith EE, Biessels GJ, et al. Neuroimaging standards for research into small vessel disease and its contribution to ageing and neurodegeneration. *Lancet Neurol* 2013; 12: 822–838.
2. Debette S and Markus HS. The clinical importance of white matter hyperintensities on brain magnetic resonance imaging: systematic review and meta-analysis. *BMJ* 2010; 341: c3666.
3. Frey BM, Petersen M, Mayer C, et al. Characterization of white matter hyperintensities in large-scale MRI-studies. *Front Neurol* 2019; 10: 238.
4. Georgakis MK, Duering M, Wardlaw JM, et al. WMH and long-term outcomes in ischemic stroke: a systematic review and meta-analysis. *Neurology* 2019; 92: e1298–e1308.
5. Dufouil C, De Kersaint-Gilly A, Besançon V, et al. Longitudinal study of blood pressure and white matter hyperintensities: the EVA MRI cohort. *Neurology* 2001; 56: 921–926.
6. Power MC, Deal JA, Sharrett AR, et al. Smoking and white matter hyperintensity progression: the ARIC-MRI study. *Neurology* 2015; 84: 841–848.
7. Du A-T, Schuff N, Chao LL, et al. White matter lesions are associated with cortical atrophy more than entorhinal and hippocampal atrophy. *Neurobiol Aging* 2005; 26: 553–559.
8. Seo SW, Lee J-M, Im K, et al. Cortical thinning related to periventricular and deep white matter hyperintensities. *Neurobiol Aging* 2012; 33: 1156–1167.e1.
9. Tuladhar AM, Reid AT, Shumskaya E, et al. Relationship between white matter hyperintensities, cortical thickness, and cognition. *Stroke* 2015; 46: 425–432.
10. Habes M, Sotiras A, Erus G, et al. White matter lesions. *Neurology* 2018; 91: e964–e975.
11. Alosco ML, Gunstad J, Jerskey BA, et al. The adverse effects of reduced cerebral perfusion on cognition and brain structure in older adults with cardiovascular disease. *Brain Behav* 2013; 3: 626–636.
12. Thong JYJ, Hilal S, Wang Y, et al. Association of silent lacunar infarct with brain atrophy and cognitive impairment. *J Neurol Neurosurg Psychiatry* 2013; 84: 1219–1225.
13. ter Telgte A, van Leijsen EMC, Wiegertjes K, et al. Cerebral small vessel disease: from a focal to a global perspective. *Nat Rev Neurol* 2018; 14: 387–398.

14. Duering M, Righart R, Wollenweber FA, et al. Acute infarcts cause focal thinning in remote cortex via degeneration of connecting fiber tracts. *Neurology* 2015; 84: 1685–1692.
15. Duering M, Righart R, Csanadi E, et al. Incident subcortical infarcts induce focal thinning in connected cortical regions. *Neurology* 2012; 79: 2025–2028.
16. Cheng B, Dietzmann P, Schulz R, et al. Cortical atrophy and transcallosal diaschisis following isolated subcortical stroke. *J Cereb Blood Flow Metab* 2020; 40: 611–621.
17. Jagodzinski A, Johansen C, Koch-Gromus U, et al. Rationale and Design of the Hamburg City Health Study. *Eur J Epidemiol* 2020; 35: 169–181.
18. D'Agostino RB, Vasan RS, Pencina MJ, et al. General cardiovascular risk profile for use in primary care. *Circulation* 2008; 117: 743–753.
19. Griffanti L, Zamboni G, Khan A, et al. BIANCA (brain intensity AbNormality classification algorithm): a new tool for automated segmentation of white matter hyperintensities. *Neuroimage* 2016; 141: 191–205.
20. Griffanti L, Jenkinson M, Suri S, et al. Classification and characterization of periventricular and deep white matter hyperintensities on MRI: a study in older adults. *Neuroimage* 2018; 170: 174–181.
21. DeCarli C, Fletcher E, Ramey V, et al. Anatomical mapping of white matter hyperintensities (WMH). *Stroke* 2005; 36: 50–55.
22. Smith RE, Tournier JD, Calamante F, et al. Anatomically-constrained tractography: Improved diffusion MRI streamlines tractography through effective use of anatomical information. *Neuroimage* 2012; 62: 1924–1938.
23. Tournier J-D, Calamante F, Connelly A. Improved probabilistic streamlines tractography by 2nd order integration over fibre orientation distributions. *Proc Int Soc Magn Reson Med* 2010; 1670.
24. Tournier J-D, Smith RE, Raffelt D, et al. MRtrix3: a fast, flexible and open software framework for medical image processing and visualisation. *bioRxiv* 2019; 551739.
25. Smith RE, Tournier JD, Calamante F, et al. SIFT2: Enabling dense quantitative assessment of brain white matter connectivity using streamlines tractography. *Neuroimage* 2015; 119: 338–351.
26. Fischl B and Dale AM. Measuring the thickness of the human cerebral cortex from magnetic resonance images. *Proc Natl Acad Sci U S A* 2000; 97: 11050–11055.
27. Fan L, Li H, Zhuo J, et al. The human brainnetome atlas: a new brain atlas based on connectional architecture. *Cereb Cortex* 2016; 26: 3508–3526.
28. Luders E, Narr KL, Thompson PM, et al. Hemispheric asymmetries in cortical thickness. *Cereb Cortex* 2006; 16: 1232–1238.
29. Sowell ER, Peterson BS, Kan E, et al. Sex differences in cortical thickness mapped in 176 healthy individuals between 7 and 87 years of age. *Cereb Cortex* 2007; 17: 1550–1560.
30. Zheng F, Liu Y, Yuan Z, et al. Age-related changes in cortical and subcortical structures of healthy adult

brains: a surface-based morphometry study. *J Magn Reson Imaging* 2019; 49: 152–163.

31. R Core Team. *R: a language and environment for statistical computing*. Vienna, Austria: R Foundation for Statistical Computing, 2018.

32. Dickie DA, Karama S, Ritchie SJ, et al. Progression of white matter disease and cortical thinning are not related in older community-dwelling subjects. *Stroke* 2016; 47: 410–416.

33. Ritchie SJ, Dickie DA, Cox SR, et al. Brain volumetric changes and cognitive ageing during the eighth decade of life. *Hum Brain Mapp* 2015; 36: 4910–4925.

34. Kloppenborg RP, Nederkoorn PJ, Grool AM, SMART Study Group, et al. Cerebral small-vessel disease and progression of brain atrophy: the SMART-MR study. *Neurology* 2012; 79: 2029–2036.

35. De Groot JC, De Leeuw FE, Oudkerk M, et al. Periventricular cerebral white matter lesions predict rate of cognitive decline. *Ann Neurol* 2002; 52: 335–341.

36. De Groot JC, de Leeuw FE, Oudkerk M, et al. Cerebral white matter lesions and depressive symptoms in elderly adults. *Arch Gen Psychiatry* 2000; 57: 1071–1076.

37. Smith CD, Johnson ES, Van Eldik LJ, et al. Peripheral (deep) but not periventricular MRI white matter hyperintensities are increased in clinical vascular dementia compared to Alzheimer's disease. *Brain Behav* 2016; 6: 1–11.

38. Van Den Heuvel DMJ, Ten Dam VH, De Craen AJM, et al. Increase in periventricular white matter hyperintensities parallels decline in mental processing speed in a non-demented elderly population. *J Neurol Neurosurg Psychiatry* 2006; 77: 149–153.

39. Yoshita M, Fletcher E, Harvey D, et al. Extent and distribution of white matter hyperintensities in normal aging, MCI, and AD. *Neurology* 2006; 67: 2192–2198.

40. Haines DE and Mihailoff GA. The Telencephalon. In: Haines DE and Mihailoff, GA (eds), *Fundamental Neuroscience for Basic and Clinical Applications*. 5th ed. Baltimore: Wolters Kluwer Health; 2018. pp. 225–240.e1.

41. Oishi K. *MRI atlas of human white matter*. Cambridge, MA: Academic Press, 2011.

42. Sarubbo S, De Benedictis A, Merler S, et al. Structural and functional integration between dorsal and ventral language streams as revealed by blunt dissection and direct electrical stimulation. *Hum Brain Mapp* 2016; 37: 3858–3872.

43. Padula MC, Schaer M, Scariati E, et al. Quantifying indices of short- and long-range white matter connectivity at each cortical vertex. *PLoS One* 2017; 12: e0187493.

44. De Laat KF, Tuladhar AM, Van Norden AGW, et al. Loss of white matter integrity is associated with gait disorders in cerebral small vessel disease. *Brain* 2011; 134: 73–83.

45. Duering M, Csanadi E, Gesierich B, et al. Incident lacunes preferentially localize to the edge of white matter hyperintensities: insights into the pathophysiology of cerebral small vessel disease. *Brain* 2013; 136: 2717–2726.

46. Tuladhar AM, van Dijk E, Zwiers MP, et al. Structural network connectivity and cognition in cerebral small vessel disease. *Hum Brain Mapp* 2016; 37: 300–310.

Free-water diffusion MRI detects structural alterations surrounding white matter hyperintensities in the early stage of cerebral small vessel disease

Carola Mayer[1] ⓘ, Felix L Nägele[1], Marvin Petersen[1] ⓘ,
Benedikt M Frey[1], Uta Hanning[2], Ofer Pasternak[3,4],
Elina Petersen[5,6], Christian Gerloff[1], Götz Thomalla[1] and
Bastian Cheng[1]

Abstract

In cerebral small vessel disease (CSVD), both white matter hyperintensities (WMH) of presumed vascular origin and the normal-appearing white matter (NAWM) contain microstructural brain alterations on diffusion-weighted MRI (DWI). Contamination of DWI-derived metrics by extracellular free-water can be corrected with free-water (FW) imaging. We investigated the alterations in FW and FW-corrected fractional anisotropy (FA-t) in WMH and surrounding tissue and their association with cerebrovascular risk factors. We analysed 1,000 MRI datasets from the Hamburg City Health Study. DWI was used to generate FW and FA-t maps. WMH masks were segmented on FLAIR and T1-weighted MRI and dilated repeatedly to create 8 NAWM masks representing increasing distance from WMH. Linear models were applied to compare FW and FA-t across WMH and NAWM masks and in association with cerebrovascular risk. Median age was 64 ± 14 years. FW and FA-t were altered 8 mm and 12 mm beyond WMH, respectively. Smoking was significantly associated with FW in NAWM ($p = 0.008$) and FA-t in WMH ($p = 0.008$) and in NAWM ($p = 0.003$) while diabetes and hypertension were not. Further research is necessary to examine whether FW and FA-t alterations in NAWM are predictors for developing WMH.

Keywords

Aging, brain imaging, cerebrovascular disease, diffusion weighted MRI, small vessel disease

Received 11 November 2021; Revised 23 February 2022; Accepted 8 March 2022

Introduction

White matter hyperintensities of presumed vascular origin (WMH) are manifestations of cerebral small vessel disease (CSVD) on fluid-attenuated inversion recovery (FLAIR) magnetic resonance imaging (MRI) and are characterized by white matter axon loss, demyelination, and gliosis.[1] They are particularly prevalent with increasing age and extent of cerebrovascular risk factors and are associated with cognitive impairment, dementia, stroke, depression, and mortality.[2–7] However, in CSVD, microstructural alterations of the white matter are not confined to the visible WMH but also extend to brain areas without apparent

[1]Department of Neurology, University Medical Center Hamburg-Eppendorf, Hamburg, Germany
[2]Department of Diagnostic and Interventional Neuroradiology, University Medical Center Hamburg-Eppendorf, Hamburg, Germany
[3]Department of Psychiatry, Brigham and Women's Hospital, Harvard Medical School, USA
[4]Department of Radiology, Brigham and Women's Hospital, Harvard Medical School, USA
[5]Clinical for Cardiology, University Heart and Vascular Center, Germany
[6]Population Health Research Department, University Heart and Vascular Center, Hamburg, Germany

Corresponding author:
Carola Mayer, Department of Neurology, University Medical Center Hamburg-Eppendorf, Martinistraße 52, 20246 Hamburg, Germany.
Email: c.mayer@uke.de

changes on FLAIR, referred to as normal-appearing white matter (NAWM).[1]

Microstructural alterations of the white matter can be quantified with metrics derived from diffusion-weighted MRI (DWI). For conventional diffusion-tensor imaging (DTI) metrics, a tensor model is applied on DWI which calculates a single compartment of the diffusion signal within each voxel of the brain. However, tensors from a single compartment are susceptible for partial volume effects which occur when several tissue types reside in the same voxel. For example, the presence of extracellular free-water (FW) can contaminate the derived DTI metrics and limit the biological specificity of DTI.[8] To overcome this limitation, an algorithm for FW elimination was developed which models two compartments of the diffusion signal. One compartment models FW as isotropic with diffusivity of water at body temperature. The voxel-wise fractional volume of the FW compartment is used to measure its contribution. The second compartment – the tissue compartment – applies a diffusion tensor to characterize diffusion in the proximity of cells, from which scalar measures such as fractional anisotropy of the tissue (FA-t) can be derived.[8] When conventional and FW-corrected DTI metrics were compared, FW-corrected measures showed the strongest association with demographic parameters and cognitive functioning and was also superior in predicting mild cognitive impairments (MCI), Alzheimer's disease and vascular dementia.[9–16]

In CSVD, the microstructural properties of NAWM are intricate. Specifically, conventional DTI metrics including fractional anisotropy (FA) and mean diffusivity (MD) indicate that the microstructural alterations of NAWM range from almost none to extensive, depending on factors such as age, WMH burden and cognitive functioning.[17–20] In this work, we set to identify if FW captures microstructural changes of the white matter depending on the distance to WMH, defining larger areas surrounding visible WMH as 'WMH penumbra'.[21] We therefore examined FW and FA-t alterations in multiple NAWM regions that are adjacent to the WMH with different distances, to better identify the WMH penumbra. Moreover, we aimed to identify if FW and FA-t are associated with cerebrovascular risk factors in WMH and WMH penumbra.

Materials and methods

Study design and participants

We analysed data from participants of the Hamburg City Health Study (HCHS). HCHS is a prospective, single-centre, epidemiologic cohort study aiming to improve the understanding of risk factors and prognosis in major chronic diseases. A detailed description of the study design was published previously.[22] In short, 45,000 citizens of Hamburg, Germany, between the age of 45 and 74 years are invited to an extensive baseline evaluation. Brain MRI is conducted in a randomly selected control group and in a subgroup of participants with increased risk for cardiovascular diseases as defined by a Framingham Risk Score >7.[23] For the current analysis, we included the first 1,000 brain MRI datasets from HCHS participants at baseline. 21 participants had to be excluded because of missing imaging data (9 without imaging data, 3 without FLAIR, 9 without DWI), 39 participants because of incomplete DWI acquisition, 1 participant because of poor FLAIR image quality, and 9 participants because of technical issues during WMH segmentation. After initial image processing, 30 participants had segmented WMH <4 voxels and were therefore excluded. The ethics committee of the State of Hamburg Chamber of Medical Practitioners (Ethik-Kommission Landesärztekammer Hamburg, PV5131) approved the HCHS, and all participants provided written informed consent. The HCHS has been registered at ClinicalTrials.gov (NCT03934957). The HCHS design ensures that all involved individuals abide by the ethical principles described in the current revision of the Declaration of Helsinki, by Good Clinical Practice (GCP) and by Good Epidemiological Practice (GEP). The data underlying this article cannot be shared publicly for the privacy of individuals that participated in the study.

Clinical data assessment

All participants of the HCHS received detailed anamnestic and clinical examination of which age, sex, (family) history of diseases and cardiovascular risk factors are of interest for the current study. A detailed study protocol has been published previously.[22] In short, diabetes was defined as either self-reported prevalence of diabetes or a blood glucose level >126 mg/dl. Hypertension was defined as either self-reported prevalence of hypertension, blood pressure >=140/90 mmHg or intake of antihypertensive medication. The smoking status (yes/no) refers to active smokers and non-smokers.

MRI sequences. All images were acquired on a single 3T Siemens Skyra MRI scanner (Siemens, Erlangen, Germany) and applied the same imaging protocol. For 3D T1-weighted anatomical images, rapid acquisition gradient-echo sequence (MPRAGE) was used with the following sequence parameters: repetition time (TR) = 2500 ms, echo time (TE) = 2.12 ms, 256 axial slices, slice thickness (ST) = 0.94 mm, and in-plane

resolution (IPR) $= 0.83 \times 0.83$ mm. 3D T2-weighted FLAIR images were acquired with the following parameters: TR $= 4700$ ms, TE $= 392$ ms, 192 axial slices, ST $= 0.9$ mm, and IPR $= 0.75 \times 0.75$ mm. For single-shell diffusion MRI, 75 axial slices were obtained covering the whole brain with gradients (b $= 1000$ s/mm^2) applied along 64 noncollinear directions with the following sequence parameters: TR $= 8500$ ms, TE $= 75$ ms, ST $= 2$ mm, IPR $= 2 \times 2$ mm with an anterior-posterior phase-encoding direction.

Imaging post-processing and definition of regions of interest

An overview of the image processing pipeline is visualized in Figure 1. FLAIR and T1-weighted images were resampled to $1 \times 1 \times 1$ mm for the purpose of the registration between modalities. To register the structural images into DWI space without degrading the image resolution to the DWI ($2 \times 2 \times 2$ mm), we created a registration target (resampled DWI into $1 \times 1 \times 1$ mm). The FLAIR and T1-weighted images were then nonlinearly registered on the 1x1x1mm DWI with nearest-neighbour interpolation. Except for the WMH segmentation which happened on the $1 \times 1 \times 1$ mm structural images, all subsequent steps of the imaging analysis were conducted on the original DWI in $2 \times 2 \times 2$ mm resolution and the registered FLAIR and T1-weighted images in $1 \times 1 \times 1$ mm resolution.

The standardized Freesurfer processing pipeline (Version 5.3) was applied on the registered T1-weighted images for the segmentation of brain structures including grey and white matter, ventricles, brainstem and cerebellum.[24] Imaging data of insufficient quality for segmentation were excluded. For the calculation of the brain volume, the brain tissue without the ventricles was summed. White matter masks were further edited by subtracting the brainstem, cerebellum, and voxels located at the boundary to the grey matter (Figure 1(a)).

Segmentation of WMH and NAWM ROIs

WMH were segmented with FSL's Brain Intensity AbNormality Classification Algorithm (BIANCA).[25] The fully automated, supervised k-nearest neighbour (k-NN) algorithm is based on native-space T1-weighted and FLAIR images and considers spatial information of each voxel after linear registration to Montreal Neurological Institute (MNI) space. As a training dataset for the k-NN algorithm, 100 FLAIR images were manually segmented by two experienced investigators (CM & MP) independently to form the training dataset (mean Dice Similarity Index of the training dataset: 0.63). Based on the segmentation of

the automatic algorithm, the WMH volume was calculated. The WMH mask was registered into DWI-space by applying the warp fields from the structural image registration. After registration, the WMH mask was resized via interpolation and binarized to match the resolution of the original DWI data ($2 \times 2 \times 2$ mm) to enable overlay on FW and FA-t maps in the subsequent analyses.

After resizing of the WMH mask, we filtered them for minimum WMH size of 4 voxels (equivalent to 0.032 ml on a $2 \times 2 \times 2$ mm image). By setting this threshold, we ensured that all imaging parameters measured within WMH are based on a representative number of voxels. Consequently, all participants with a WMH volume <0.032 ml were excluded. WMH load was defined as the ratio of WMH volume and brain volume. We further calculated the logarithm of the WMH load, referred to as 'log WMH load', to obtain normally distributed data. For the analysis of NAWM, regions of interest (ROIs) were created by multiple dilations in the 3-dimensional space in white matter areas adjacent to the WMH in 1 voxel increments (2 mm). This process was repeated 8 times, creating 8 NAWM masks representing increasing distance to the WMH. We avoided duplicate inclusion of voxels in more than one ROI by excluding all voxels overlapping with the previously created ROI in each dilation. In the final step, a total of 8 rim-shaped ROIs (each 2 mm size, in total a diameter of 16 mm surrounding WMH) were available and refined by including only voxels from the pre-defined white matter segmentation (Figure 1(b)). The size of the WMH penumbra was chosen based on previous literature.[26,27]

Calculation of FW & FA-t

The bi-tensor model optimized for single-shell DWI was fitted to the original DWI data to calculate the signal attenuation for extracellular FW and tissue compartments separately.[8] The regularized non-linear fit yielded FW maps, and FW-corrected diffusion tensors of the tissue compartment, from which the FW-corrected fractional anisotropy (FA-t) was calculated. Utilizing WMH and surrounding NAWM ROIs, FW and FA-t were extracted and subsequently averaged for each ROI for further statistical analysis (Figure 1(c)).

Statistical analysis

Demographic data was summarized and reported with median and interquartile range (IQR). Normality of the data was checked with skewness and kurtosis, with the thresholds suggested for large datasets.[28] We conducted two separate statistical analyses. First, we tested for differences of FW and FA-t between WMH
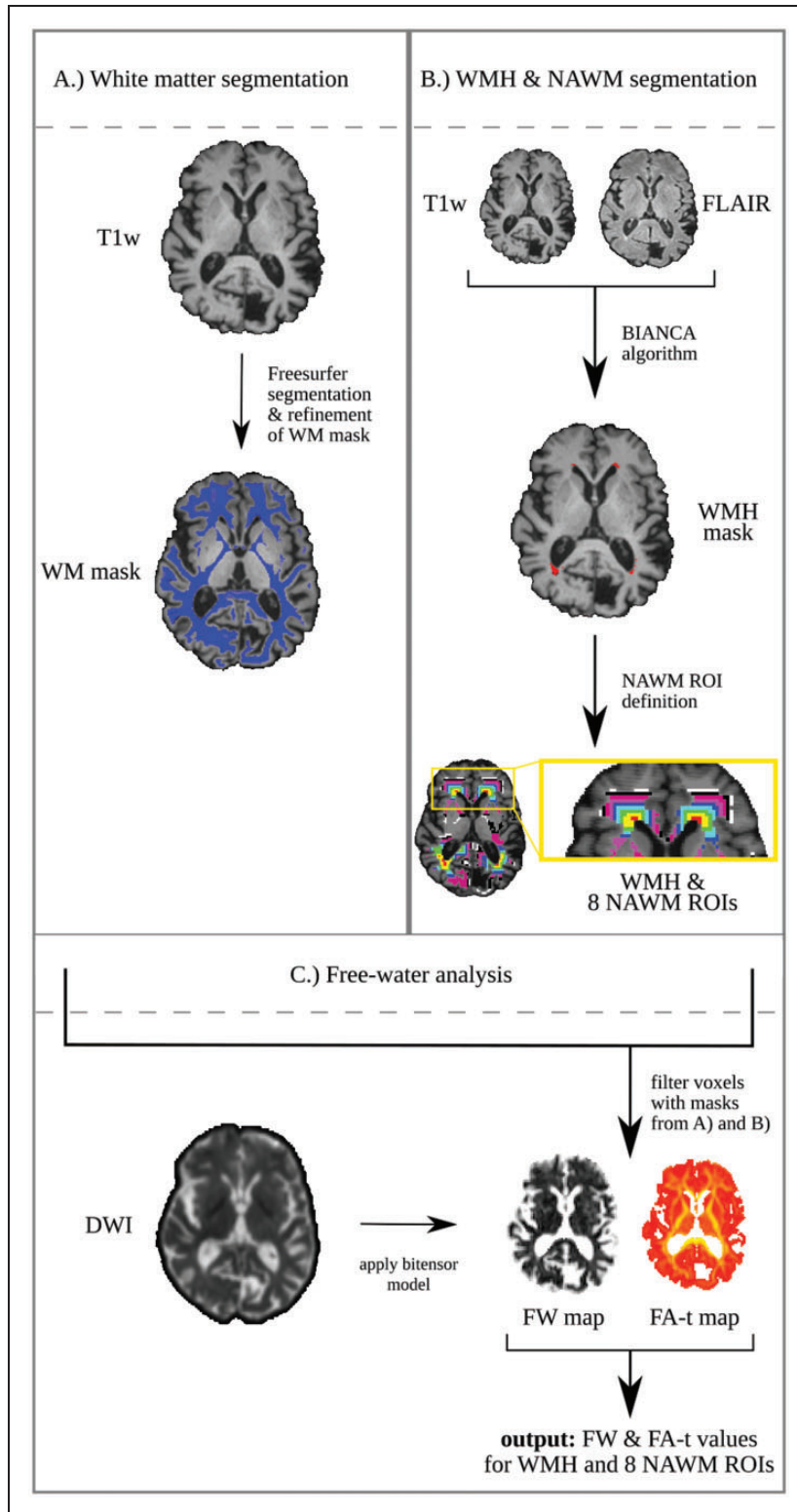
Figure 1. Visualization of the image processing pipeline. (a) Definition of white matter (WM) masks using T1-weighted images and Freesurfer.[24] The WM mask was further refined by excluding structures such as brainstem and cerebellum. (b) T1-weighted images and FLAIR were used for segmentation of the white matter hyperintensities (WMH) with a trained automatic algorithm (BIANCA).[25] The WMH mask was registered and resized to match the original DWI data resolution (2x2x2mm). Registered WMH masks were repeatedly dilated by one voxel and filtered with the white matter mask. (c) A bi-tensor model was applied on original DWI data to extract a tissue compartment and a free-water compartment from which free-water and free-water corrected FA (FA-t) maps were extracted. The WMH and NAWM ROIs were applied on the free-water and FA-t maps to calculate the average values for each region. DWI: diffusion-weighted image; FA: fractional anisotropy; FLAIR: fluid-attenuated inversion recovery; FW: free-water; NAWM: normal-appearing white matter; ROI: region of interest T1w: T1-weighted image; WM: white matter; WMH: white matter hyperintensities.

and surrounding NAWM ROIs with increasing distance to the WMH. For this purpose, we conducted separate linear mixed-effects models with either FW or FA-t as the dependent variable. We added a variable with 9 categories (i.e., WMH and 8 NAWM ROIs) and pre-defined contrasts with forward difference coding to compare each white matter ROI with the next rim of NAWM ROI. Age, sex, and log WMH load were added as independent variables. Since FA-t and FW were measured at multiple regions within subjects, a random effect was included to control for individual differences. Based on the results from this model, NAWM ROIs with significantly different FW values were merged into one single ROI, termed 'WMH-FW-penumbra'. In the second analysis, we tested the association of FW and FA-t values in WMH and WMH-FW-penumbra ROIs with cerebrovascular risk factors separately in two multivariate linear regressions. As before, age, sex, and log WMH load were added as independent variables next to variables of vascular risk (i.e., diabetes, smoking and hypertension). Results of all linear regressions are presented with standardized coefficients (β) and p-values (p). Effects were interpreted as significant if $p < 0.05$. All analysis was carried out using R Version 3.6.3.[29]

Supplementary analysis. To investigate the contribution of physiological, CSVD-independent effects on alterations of free-water in WMH-FW-penumbra, we conducted two post-hoc, supplementary analyses: 1) we separately calculated periventricular alterations of free-water in the WMH-FW-penumbra of deep and periventricular WMH. This was done to investigate if similar effects in the WMH-FW-penumbra would be observed in deep WMH, which occur in a much more heterogeneous spatial pattern as compared to periventricular WMH, which are more stereotypically located in the white matter in close proximity to the ventricles.[30,31] 2) We compared free-water extent in the WMH-FW-penumbra in both participants from the first (lowest) and forth (highest) quartile of WMH volume. This approach was chosen to investigate if the extent of free-water changes would occur at similar distances from WMH independent of WMH extent. Methods and detailed results can be found in the supplement.

Results

Study sample characteristics

We included MRI data of the first N = 1,000 participants of the HCHS in our analysis. The final dataset comprises 900 participants (412 females; 45.8%) with a median age of 64 years (IQR = 14). The sample characteristics are summarized in Table 1.

Differences in white matter microstructure across ROIs

Results from linear mixed-effects models demonstrated significant differences in FW between concentrically adjacent ROIs including WMH and the first 4 NAWM ROIs (2 mm–8 mm) with the highest FW in the WMH and lower FW values with increasing distance from the WMH (Table 2, Figure 2). The differences between ROIs were significant after controlling for age, sex, and log WMH load. There were no significant differences of FW in adjacent ROIs between 10 mm–16 mm. Independent from the region, the results show that FW values were higher with increasing age ($\beta = 0.008$, $p < 0.001$) and higher log WMH load ($\beta = 0.007$, $p < 0.001$) while sex was not significant ($\beta = 0.003$, $p = 0.051$).

The linear mixed-effects model also revealed that FA-t differs significantly in all concentrically adjacent ROIs between WMH and 14 mm distance from the WMH. These differences were significant after controlling for age, sex, and log WMH load (Table 2, Figure 3). FA-t was the lowest in WMH, increased to a peak at the 4 mm ROI and declined with further increasing distance. Of all comparisons of concentrically adjacent ROIs, only the comparison of FA-t between the ROI at 14 mm with the ROI at 16 mm did not show a significant difference. Independent of the white matter region, FA-t was generally significantly lower with higher age ($\beta = -0.002$, $p = 0.01$) and higher log WMH load ($\beta = -0.004$, $p < 0.001$) while sex did not have a significant effect ($\beta = -0.001$, $p = 0.35$).

Table 1. Sample characteristics with demographic data, cerebrovascular risk factors, and MRI measures.

Demographic characteristics	
Female sex, n (%)	412 (45.8%)
Age [years], median (IQR)	64 (14)
Cerebrovascular risk factors	
Active smoker, n (%)	141 (15.7%)
Diabetes mellitus,[a] n (%)	73 (8.1%)
Hypertension,[b] n (%)	618 (68.7%)
Conventional MRI measures	
Total brain volume [ml], median (IQR)	1,483 (203)
WMH volume [ml], median (IQR)	0.66 (1.4)
WMH load [%], median (IQR)	0.04 (0.1)

IQR: interquartile range; ml: millilitre; n: number of participants; WMH: white matter hyperintensities.
[a]Prevalence of diabetes mellitus was defined as blood glucose level >126 mg/dl or self-report.
[b]Prevalence of hypertension was defined as blood pressure >= 140/90 mm/Hg, intake of antihypertensive medication or self-report.

Table 2. Results of multivariate mixed-effects linear regression analysing free-water and FA-t in WMH and adjacent NAWM ROIs.
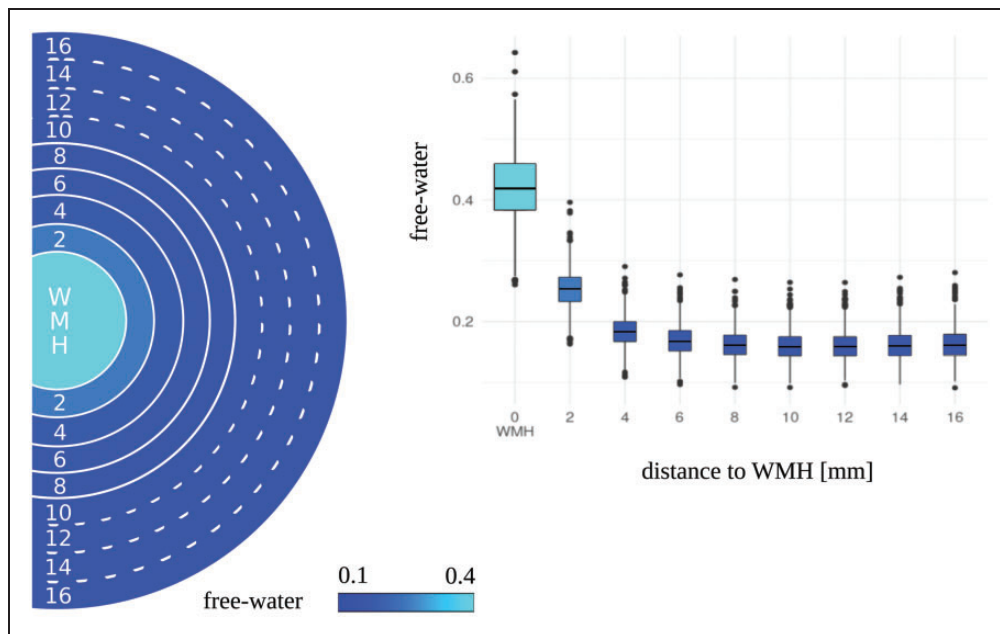
	Free-water		FA-t	
	β	P	β	P
Intercept	0.205	**<0.001**	0.456	**<0.001**
age	0.008	**<0.001**	−0.002	**0.01**
Sex–female	0.003	0.051	−0.001	0.35
log WMH load	0.007	**<0.001**	−0.004	**<0.001**
ROI contrasts				
WMH – 2 mm	0.166	**<0.001**	−0.059	**<0.001**
2mm–4 mm	0.07	**<0.001**	−0.008	**<0.001**
4mm–6 mm	0.015	**<0.001**	0.019	**<0.001**
6mm–8 mm	0.006	**<0.001**	0.015	**<0.001**
8mm–10 mm	0.002	**0.017**	0.011	**<0.001**
10mm–12 mm	<−0.001	0.932	0.007	**<0.001**
12mm–14 mm	−0.001	0.154	0.004	**0.003**
14mm–16 mm	−0.001	0.18	0.002	0.141

Two multivariate linear regression models were conducted with either free-water or FA-t as the dependent variable, as indicated above. P-values <0.05 are indicated in bold. Models are additionally adjusted for random effects of individual differences.

β: standardized estimate; FA-t: free-water corrected fractional anisotropy; log: logarithmic; mm: millimetre; NAWM: normal-appearing white matter; p: p-value; ROI: region of interest; WMH: white matter hyperintensities.

Association of microstructural integrity with cerebrovascular risk factors

Based on the results of the ROI analysis, the 'WMH-FW-penumbra' was defined and included the first 4 NAWM ROIs (2 mm – 8 mm) where significantly increased FW was found between concentrically adjacent ROIs. In the second part of the analysis, we examined the association of FW and FA-t with cerebrovascular risk factors both in WMH and in the WMH-FW-penumbra. Results from multivariate linear regression demonstrated higher FW in WMH-FW-penumbra in active smokers ($\beta = 0.006$, p = 0.008) compared to non-smokers; no significant differences between smokers and non-smokers were found in WMH ($\beta = 0.001$, p = 0.793). Additional cerebrovascular risk factors were not significantly associated with FW. Moreover, FW in WMH and WMH-FW-penumbra was higher with increasing age (effect in WMH: $\beta = 0.008$, p < 0.001; effect in penumbra: $\beta = 0.007$, p < 0.001) and higher log WMH load (effect in WMH: $\beta = 0.017$, p < 0.001; effect in penumbra: $\beta = 0.004$, p < 0.001), next to a significant main effect of sex on FW in WMH ($\beta = -0.008$, p = 0.031). See Table 3 for all results of the linear regression.

Figure 2. Distribution of free-water in white matter hyperintensities (WMH) and adjacent normal-appearing white matter regions. The boxplot displays the raw free-water distribution across the regions. The visualized circle displays the color-coded free-water in each region. A solid line between two adjacent regions represents a significant difference in free-water, based on the outcome of the multivariate linear regression. A dotted line represents no significant difference between the adjacent regions.
mm: millimetre; WMH: white matter hyperintensities.
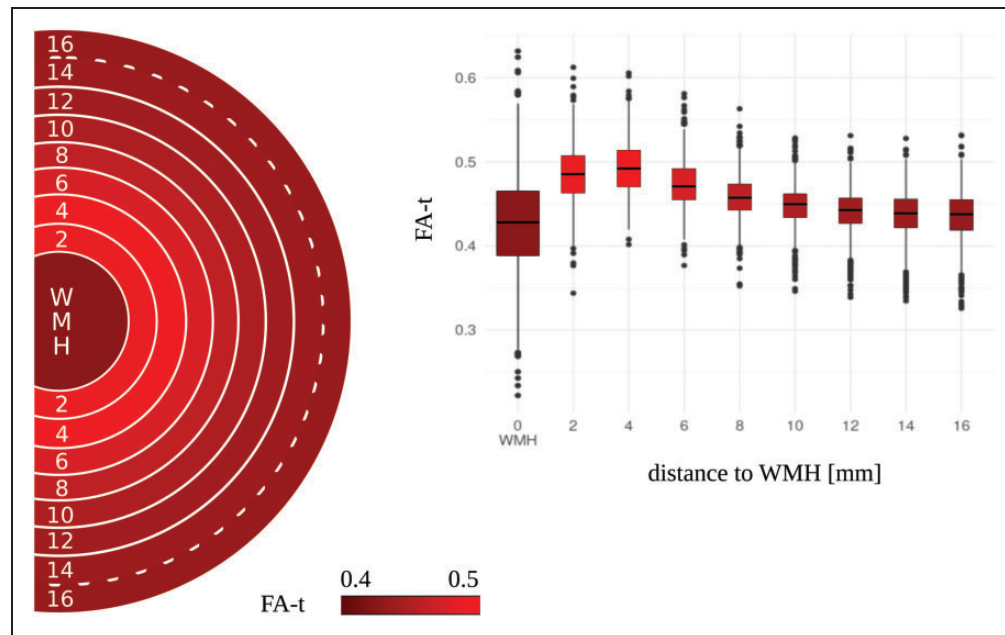
Figure 3. Distribution of free-water corrected fractional anisotropy (FA-t) in white matter hyperintensities (WMH) and adjacent normal-appearing white matter regions. The boxplot displays the raw FA-t distribution across the regions. The visualized circle displays the color-coded FA-t in each region. A solid line between two adjacent regions represents a significant difference in FA-t, based on the outcome of the multivariate linear regression. A dotted line represents no significant difference between the adjacent regions.
FA-t: free-water corrected fractional anisotropy; mm: millimetre; WMH: white matter hyperintensities.

For FA-t, results of multivariate linear regression showed that active smokers had significantly lower FA-t values in WMH and WMH-FW-penumbra compared to non-smokers (effect in WMH: $\beta = -0.015$, $p = 0.008$; effect in penumbra: $\beta = -0.007$, $p = 0.003$). Other vascular risk factors, i.e., diabetes and hypertension, were not significantly associated with FA-t. Moreover, FA-t in both WMH and WMH penumbra was significantly depending on age (effect in WMH: $\beta = 0.008$, $p = 0.001$; effect in penumbra: $\beta = -0.004$, $p < 0.001$) next to significant main effects of sex on FA-t in WMH ($\beta = -0.011$, $p = 0.008$) and log WMH load on FA-t in WMH-FW-penumbra ($\beta = -0.003$, $p = 0.003$). See Table 3 for all results of the linear regression.

Supplementary analysis

Results from our post-hoc analysis show that 1) both WMH in the periventricular and deep white matter have increased FW in the surrounding tissue, and that 2) the extent of FW increase in the surrounding tissue was present similarly both in the first and last quartile of the periventricular WMH volumes.

Discussion

We examined the microstructural alterations of white matter in WMH and surrounding tissue in a large population-based cohort at increased risk for cerebrovascular diseases using DTI derived metrics of extracellular FW and FA-t. We further examined the association of FW and FW-corrected FA with major vascular risk factors both in WMH and in the WMH-FW-penumbra. Our results show that FW was significantly higher in the NAWM up to 8 mm surrounding the WMH with a distance-dependent decline. Additional, post-hoc analysis revealed that the FW alterations in the NAWM is present both in periventricular and deep WMH and independent from the degree of periventricular WMH volume, indicating an anatomically independent effect. The spatial relationship of FA-t values was more complex with the highest value located in NAWM of 4 mm distance to WMH and decreasing further distant. As a second finding, active smokers had significantly higher FW and lower FA-t in the WMH-FW-penumbra while diabetes and hypertension were not significantly associated. This study therefore helps to determine the dimension of microstructural deterioration in the penumbra of

Table 3. Results of multivariate linear regression models with cerebrovascular risk factors and free-water/FA-t in WMH and WMH-FW-penumbra.

| | Free-water | | | | FA-t | | | |
| | WMH | | penumbra | | WMH | | penumbra | |
	β	P	β	P	β	P	β	P
Intercept	0.424	**<0.001**	0.192	**<0.001**	0.431	**<0.001**	0.478	**<0.001**
age	0.008	**<0.001**	0.007	**<0.001**	0.008	**0.001**	−0.004	**<0.001**
sex − female	−0.008	**0.031**	−0.003	0.084	−0.011	**0.008**	−0.002	0.336
log WMH load	0.017	**<0.001**	0.004	**<0.001**	0.001	0.775	−0.003	**0.003**
smoking − active	0.001	0.793	0.006	**0.008**	−0.015	**0.008**	−0.007	**0.003**
diabetes − yes	−0.003	0.639	<−0.001	0.953	0.007	0.607	0.002	0.533
hypertension − yes	<0.001	0.997	0.002	0.227	0.002	0.316	0.003	0.212

The dependent variable is either free-water or FA-t measured in WMH and in WMH-FW-penumbra, as indicated in the table. The penumbra is defined as the normal-appearing white matter in the direct surrounding of WMH with higher free-water (diameter 8 mm). P-values < 0.05 are indicated in bold. β: standardized estimate; FA-t: free-water corrected fractional anisotropy; log: logarithmic; p: p-value; WMH: white matter hyperintensities.

WMH based on FW measurements and to assess the relationship between FW in this penumbra and cerebrovascular risk factors.

In CSVD, the NAWM surrounding apparent WMH is affected by microstructural alterations not visible on FLAIR and was previously described as the 'WMH penumbra', characterized by a stronger tendency to convert to WMH.[21,32,33] Several studies examined the extent of alterations in the white matter by analysing DWI and perfusion data, indicating that the degree of microstructural deterioration in NAWM increases in closer proximity to WMH.[20,21,26,34] However, results show heterogeneity in defining the diameter of the WMH penumbra which depends on the imaging parameter used – it varies from a 4 mm penumbra defined by decreased FA and increased MD up to a 12 mm penumbra defined by CBF, and 20 mm for a penumbra defined by blood-brain barrier leakage.[20,21,27,34] Despite inconsistent findings regarding the spatial extent of the WMH penumbra, all studies found that WMH represent the peak of microstructural degeneration in CSVD.[20,21,26,27,34]

In the current analysis, we characterized the extent of the WMH penumbra based on free-water imaging, reflecting the microstructural properties of the WMH and surrounding NAWM. In line with the notion of microstructural damage peaking in WMH, we found that WMH were characterized by the highest FW and the lowest FA-t values. In addition, there was a constant increase in FW with closer proximity to WMH starting in NAWM of 8 mm distance to WMH. Previous literature already indicates that FW in NAWM varies depending on the diagnosis of Alzheimer's Disease, presence of MCI, and dementia severity.[11,35] However, the spatial distribution of FW in NAWM was not previously examined. Increased

extracellular FW may be an indicator for microvascular degeneration, demyelination and fibre loss which are pathological markers of CSVD.[36,37] Neuroinflammatory processes and blood-brain-barrier leakage next to damage of the ependyma leading to cerebrospinal fluid entering the brain parenchyma are additional pathological mechanisms which could result in increases of the extracellular FW in WMH and NAWM.[38–40] Taken together, the results of our study suggest that pathological white matter alterations implied in CSVD are detectable with free-water imaging in and, most importantly, beyond visible WMH. Longitudinal studies will help to delineate factors which influence the progression of the WMH-FW-penumbra.

Next to FW, FA-t demonstrated a more complex pattern in the NAWM ROIs with highest values in NAWM of 4 mm distance and decreasing in both closer and more distant ROIs. The counterintuitive results were already observed in other studies examining FW-uncorrected FA-values.[20,41] The peak of FA-t values as a halo surrounding the WMH is a finding discordant to the linear decrease of FW. A possible explanation for the peak in the direct surrounding of WMH is the majority of WMH in this study being located in the caps of the ventricles which contain densely bundles white matter tracts and, subsequently, have by nature higher FA-t values compared to white matter with a low density of tracts.[30,42,43] Consequently, FA-t (or FA in general) is prone to local differences by higher values in regions with densely bundles white matter tract compared to regions outside the main fibre tracts. This bias can be unmasked with free-water imaging. Previous studies already found that FW is more correlated with clinical deficits and provides a greater biological specificity than

conventional DTI metrics, where alterations in FA and MD can be explained by increases in FW.[8–10,12]

We examined the association of FW and FA-t with cerebrovascular risk factors represented by hypertension, smoking, and diabetes. Our results show a significant association of FW with smoking in the WMH-FW-penumbra. However, neither the relationship between smoking status and FW in WMH was significant nor was FW associated with other vascular risk factors. For FA-t, active smoking status was significantly associated with lower FA-t values in both WMH and the WMH-FW-penumbra, while diabetes and hypertension were not significantly associated. The results are in line with previous literature showing that chronic smokers have significantly lower FA and smoking cessation is positively related to lower FA in NAWM, but no study examined the effect of smoking on changes of FW in the NAWM so far.[44–46] As a potential pathophysiological mechanism underlying the association with FW, chemical constituents of the cigarette smoke are suggested to cause neurotoxic swelling of the brain and plasma fluid leaking into the interstitial space which leads to more extracellular water.[47,48] Previous literature also indicates an association of diabetes and hypertension with uncorrected FA in the brain white matter but their association with FW has not been examined previously.[46,49–51] Our analysis revealed that FA-t and FW were not significantly associated with diabetes or hypertension. As an important limitation, we did not consider the time since diagnosis or differences between participants with or without antihypertensive medication - two factors which were shown to be associated with WMH severity.[3,52] Additional analysis is necessary to examine whether diabetes and hypertension might have an influence on FW in a cohort with severe manifestations of CSVD, syndromes of neurodegeneration or other neurological diseases affecting the brain microstructure.

Generally, all significant effects reported in this paper were found in a cohort which displayed a relatively low degree of CSVD manifestation on MRI. Therefore, our study provides novel findings for early stages of CSVD demonstrating subtle alterations in the cerebral white matter surrounding WMH. Due to the selection of the participants from a population-based study, we cannot exclude an impact of physiological white matter microstructure on our findings. However, given the results from our post-hoc analysis, we would argue that our findings nonetheless indicate pathophysiological processes occurring in CSVD as a spectrum of increasing alterations of the white matter. The cross-sectional nature of our study is an additional limitation and further studies are needed to investigate the course of deterioration longitudinally and to examine whether increased FW is a predictor of conversion into WMH. Moreover, given the selection of participants from a population-based study, it is not possible to provide an a-priori categorization of unaffected individuals. While our results are based on the application of a bi-tensor model which accounts for signal contribution from tissue and extracellular, i.e., FW, compartments, it has been shown that perfusion significantly affects the estimation of the FW fraction.[53] Therefore, novel three-compartment diffusion MRI methods which account for the signal contribution of blood perfusion, in addition to that of FW and tissue compartments, might be helpful to delineate the complex interplay of vascular and tissue-changes observed in CSVD.[53] Such models require the acquisition of multi-shell diffusion data, for which more robust estimation of FW is also available.[54]

To conclude, we presented results of the, so far, largest free-water imaging analysis in a population-based study in the context of CSVD. We showed that the WMH-FW-penumbra has a size of 8 mm surrounding WMH and that FW increases in closer proximity to WMH. In contrast to that, FA-t shows a more complex spatial distribution to WMH with peaks at 4 mm distance which is congruent with previous studies. In addition, our analysis found significantly higher FW and lower FA-t in active smokers compared to non-smokers. Further research will be necessary to better understand the longitudinal trajectory of FW and cellular tissue alterations in NAWM and their spatial relationship to WMH. This might ultimately help to identify which factors are beneficial in preventing NAWM from the progression to WMH.

Funding

Declaration of conflicting interests

The author(s) declared no potential conflicts of interest with respect to the research, authorship, and/or publication of this article.

Authors' contributions

CM designed and conceptualized the study, analysed, and interpreted the data, and wrote and revised the paper. FLN made major contributions in revising the manuscript. MP and BMF analysed and interpreted the data and contributed analysis tools and revised the manuscript. UH and EP participated in the data acquisition. OP contributed analysis tools and made major contributions in revising the manuscript. CG collected the data and critically revised the manuscript. GT and BC made major contributions in designing, conceptualizing, and supervising the study and in drafting and revising the manuscript.

ORCID iDs

Carola Mayer (iD) https://orcid.org/0000-0002-8065-8683
Marvin Petersen (iD) https://orcid.org/0000-0001-6426-7167

Supplemental material

Supplemental material for this article is available online.

References

1. Wardlaw JM, Smith C and Dichgans M. Small vessel disease: mechanisms and clinical implications. *Lancet Neurol* 2019; 18: 684–696.
2. Debette S and Markus HS. The clinical importance of white matter hyperintensities on brain magnetic resonance imaging: systematic review and Meta-analysis. *BMJ* 2010; 341: c3666.
3. Dufouil C, de Kersaint-Gilly A, Besancon V, et al. Longitudinal study of blood pressure and white matter hyperintensities: the EVA MRI cohort. *Neurology* 2001; 56: 921–926.
4. Kloppenborg RP, Nederkoorn PJ, Geerlings MI, et al. Presence and progression of white matter hyperintensities and cognition: a meta-analysis. *Neurology* 2014; 82: 2127–2138.
5. Power MC, Deal JA, Sharrett AR, et al. Smoking and white matter hyperintensity progression: the ARIC-MRI study. *Neurology* 2015; 84: 841–848.
6. Taylor WD, Steffens DC, MacFall JR, et al. White matter hyperintensity progression and late-life depression outcomes. *Arch Gen Psychiatry* 2003; 60: 1090–1096.
7. Zhuang F-J, Chen Y, He W-B, et al. Prevalence of white matter hyperintensities increases with age. *Neural Regen Res* 2018; 13: 2141–2146.
8. Pasternak O, Sochen N, Gur Y, et al. Free water elimination and mapping from diffusion MRI. *Magn Reson Med* 2009; 62: 717–730.
9. Duering M, Finsterwalder S, Baykara E, et al. Free water determines diffusion alterations and clinical status in cerebral small vessel disease. *Alzheimer's Dementia* 2018; 14: 764–774.
10. Gullett JM, O'Shea A, Lamb DG, et al. The association of white matter free water with cognition in older adults. *Neuroimage* 2020; 219: 117040.
11. Ji F, Pasternak O, Liu S, et al. Distinct white matter microstructural abnormalities and extracellular water increases relate to cognitive impairment in Alzheimer's disease with and without cerebrovascular disease. *Alzheimers Res Ther* 2017; 9: 63.
12. Maillard P, Fletcher E, Singh B, et al. Cerebral white matter free water: a sensitive biomarker of cognition and function. *Neurology* 2019; 92: e2221–e2231.
13. Huang P, Zhang R, Jiaerken Y, et al. White matter free water is a composite marker of cerebral small vessel degeneration. *Transl Stroke Res* 2022; 13: 56–64.
14. Chad JA, Pasternak O, Salat DH, et al. Re-examining age-related differences in white matter microstructure with free-water corrected diffusion tensor imaging. *Neurobiol Aging* 2018; 71: 161–170.
15. Edde M, Theaud G, Rheault F, et al. Free water: a marker of age-related modifications of the cingulum white matter and its association with cognitive decline. *PLoS One* 2020; 15: e0242696.
16. Bergamino M, Walsh RR and Stokes AM. Free-water diffusion tensor imaging improves the accuracy and sensitivity of white matter analysis in Alzheimer's disease. *Sci Rep* 2021; 11: 6990.
17. Muñoz Maniega S, Chappell FM, Valdés Hernández MC, et al. Integrity of normal-appearing white matter: influence of age, visible lesion burden and hypertension in patients with small-vessel disease. *J Cereb Blood Flow Metab* 2017; 37: 644–656.
18. Sexton CE, Walhovd KB, Storsve AB, et al. Accelerated changes in white matter microstructure during aging: a longitudinal diffusion tensor imaging study. *J Neurosci* 2014; 34: 15425–15436.
19. Vernooij MW, Ikram MA, Vrooman HA, et al. White matter microstructural integrity and cognitive function in a general elderly population. *Arch Gen Psychiatr* 2009; 66: 545–553.
20. Wardlaw JM, Makin SJ, Valdés Hernández MC, et al. Blood-brain barrier failure as a core mechanism in

cerebral small vessel disease and dementia: evidence from a cohort study. *Alzheimer's Dementia* 2017; 13: 634–643.

21. Maillard P, Fletcher E, Harvey D, et al. White matter hyperintensity penumbra. *Stroke* 2011; 42: 1917–1922.

22. Jagodzinski A, Johansen C, Koch-Gromus U, et al. Rationale and design of the Hamburg city health study. *Eur J Epidemiol* 2020; 35: 169–181.

23. D'Agostino RB, Vasan RS, Pencina MJ, et al. General cardiovascular risk profile for use in primary care. *Circulation* 2008; 117: 743–753.

24. Fischl B and Dale AM. Measuring the thickness of the human cerebral cortex from magnetic resonance images. *Proc Natl Acad Sci U S A* 2000; 97: 11050–11055.

25. Griffanti L, Zamboni G, Khan A, et al. BIANCA (brain intensity AbNormality classification algorithm): a new tool for automated segmentation of white matter hyperintensities. *Neuroimage* 2016; 141: 191–205.

26. Wu X, Ge X, Du J, et al. Characterizing the penumbras of white matter hyperintensities and their associations with cognitive function in patients with subcortical vascular mild cognitive impairment. *Front Neurol* 2019; 10: 348.

27. Promjunyakul N, Lahna D, Kaye JA, et al. Characterizing the white matter hyperintensity penumbra with cerebral blood flow measures. *NeuroImage Clin* 2015; 8: 224–229.

28. Kim H-Y. Statistical notes for clinical researchers: assessing normal distribution (2) using skewness and kurtosis. *Restor Dent Endod* 2013; 38: 52–54.

29. R Core Team. *R: A language and environment for statistical computing*. Vienna, Austria: R Foundation for Statistical Computing, 2018.

30. Griffanti L, Jenkinson M, Suri S, et al. Classification and characterization of periventricular and deep white matter hyperintensities on MRI: a study in older adults. *Neuroimage* 2018; 170: 174–181.

31. Kim KW, MacFall JR and Payne ME. Classification of white matter lesions on magnetic resonance imaging in elderly persons. *Biol Psychiatr* 2008; 64: 273–280.

32. Maillard P, Carmichael O, Harvey D, et al. FLAIR and diffusion MRI signals are independent predictors of white matter hyperintensities. *AJNR Am J Neuroradiol* 2013; 34: 54–61.

33. de Groot M, Verhaaren BFJ, de Boer R, et al. Changes in normal-appearing white matter precede development of white matter lesions. *Stroke* 2013; 44: 1037–1042.

34. Nasrallah IM, Hsieh M-K, Erus G, et al. White matter lesion penumbra shows abnormalities on structural and physiologic MRIs in the coronary artery risk development in young adults cohort. *Am J Neuroradiol* 2019; 40: 1291–1298.

35. Ofori E, DeKosky ST, Febo M, et al. Free-water imaging of the hippocampus is a sensitive marker of Alzheimer's disease. *NeuroImage Clin* 2019; 24: 101985.

36. Wardlaw JM, Valdés Hernández MC and Muñoz-Maniega S. What are white matter hyperintensities made of?. *J Am Heart Assoc* 2015; 4: 001140.

37. Gouw AA, Seewann A, Vrenken H, et al. Heterogeneity of white matter hyperintensities in Alzheimer's disease: post-mortem quantitative MRI and neuropathology. *Brain* 2008; 131: 3286–3298.

38. Kalaria RN. Neuropathological diagnosis of vascular cognitive impairment and vascular dementia with implications for Alzheimer's disease. *Acta Neuropathol* 2016; 131: 659–685.

39. Fazekas F, Kleinert R, Offenbacher H, et al. Pathologic correlates of incidental MRI white matter signal hyperintensities. *Neurology* 1993; 43: 1683–1689.

40. Gouw AA, Seewann A, Van Der Flier WM, et al. Heterogeneity of small vessel disease: a systematic review of MRI and histopathology correlations. *J Neurol Neurosurg Psychiatry* 2011; 82: 126–135.

41. Muñoz Maniega S, Valdés Hernández MC, Clayden JD, et al. White matter hyperintensities and normal-appearing white matter integrity in the aging brain. *Neurobiol Aging* 2015; 36: 909–918.

42. Haines DE and Mihailoff GA. The Telencephalon. In: Haines DE and Mihailoff, GA (eds), *Fundamental Neuroscience for Basic and Clinical Applications*. 5th ed. Baltimore: Wolters Kluwer Health, 2018. pp. 225–240.e1.

43. Mayer C, Frey BM, Schlemm E, et al. Linking cortical atrophy to white matter hyperintensities of presumed vascular origin. *J Cereb Blood Flow Metab* 2021; 41: 1682–1691.

44. Gons RAR, van Norden AGW, de Laat KF, et al. Cigarette smoking is associated with reduced microstructural integrity of cerebral white matter. *Brain* 2011; 134: 2116–2124.

45. Paul R, Grieve S, Niaura R, et al. Chronic cigarette smoking and the microstructural integrity of white matter in healthy adults: a diffusion tensor imaging study. *Nicotine Tob Res* 2008; 10: 137–147.

46. de Groot M, Ikram MA, Akoudad S, et al. Tract-specific white matter degeneration in aging: the Rotterdam study. *Alzheimers Dement* 2015; 11: 321–330.

47. Hawkins BT, Brown RC and Davis TP. Smoking and ischemic stroke: a role for nicotine? *Trends Pharmacol Sci* 2002; 23: 78–82.

48. Gazdzinski S, Durazzo TC, Studholme C, et al. Quantitative brain MRI in alcohol dependence: preliminary evidence for effects of concurrent chronic cigarette smoking on regional brain volumes. *Alcohol Clin Exp Res* 2005; 29: 1484–1495.

49. Falvey CM, Rosano C, Simonsick EM, et al. Macro- and microstructural magnetic resonance imaging indices associated with diabetes among community-dwelling older adults. *Diabetes Care* 2013; 36: 677–682.

50. Hsu J-L, Chen Y-L, Leu J-G, et al. Microstructural white matter abnormalities in type 2 diabetes mellitus: a diffusion tensor imaging study. *Neuroimage* 2012; 59: 1098–1105.

51. Reijmer YD, Brundel M, de Bresser J, et al. Microstructural white matter abnormalities and cognitive

functioning in type 2 diabetes: a diffusion tensor imaging study. *Diabetes Care* 2013; 36: 137–144.

52. de Leeuw F, -E, de Groot JC, Oudkerk M, et al. Hypertension and cerebral white matter lesions in a prospective cohort study. *Brain* 2002; 125: 765–772.

53. Rydhög AS, Szczepankiewicz F, Wirestam R, et al. Separating blood and water: perfusion and free water

elimination from diffusion MRI in the human brain. *Neuroimage* 2017; 156: 423–434.

54. Bergmann Ø, Henriques R, Westin C, et al. Fast and accurate initialization of the free-water imaging model parameters from multi-shell diffusion MRI. *NMR Biomed* 2020; 33: e4219.

Supplementary Material

Free-water diffusion MRI detects structural alterations surrounding white matter hyperintensities in the early stage of cerebral small vessel disease

Carola Mayer[1], Felix L Nägele[1], Marvin Petersen[1], Benedikt M Frey[1], Uta Hanning[2], Ofer Pasternak[3,4], Elina Petersen[5,6], Christian Gerloff[1], Götz Thomalla[1] and Bastian Cheng[1]

[1] Department of Neurology, University Medical Center Hamburg-Eppendorf, Germany

[2] Department of Diagnostic and Interventional Neuroradiology, University Medical Center Hamburg-Eppendorf, Germany

[3] Department of Psychiatry, Brigham and Women's Hospital, Harvard Medical School, United States

[4] Department of Radiology, Brigham and Women's Hospital, Harvard Medical School, United States

[5] Clinical for Cardiology, University Heart and Vascular Center, Germany

[6] Population Health Research Department, University Heart and Vascular Center, Germany

Corresponding author

Carola Mayer, Department of Neurology, University Medical Center Hamburg-Eppendorf, Martinistraße 52, 20246 Hamburg, Germany. Email: c.mayer@uke.de

Supplement Material S1. Analysis of penumbral tissue for periventricular and deep WMH

Methods

In this additional analysis, we measured free-water (FW) measurements in the WMH and penumbra of periventricular and deep WMH separately to investigate if similar effects in the WMH penumbra would be observed in deep WMH, which occur in a much more heterogeneous spatial pattern as compared to periventricular WMH, which are confined to the white matter in close proximity to the ventricles.[1,2] To differentiate between periventricular and deep WMH, we applied a threshold of 10mm from the ventricles, as proposed previously.[1] After the differentiation, we applied the same analysis steps as in the main manuscript, separately for the deep WMH and periventricular WMH. Regions of interest (ROIs) were created by dilating the periventricular / deep WMH mask in the 3-dimensional space in 1 voxel increments (2mm). This process was repeated 8 times to create 8 normal-appearing white matter (NAWM) masks. To avoid confounding effects of periventricular WMH located in the penumbral tissue of deep WMH and vice versa, we excluded both the WMH mask and the first penumbral tissue mask (2mm surrounding WMH) of each WMH type from the other WMH type. Then, FW was extracted and averaged for each ROI.

The statistical analysis contained the same linear mixed-effects models as applied in the main manuscript, with FW as the dependent variable. Models were defined separately for periventricular and deep WMH.

Results

The linear mixed-effects models showed, that both WMH in the periventricular and deep white matter have increased FW in the surrounding tissue (table 1). For a visualization of the distribution of the deep and periventricular WMH, see figure 1. Although the effect is less extensive in the case of deep WMH (FW increased in up to 4mm distance to the lesion), the significant results both in periventricular and deep WMH indicate that FW alterations are not solely associated with the distance to the ventricles. Additionally, we see that the standardized effect sizes (β) decrease with increasing distance to both periventricular and deep WMH, indicating a direct relationship between FW in the penumbra and WMH.

Figure 1. Heatmap of the periventricular and deep WMH of the study sample (N = 900).

periventricular WMH
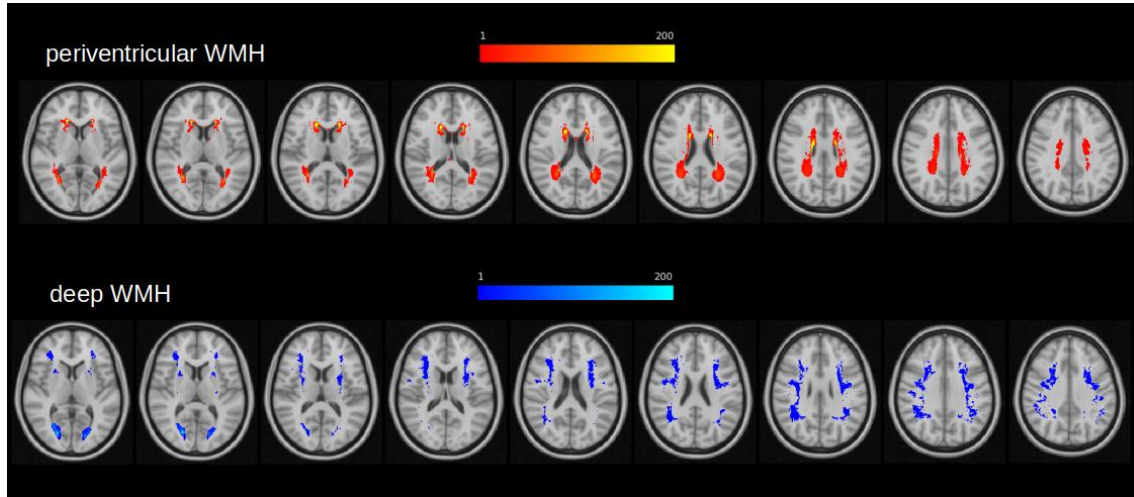
deep WMH

Table 1. Results of the linear mixed-effects models analyzing the free-water content in the deep and periventricular WMH.

		Free-water in periventricular WMH		Free-water in deep WMH	
		β	p	β	p
Intercept		0.212	**<0.001**	0.197	**<0.001**
age		0.008	**<0.001**	0.005	**<0.001**
sex - female		-0.003	0.056	-0.006	**0.009**
log WMH load		0.008	**<0.001**	0.009	**<0.001**
ROI contrasts	WMH – 2mm	0.175	**<0.001**	0.119	**<0.001**
	2mm – 4mm	0.07	**<0.001**	0.052	**<0.001**
	4mm – 6mm	0.016	**<0.001**	0.011	**<0.001**
	6mm – 8mm	0.007	**<0.001**	< 0.001	0.623
	8mm – 10mm	0.004	**0.001**	-0.001	0.433
	10mm – 12mm	< 0.001	0.392	-0.001	0.31
	12mm – 14mm	< -0.001	0.7	-0.002	0.174
	14mm – 16mm	< -0.001	0.461	-0.002	0.248

Two multivariate linear regression models were conducted with free-water as the dependent variable. As indicated above, free-water in either the periventricular or deep WMH were included. P-values < 0.05 are indicated in bold. Models are additionally adjusted for random effects of individual differences.

Abbreviations: β = standardized estimate, log = logarithmic, mm = millimetre, p = p-value, ROI = region of interest, WMH = white matter hyperintensities.

Supplement Material S2. Analysis of penumbral tissue for lowest and highest quartile of periventricular WMH volume

Methods

As a second approach, we examined FW in the penumbra of periventricular WMH separately for participants in the first (<25%, Q1) and last (>75%, Q4) quartile of WMH volumes. For this, we divided the cohort into four quartiles based on their periventricular WMH volume and only considered the lowest and highest quartile for further analysis. Mean volumes for periventricular WMH were 0.08ml (IQR = 0.073) for Q1 and 3.4ml (IQR = 2.55) for Q4. A heatmap of the periventricular WMH volumes in both groups (Q1/Q4) is visualized in figure 2.

Results

Again, we applied two linear mixed-effects models as described in the main manuscript. In this analysis, only FW in the WMH and penumbral tissue of either Q1 or Q4 of the periventricular WMH was considered. The results are shown in table 2. In short, although the groups varied in periventricular WMH volume (i.e. the extent of WMH into periventricular white matter), the extent of FW increase in the WMH penumbra was similar for WMH in Q1 and Q4. The results indicate that the FW increases in proximity to WMH do not solely reflect the underlying, physiological anatomical structure.

Figure 2. Heatmap of the lowest and highest quartile of periventricular WMH volume in the study sample (N = 900).

periventricular WMH Q1

periventricular WMH Q4
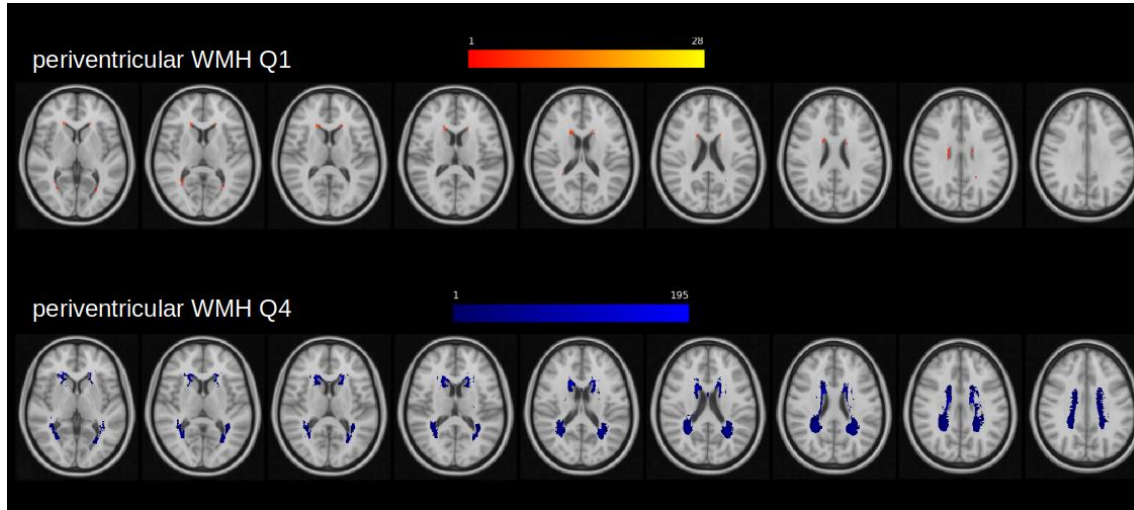
Table 2. Results of the linear mixed-effects models analyzing the free-water content in the first and fourth quartile of the periventricular WMH volume.

		Free-water in Q1 periventricular WMH volume		Free-water in Q4 periventricular WMH volume	
		β	p	β	p
Intercept		0.189	**<0.001**	0.222	**<0.001**
age		0.005	**<0.001**	0.006	**<0.001**
sex - female		< -0.001	0.962	-0.009	**0.008**
log WMH load		0.001	0.657	0.006	**<0.001**
ROI contrasts	WMH – 2mm	0.142	**<0.001**	0.183	**<0.001**
	2mm – 4mm	0.069	**<0.001**	0.069	**<0.001**
	4mm – 6mm	0.017	**<0.001**	0.013	**<0.001**
	6mm – 8mm	0.007	**0.001**	0.005	**0.001**
	8mm – 10mm	0.003	0.208	0.001	0.452
	10mm – 12mm	0.001	0.724	-0.002	0.295
	12mm – 14mm	< 0.001	0.916	-0.003	**0.031**
	14mm – 16mm	< 0.001	0.893	-0.003	0.061

Two multivariate linear regression models were conducted with free-water as the dependent variable. As indicated above, either participants in the first or fourth quartile of the periventricular WMH volume were included. P-values < 0.05 are indicated in bold. Models are additionally adjusted for random effects of individual differences.

Abbreviations: β = standardized estimate, log = logarithmic, mm = millimetre, p = p-value, Q1= first quartile (<25%), Q4 = fourth quartile (>75%), ROI = region of interest, WMH = white matter hyperintensities.

References

1.   Griffanti L, Jenkinson M, Suri S, et al. Classification and characterization of periventricular and deep white matter hyperintensities on MRI: A study in older adults. *Neuroimage* 2018; 170: 174–181.

2.   Kim KW, MacFall JR, Payne ME. Classification of White Matter Lesions on Magnetic Resonance Imaging in Elderly Persons. *Biol Psychiatry* 2008; 64: 273–280.

Article

Association between Coffee Consumption and Brain MRI Parameters in the Hamburg City Health Study

Carola Mayer [1,*], Felix L. Nägele [1], Marvin Petersen [1], Maximilian Schell [1], Ghazal Aarabi [2], Thomas Beikler [2], Katrin Borof [2], Benedikt M. Frey [1], Julius Nikorowitsch [3], Juliana Senftinger [3], Carolin Walther [2], Jan-Per Wenzel [3], Birgit-Christiane Zyriax [4], Bastian Cheng [1] and Götz Thomalla [1,*]

1 Department of Neurology, University Medical Center Hamburg-Eppendorf, 20246 Hamburg, Germany
2 Department of Periodontics, Preventive and Restorative Dentistry, University Medical Center Hamburg-Eppendorf, 20246 Hamburg, Germany
3 Department of Cardiology, University Heart and Vascular Center, 20246 Hamburg, Germany
4 Midwifery Science—Health Service Research and Prevention, Institute for Health Services Research in Dermatology and Nursing (IVDP), University Medical Center Hamburg-Eppendorf, 20246 Hamburg, Germany
* Correspondence: c.mayer@uke.de (C.M.); thomalla@uke.de (G.T.)

Abstract: Despite associations of regular coffee consumption with fewer neurodegenerative disorders, its association with microstructural brain alterations is unclear. To address this, we examined the association of coffee consumption with brain MRI parameters representing vascular brain damage, neurodegeneration, and microstructural integrity in 2316 participants in the population-based Hamburg City Health Study. Cortical thickness and white matter hyperintensity (WMH) load were measured on FLAIR and T1-weighted images. Microstructural white matter integrity was quantified as peak width of skeletonized mean diffusivity (PSMD) on diffusion-weighted MRI. Daily coffee consumption was assessed in five groups (<1 cup, 1–2 cups, 3–4 cups, 5–6 cups, >6 cups). In multiple linear regressions, we examined the association between brain MRI parameters and coffee consumption (reference group <1 cup). After adjustment for covariates, 3–4 cups of daily coffee were associated with lower PSMD ($p = 0.028$) and higher cortical thickness ($p = 0.015$) compared to <1 cup. Moreover, 1–2 cups per day was also associated with lower PSMD ($p = 0.022$). Associations with WMH load or other groups of coffee consumption were not significant ($p > 0.05$). The findings indicate that regular coffee consumption is positively associated with microstructural white matter integrity and cortical thickness. Further research is necessary to determine longitudinal effects of coffee on brain microstructure.

Keywords: cerebral small vessel disease; coffee consumption; cortical atrophy; diffusion-weighted magnetic resonance imaging; microstructural integrity; neurodegenerative diseases; white matter hyperintensities

1. Introduction

Coffee is one of the most consumed beverages worldwide. Even subtle effects of coffee on health might have wide-ranging implications on the population level [1]. Since coffee constituents such as caffeine can easily cross the blood-brain barrier, coffee is suggested to impact neurological health [2]. For example, regular coffee consumption was associated with a lower risk of cerebrovascular and neurodegenerative disease such as stroke, Parkinson's disease, dementia, and cognitive decline [3–8]. These neuroprotective associations can be explained by the various ingredients of coffee which have anti-inflammatory properties, reduce amyloid-β levels in the cells, and decrease cardiovascular risk [9–12].

Despite the association of regular coffee consumption with fewer neurodegenerative diseases, it remains unclear how coffee is associated with pre-clinical brain pathologies

such as lesions in the white matter, degeneration of the cortex, or alterations of the microstructural integrity. White matter hyperintensities (WMH) are hyperintense lesions on T2-weighted images and are associated with an increased risk for stroke and depression, cognitive deterioration, and gait disorders [13–15]. As a marker of cerebral small vessel disease (CSVD) and vascular brain damage, WMH can vary in the degree of expression, depending on the age and the presence of cardiovascular risk factors, e.g., smoking or hypertension [16–18]. Previous studies have reported diverging results on the association of consumed coffee with imaging markers of CSVD. They found either beneficial associations of coffee with lacunar infarcts [7], beneficial [19] or detrimental [20] associations with WMH volume, or no significant associations at all [21,22].

A recently developed and valid imaging marker of microstructural integrity is the peak width of skeletonized mean diffusivity (PSMD), calculated as the distribution of the mean diffusivity (MD) between the 5th and 95th percentile in the white matter skeleton [23]. Only one study analyzed the association of coffee consumption with microstructural integrity, as quantified by fractional anisotropy, with a higher coffee consumption being associated with higher integrity of the white matter microstructure [24].

Damage to the brain structure is not restricted to white matter, but also extents to the cortex, e.g., in the form of atrophy. Except for one study focusing on the quantification of cortical thickness in regions susceptible for Alzheimer's Disease [22], the link between coffee consumption and cortical thickness was only indirectly examined by measuring total brain volume or grey matter volume, with incongruent results between studies [7,21,25,26]. This study aimed at investigating whether coffee consumption is associated with multiple brain MRI markers of vascular brain damage and neurodegeneration, including WMH, PSMD, and cortical thickness in a large, population-based cohort.

2. Materials and Methods

2.1. Study Design

This study included data from the Hamburg City Health Study (HCHS), an ongoing population-based, single-center, prospective cohort study investigating risk factors of major chronic diseases to improve prognosis and treatment options. A detailed description of the study design was published previously [27]. To describe briefly, 45,000 citizens of the city of Hamburg, Germany, between the age of 45 and 74 years are invited to receive an extensive baseline clinical evaluation. An MRI of the brain is conducted in a subgroup which comprises participants with increased cardiovascular diseases risk (determined by a Framingham Risk Score >7) and control participants [28]. This study included data from the first 10,000 participants, of which 2652 received a brain MRI. A total of 17 participants were excluded because of at least one missing MR sequence (12 without FLAIR, 14 without T1, 14 without diffusion-weighted MRI), 26 participants had to be excluded because of anomalies in the neuroradiological evaluation, 29 participants had to be excluded because of insufficient FLAIR (N = 23) or T1-weighted (N = 6) image quality, and 80 participants had to be excluded because of technical issues during brain parcellation (N = 53) or WMH segmentation (N = 27). Of the remaining participants, 2316 had complete data on coffee consumption.

2.2. Clinical Data Assessment

Coffee consumption was quantified as the average number of cups consumed per day over the last 12 months, based on the participants' responses on a validated food frequency questionnaire (FFQ) [29]. The FFQ also examined the regular consumption of decaffeinated coffee. The questions were stated as follows: "Over the last 12 months, how often did you consume caffeinated/decaffeinated coffee? This also includes the consumption of espresso, cappuccino, café latte, and other preparation types." One coffee corresponds to 150 milliliters. The frequency of coffee consumption was classified into five groups: less than one cup per day (<1 c/d), one to two cups per day (1–2 c/d), three to four cups per day (3–4 c/d), five to six cups per day (5–6 c/d), or more than six cups per day (>6 c/d). In addition, all participants received detailed anamnestic and clinical

examination. For the current analysis, the covariates age, sex, educational status, diabetes, hypertension, smoking status, body mass index (BMI), adherence to the Mediterranean diet, and alcohol consumption were included. In short, educational status was evaluated on a scale from 1–3, based on the International Standard Classification of Education (ISCED) [30]. Diabetes mellitus was determined from self-reported prevalence, fasting serum glucose level (>126 mg/dL) or non-fasting serum glucose level (>200 mg/dL). Hypertension was determined based on self-reported prevalence, blood pressure ($\geq$140/90 mmHg), or intake of antihypertensive medication. Smoking status was classified as active smokers or non-smokers. Adherence to the Mediterranean diet was calculated with the German version of the original Mediterranean Diet Adherence Screener (MEDAS) [31]. Alcohol consumption was measured as the frequency of alcohol consumption on a scale from 0–4, and converted into the monthly frequency.

2.3. MRI Acquisition and Processing

MR images were acquired on a single 3T Siemens Skyra MRI scanner (Siemens, Erlangen, Germany). All participants received the same imaging protocol. Structural imaging consisted of a 3D T1-weighted rapid acquisition gradient-echo sequence (MPRAGE; 256 axial slices, echo time (TE) = 2.12 ms, slice thickness (ST) = 0.94 mm, repetition time (TR) = 2500 ms, in-plane resolution (IPR) = 0.83 $\times$ 0.83 mm) and a 3D T2-weighted fluid-attenuated inversion recovery (FLAIR) image (192 axial slices, TR = 4700 ms, TE = 392 ms, 192 axial slices, ST = 0.9 mm, IPR = 0.75 $\times$ 0.75 mm). For single-shell diffusion MRI (dMRI), 75 axial slices were obtained covering the whole brain with gradients (b = 1000 s/mm^2) applied along 64 noncollinear directions (TR = 8500 ms, TE = 75 ms, ST = 2 mm, IPR = 2 $\times$ 2 mm with anterior-posterior phase-encoding direction). MR data were preprocessed as described previously and full documentation of the MRI processing pipeline is available in a GitHub repository (https://github.com/csi-hamburg/CSIframe/wiki; accessed on 30 December 2022) [32]. In short, dMRI and T1-weighted images were preprocessed with QSIPrep 0.14.2. as implemented in Nipype 1.6.1. [33,34]. Among other steps, the pipeline includes intensity normalization, skull-stripping, MP-PCA denoising, removal of ringing artefacts, and correction for B1 field inhomogeneity, head motion, eddy current, and susceptibility distortions [34].

For the measurement of the brain volume and cortical thickness, brain parcellation was conducted on T1-weighted images using Freesurfer v.6.0.1. [35,36]. All images were thoroughly inspected both visually and quantitatively (outliers defined as measures exceeding 2 standard deviations from the median), and output of insufficient quality (i.e., segmentation errors) was excluded.

WMH were segmented as described in detail previously [32]. In short, we applied the Brain Intensity AbNormality Classification Algorithm (BIANCA) implemented in FSL with LOCally Adaptive Threshold Estimation (LOCATE) on preprocessed FLAIR images and T1-weighted images [37,38]. After applying both algorithms, the segmentations were refined using Freesurfer v.6.0.1 parcellations to exclude non-white matter regions (among others, corpus callosum and basal ganglia) [35]. Finally, the lesion load was calculated by normalization for intracranial volume, as calculated by Freesurfer v.6.0.1. [35]. The normalized lesion load is further referred to as 'log WMH load'.

PSMD was calculated based on standard procedures and adapted for our purposes by using non-linear registration with the Advanced Normalization Tools (ANTs) SyN registration [23,39]. PSMD is calculated as the difference between the 95th and 5th percentile of MD values on the white matter skeleton in standard (MNI) space. White matter areas susceptible to partial volume effects of cerebrospinal fluid were excluded by masking.

2.4. Statistical Analyses

Demographical data were summarized and reported with median and interquartile range (IQR) for continuous variables and number and percentage (n, %) for categorical variables. Demographical characteristics and cardiovascular risk factors were tested for significant difference between groups of coffee consumption by applying Pearson

Chi-square test for categorical variables and Kruskal-Wallis-test for continuous variables. To investigate the association between coffee consumption and MRI markers, we conducted multiple linear regression models with MRI markers as the dependent variables (mean cortical thickness, log WMH load, PSMD). Coffee consumption and covariates (age, sex, education, smoking status, diabetes, hypertension, BMI, adherence to Mediterranean diet, alcohol consumption) were added as independent variables to the models. The lowest group of coffee consumption (<1 cup per day) was set as the reference group. The output of the linear regression analysis was reported with standardized coefficients (β) and *p*-Values (*p*). A $p < 0.05$ was interpreted as significant. All statistical analyses were carried out using R software v.4.2.2. [40].

3. Results

3.1. Study Sample Characteristics

The final cohort consisted of data from N = 2316 participants who had a median age of 65 (IQR = 14) years, with 44.3% female participants. Of all participants included, 19.8% consumed <1 cup of coffee per day, 44% consumed 1–2 cups per day, 25.1% consumed 3–4 cups per day, 7.6% consumed 5–6 cups per day, and 3.5% consumed >6 cups of coffee per day. The consumption of decaffeinated coffee was less prevalent. In total, N = 127 (5.5%) reported consuming decaffeinated coffee on a regular basis (at least 1 cup per day). However, 120 of the 127 (94.5%) participants also drank caffeinated coffee, leaving only seven individuals exclusively consuming decaffeinated coffee. Since this group was too small for statistical analysis, we only included the consumption of caffeinated coffee.

Subjects consuming more caffeinated coffee were more often younger, male, of higher education, and possessing a higher BMI. Moreover, a higher coffee consumption was positively associated with smoking and negatively associated with diabetes mellitus and hypertension (Table 1). The median WMH volume was 1.48 mL (IQR = 2.22) and the median cortical thickness was 2.61 mm (IQR = 0.13). For a detailed description of the study sample, see Table 1. In Figure 1A.1,B.1,C.1, the distribution of the MRI parameters across the groups of coffee consumption are visualized.

Table 1. Descriptive statistics of the overall cohort, as well as for each group of coffee consumption.

Characteristics	Coffee Consumption						*p*-Value *
	Overall Cohort	<1 c/d	1–2 c/d	3–4 c/d	5–6 c/d	>6 c/d	
Group size	**2316**	**459**	**1020**	**581**	**176**	**80**	
Sociodemographic characteristics							
Age, median (IQR)	65 (14)	67 (13)	67 (13)	62 (14)	61 (13)	60 (9)	**<0.001**
Female sex, n (%)	1026 (44.3)	191 (41.61)	501 (49.12)	254 (43.72)	55 (31.25)	25 (31.25)	**<0.001**
Education [1]							**<0.001**
Low, n (%)	98 (4.23)	25 (5.75)	47 (4.78)	18 (3.2)	6 (3.49)	2 (2.53)	
Medium, n (%)	1087 (46.93)	219 (50.34)	472 (47.97)	275 (48.85)	80 (46.51)	41 (51.9)	
High, n (%)	1048 (45.25)	191 (43.91)	465 (47.26)	270 (47.96)	86 (50)	36 (45.57)	

Table 1. *Cont.*

Characteristics	Coffee Consumption						*p*-Value *
	Overall Cohort	<1 c/d	1–2 c/d	3–4 c/d	5–6 c/d	>6 c/d	
Cardiovascular risk factors							
Smoking, n (%)	320 (13.82)	37 (9.3)	113 (12.58)	110 (21.07)	39 (24.68)	21 (28.77)	**<0.001**
Diabetes mellitus, n (%) [2]	210 (9.07)	61 (13.96)	88 (9.23)	45 (8.43)	12 (7.14)	4 (5.33)	**0.01**
Hypertension, n (%) [3]	1611 (69.56)	330 (73.99)	734 (74.37)	380 (68.1)	121 (69.94)	46 (61.33)	**0.015**
BMI, median (IQR)	26.15 (9.45)	26.18 (5.59)	25.96 (5.44)	26.11 (5.43)	26.49 (4.59)	28 (4.9)	**0.02**
Alcohol consumption [monthly frequency], median (IQR)	3 (9)	3 (9)	3 (7)	10 (13)	10 (14)	3 (9)	**0.001**
Adherence to the Mediterranean diet, median (IQR)	4 (3)	4 (3)	4 (3)	4 (3)	5 (3)	4 (2)	0.945
MRI parameters							
Brain volume [mL], median (IQR)	1210.3 (166.6)	1204.38 (157.79)	1195.82 (168.59)	1226.89 (162.09)	1238.15 (162.73)	1240.43 (150.83)	**<0.001**
Mean cortical thickness [mm], median (IQR)	2.61 (0.13)	2.6 (0.13)	2.61 (0.13)	2.62 (0.13)	2.61 (0.11)	2.62 (0.11)	**<0.001**
WMH volume [mL], median (IQR)	1.48 (2.22)	1.61 (2.18)	1.59 (2.51)	1.29 (2.09)	1.32 (1.93)	1.28 (1.71)	**0.002**
PSMD [$\times 10^5$], median (IQR)	22.3 (4.31)	22.77 (4.61)	22.52 (4.36)	21.96 (4.05)	22.24 (4.37)	21.44 (2.81)	**<0.001**

All demographic variables were tested for significant difference between groups of coffee consumption. *p*-Values < 0.05 were interpreted as significant and are indicated in bold. * Pearson Chi-square test applied for categorical variables; Kruskal–Wallis test applied for continuous variables. [1] Educational level as defined by the International Standard Classification of Education (ISCED). [2] Prevalence of diabetes mellitus was determined based on fasting serum glucose level (>126 mg/dL), non-fasting serum glucose level (>200 mg/dL), or self-report. [3] Prevalence of hypertension was determined based on blood pressure ($\geq$140/90 mmHg), intake of antihypertensive medication, or self-report. Abbreviations: BMI = body mass index, c/d = cups per day, IQR = interquartile range, mL = milliliter, mm = millimeter, MRI = magnetic resonance imaging, PSMD = peak width of skeletonized mean diffusivity, WMH = white matter hyperintensities.

3.2. Association of Coffee Consumption with MRI Parameters

After controlling for age, sex, level of education, diabetes mellitus, hypertension, smoking, BMI, Mediterranean diet, and alcohol consumption, the amount of coffee consumed was associated with PSMD and mean cortical thickness, but not with log WMH load (Table 2). A daily coffee consumption of <1 cup per day was set as the reference group. Drinking 1–2 cups of coffee per day was associated with lower PSMD, compared to the reference group (ß = −0.542, *p* = 0.022). Moreover, 3–4 cups of coffee consumption per day was associated with lower PSMD, compared to group drinking <1 cup per day (ß = −0.591, *p* = 0.028). Drinking 5–6 cups per day (ß = −0.014, *p* = 0.97) or >6 cups per day (ß = −0.461, *p* = 0.386) was not associated with a different PSMD, compared to the reference group. For cortical thickness, 3–4 cups of coffee were associated with significantly higher cortical thickness (ß = 0.018, *p* = 0.015), compared to <1 cup per day. Drinking 1–2 cups of coffee per day was not significantly associated with a difference in cortical thickness (ß = 0.004, *p* = 0.544) when compared to drinkers with <1 cup of daily consumption. The result was also insignificant for a daily consumption of 5–6 cups per day (ß = 0.002, *p* = 0.831) and >6 cups per day (ß = −0.001, *p* = 0.941). The association with log WMH load was not significantly different between the groups of coffee consumption,

with <1 cup per day as the reference group (1–2 cups per day: $\beta = -0.025$, $p = 0.71$; 3–4 cups per day: $\beta = 0.061$, $p = 0.429$; 5–6 cups per day: $\beta = 0.001$, $p = 0.994$; >6 cups per day: $\beta = -0.01$, $p = 0.944$). See Table 2 for the detailed output of the linear regression.
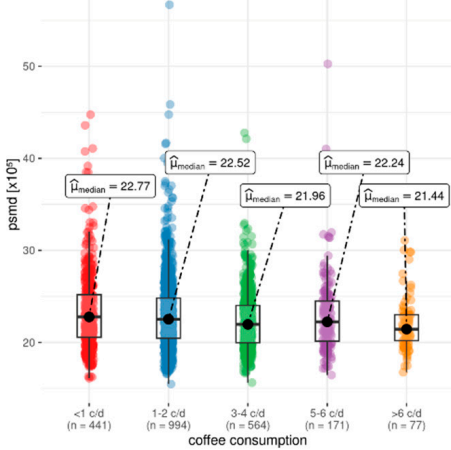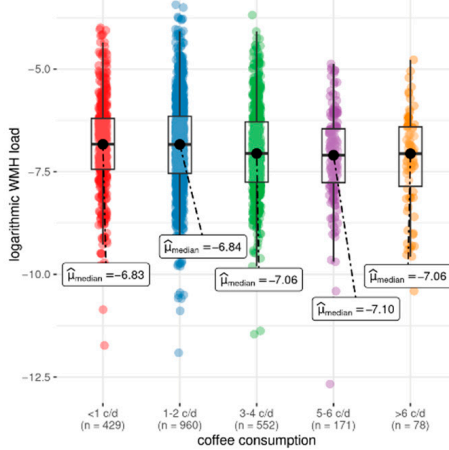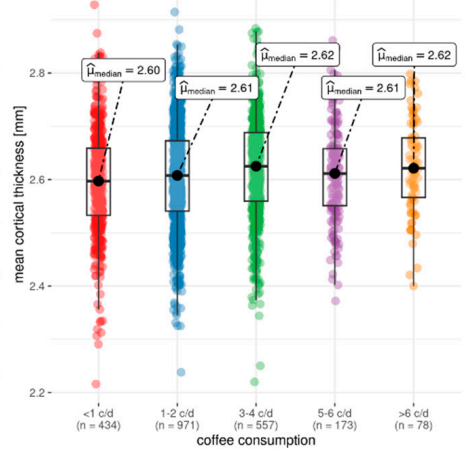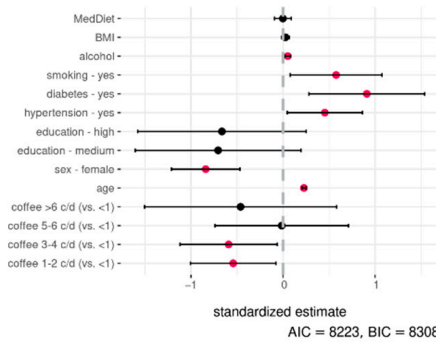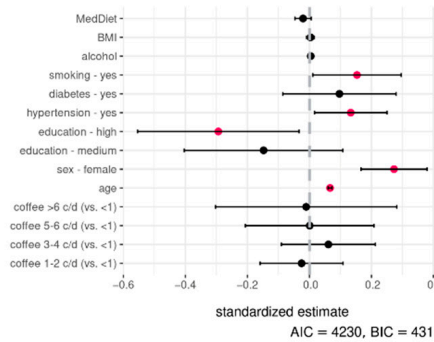
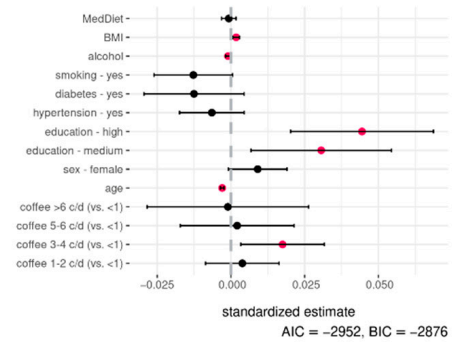

Figure 1. Summary statistics of the association between coffee consumption and the MRI parameters. Daily coffee consumption is indicated in cups per day (c/d) and categorized in five groups (<1 c/d, 1–2 c/d, 3–4 c/d, 5–6 c/d, >6 c/d). The upper row shows boxplots with the groups of coffee consumption on the x-axis and peak width of skeletonized mean diffusivity (PSMD, (**A.1**)) logarithmic white matter hyperintensity load (log WMH load, (**B.1**)) and mean cortical thickness (**C.1**) on the y-axis. The inferential test results above the boxplots indicate the output from the non-parametric Kruskal–Wallis test. The bottom row shows the results of the linear regression models where the dependent variable is either PSMD (**A.2**), log WMH load (**B.2**), or mean cortical thickness (**C.2**). Independent variables are the same in all regressions and presented on the y-axis. The standardized estimates are presented on the x-axis. Pink dots indicate a significant association and black dots a non-significant association of the independent variable. Abbreviations: AIC = Akaike information criterion; BIC = Bayesian information criterion; c/d = cups per day; MedDiet = adherence to the Mediterranean diet; mm = millimeter; n_{obs} = number of observations; p = p-Value; μ_{median} = median; χ^2 = chi-square from the Kruskal–Wallis test.

Table 2. Results of the linear regression models examining the association between coffee consumption and microstructural brain parameters.

Dependent Variable	PSMD [$\times 10^5$]		Mean Cortical Thickness [mm]		log WMH Load [4]	
	β	*p*	β	*p*	β	*p*
Intercept	23.96	**<0.001**	2.571	**<0.001**	−6.967	**<0.001**
Age	1.917	**<0.001**	−0.025	**0.001**	0.558	**<0.001**
Sex—female	−0.84	**<0.001**	0.009	0.074	0.273	**<0.001**
Education—medium [1]	−0.705	0.125	0.031	**0.012**	−0.148	0.257
Education—high [1]	−0.663	0.155	0.044	**<0.001**	−0.294	**0.027**
Hypertension—yes [2]	0.455	**0.029**	−0.006	0.245	0.133	**0.026**
Diabetes—yes [3]	0.911	**0.005**	−0.013	0.147	0.097	0.299
Smoking—yes	0.577	**0.023**	−0.013	0.06	0.153	**0.035**
Alcohol consumption	0.303	**0.001**	−0.006	**0.017**	0.025	0.358
BMI	0.114	0.221	0.008	**0.002**	0.015	0.586
Mediterranean diet	−0.002	0.986	−0.001	0.569	−0.039	0.123
Coffee consumption—1–2 c/d	−0.542	**0.022**	0.004	0.544	−0.025	0.71
Coffee consumption—3–4 c/d	−0.591	**0.028**	0.018	**0.015**	0.061	0.429
Coffee consumption—5–6 c/d	−0.014	0.97	0.002	0.831	0.001	0.994
Coffee consumption—>6 c/d	−0.461	0.386	−0.001	0.941	−0.01	0.944

Three linear regression models were conducted with either PSMD, mean cortical thickness or log WMH load as the dependent variable. Coffee consumption was quantified in groups with <1 cup per day set as reference category. Numbers indicate coefficients and *p*-Values. The *p*-Values < 0.05 were interpreted as significant and are indicated in bold. [1] Educational level as defined by the International Standard Classification of Education (ISCED). Low educational level was set as reference. [2] Prevalence of hypertension was determined based on blood pressure (≥140/90 mmHg), intake of antihypertensive medication, or self-report. [3] Prevalence of diabetes mellitus was determined based on fasting serum glucose level (>126 mg/dL), non-fasting serum glucose level (>200 mg/dL), or self-report. [4] Log WMH load refers to the logarithm of WMH volume and normalization for estimated total intracranial volume. Abbreviations: β = standardized coefficient, BMI = body mass index, c/d = cups per day, log = logarithmic, mm = millimeter, *p* = *p*-Value, PSMD = peak width of skeletonized mean diffusivity, WMH = white matter hyperintensities.

4. Discussion

In this study, we examined the association of cortical thickness, cerebral small vessel disease (in the form of WMH), and microstructural integrity with coffee consumption in a population-based cohort including data from 2316 middle-aged to elderly participants. Our results show that individuals with a regular and moderate coffee consumption of 3 to 4 cups per day had higher cortical thickness and less microstructural white matter alteration, as quantified by the PSMD. Individuals drinking 5 or more cups per day did not significantly differ on any MRI parameter from individuals drinking <1 cup per day, indicating a U-shaped relationship. Moreover, there was no significant association of coffee with CSVD quantified by WMH, which is in congruence with the few studies examining the same association [7,21,22]. While PSMD measures subtle changes in the white matter microstructure and already captures early signs of structural damage, WMH reflects an end stage of white matter damage. Thus, our findings are novel in providing evidence for an association of a moderate coffee consumption with findings of early microstructural brain damage.

Multiple factors that are known to induce neurodegeneration and vascular brain damage can be beneficially influenced by the consumption of coffee, i.e., systemic inflammatory processes, deposition of amyloid-ß, and the development of cardiovascular risk factors. In the following section, we will discuss each factor in the context of coffee consumption and reflect these on the results of our analysis.

Of the more than 1000 bioactive compounds of coffee, multiple constituents (such as caffeine, polyphenols, or heterocyclic compounds) have anti-inflammatory and anti-oxidant properties, measured by reduced CRP levels and a lower risk of mortality from inflammatory diseases in regular coffee drinkers [9,41,42]. Chronic inflammatory processes, on the other hand, increase the risk for vascular dementia, Alzheimer's Disease, and stroke, and are associated with an increased WMH prevalence at baseline, an increased WMH

progression over time, and a reduced white matter integrity 20 years later [43–47]. The negative relationship between coffee consumption, vascular brain damage and cognitive decline can therefore be explained by the anti-inflammatory properties of coffee [3,4]. Only one previous study analyzed the microstructural integrity in the context of coffee [24]. They found that a moderate-to-high coffee consumption—reflecting approximately 1–6 cups of coffee per day—was associated with better microstructural integrity in 145 elderly individuals [24]. The results are comparable to our findings, including the more sensitive marker PSMD, with a lower PSMD in middle-aged to elderly individuals with a moderate coffee consumption of 1–4 cups per day.

Next to its anti-inflammatory mechanisms, coffee consumption has an influence on the central nervous system through its binding to adenosine receptors. The constituent caffeine is highly soluble in lipid and water, which allows caffeine to easily cross the blood-brain barrier. Caffeine has a chemically similar structure to adenosine and can, once in the brain, act as an adenosine receptor antagonist by binding to A1 and A2a receptors [2]. Via blockage of adenosine receptor A2a, caffeine can reduce amyloid-β induced toxicity [10]. In humans, coffee consumption was associated with a lower amyloid-β positivity on PET scans and, subsequently, a lower risk of dementia [4,22]. A midlife coffee consumption of 3–5 cups per day was associated with a 70% lower risk of incident dementia [3]. Cortical thickness as an MR imaging marker of neurodegeneration was higher in individuals with a coffee consumption of 3–4 cups per day in our cohort. Only one previous study considered cortical thickness in predefined regions of interest in the context of coffee consumption [22]. Previous results measuring cortical thickness indirectly via grey matter volume are heterogeneous with either positive, negative, or no associations of coffee consumption [21,25,26,48]. Moreover, adenosine receptor antagonists were protective against hippocampal damage after induced neurotoxicity and brain damage after ischemic stroke, most probably due to the suppression of glutamate release [49,50]. Similar mechanisms are suggested for the neuroprotective associations of caffeine, e.g., against the depletion of striatal dopamine levels in a Parkinson's Disease mice model [51]. In humans, a daily coffee consumption of 3 cups was associated with a lower risk of Parkinson's Disease in a large meta-analysis including 901,764 participants, and associated with 20% lower risk of incident stroke [8,52,53].

Coffee consumption may also be neuroprotective in an indirect way by reducing cardiovascular risk factors such as diabetes or metabolic syndrome [11,12]. A large umbrella review including 218 meta-analyses revealed that the reduced risk of diabetes mellitus is one of the most beneficial outcomes of regular coffee consumption [1]. Since cardiovascular risk factors are the major cause in the development of CSVD, coffee might help in reducing the degree of CSVD in individuals with high cardiovascular risk [54]. Although our study is limited in its cross-sectional design, we observed that the prevalence of diabetes mellitus was 13.96% in participants drinking less than 1 cup of coffee per day, compared to a prevalence of 5.33% in participants consuming more than 6 cups of coffee per day (Table 1).

A U-shaped relationship between coffee consumption and health outcomes has been reported in previous studies, with a moderate coffee consumption found in individuals with the most beneficial health parameters. Drinking 2.5–5 cups of coffee per day was associated with a reduced risk of dementia and metabolic syndrome, and a consumption of 1–3 cups per day was associated with a reduced risk for stroke, cardiovascular diseases, coronary heart disease, Parkinson's Disease, and overall mortality [3,8,11,41,52]. Our findings also indicate a U-shaped association between microstructural white matter integrity, cortical thickness, and coffee consumption with better associations on the structural MRI for a consumption of 1–4 cups per day, while individuals with a daily consumption of 5 or more cups did not significantly differ from individuals drinking <1 cup in any MRI parameter. It is suggested that coffee has both beneficial and detrimental associations with health, where the detrimental mechanisms of a very high coffee consumption outweighs the positive, serving a possible explanation for the U-shaped association of coffee with health parameters [52]. At the same time, the comparability of studies is limited due to

differences in portion sizes leading to a high risk of bias and very low quality of evidence in meta-analyses [55].

This study has strengths and limitations. In a large middle-aged to elderly population, we examined the relationship between coffee consumption and several brain MRI parameters. We quantified PSMD as novel imaging marker of microstructural integrity, and additionally included measures of vascular brain damage and neurodegeneration to better understand the association of coffee consumption with structural brain alterations. The study included data from a large population-based cohort, and we applied an advanced processing protocol on the MR images. Still, only cross-sectional data are currently available, and no conclusions about causality can be drawn from observational, cross-sectional data. The lack of longitudinal data in our analysis should be considered a limitation. As observed in this cohort, coffee consumption was positively correlated with the consumption of alcohol and smoking, which are known to negatively influence both overall and neurological health. Therefore, the true strength of the association between coffee and health parameters might even be underestimated. At the same time, individuals consuming more coffee tended to be younger, higher educated, and less often diagnosed with hypertension or diabetes. Despite the inclusion of important covariates in the linear regression models, we cannot rule out potential residual confounding factors. This study was intended to be exploratory, given that multiple predictors were assessed and adjustment for multiple testing was not performed. In addition, we did not compare the association of caffeinated with decaffeinated coffee, because of the small sample size drinking exclusively decaffeinated coffee (N = 7). The suggested associations of caffeine on neurological health need to be studied in detail in larger cohorts.

5. Conclusions

To summarize, a coffee consumption of 1–4 cups per day is associated with a lower PSMD, indicating better microstructural integrity. Moreover, we found that a coffee consumption of 3–4 cups per day was associated with preserved cortical thickness. In total, a moderate coffee consumption was related to better structural brain parameters than a low coffee consumption in a population-based cohort with middle-aged to elderly individuals. Further research is necessary to determine whether coffee consumption has a potentially protective effect against microstructural brain alterations longitudinally.

References

1. Poole, R.; Kennedy, O.J.; Roderick, P.; Fallowfield, J.A.; Hayes, P.C.; Parkes, J. Coffee consumption and health: Umbrella review of meta-analyses of multiple health outcomes. *BMJ* **2017**, *359*, j5024. [CrossRef] [PubMed]
2. Fredholm, B.B.; Bättig, K.; Holmén, J.; Nehlig, A.; Zvartau, E.E. Actions of caffeine in the brain with special reference to factors that contribute to its widespread use. *Pharmacol. Rev.* **1999**, *51*, 83–133. [PubMed]
3. Eskelinen, M.H.; Ngandu, T.; Tuomilehto, J.; Soininen, H.; Kivipelto, M. Midlife Coffee and Tea Drinking and the Risk of Late-Life Dementia: A Population-Based CAIDE Study. *J. Alzheimer's Dis.* **2009**, *16*, 85–91. [CrossRef] [PubMed]
4. Driscoll, I.; Shumaker, S.A.; Snively, B.M.; Margolis, K.L.; Manson, J.E.; Vitolins, M.Z.; Rossom, R.C.; Espeland, M.A. Relationships Between Caffeine Intake and Risk for Probable Dementia or Global Cognitive Impairment: The Women's Health Initiative Memory Study. *J. Gerontol. Ser. A Biol. Sci. Med. Sci.* **2016**, *71*, 1596–1602. [CrossRef] [PubMed]
5. Larsson, S.C.; Virtamo, J.; Wolk, A. Coffee Consumption and Risk of Stroke in Women. *Stroke* **2011**, *42*, 908–912. [CrossRef]
6. Lee, J.; Lee, J.-E.; Kim, Y. Relationship between coffee consumption and stroke risk in Korean population: The Health Examinees (HEXA) Study. *Nutr. J.* **2017**, *16*, 7. [CrossRef]
7. Araújo, L.F.; Mirza, S.S.; Bos, D.; Niessen, W.J.; Barreto, S.M.; van der Lugt, A.; Vernooij, M.W.; Hofman, A.; Tiemeier, H.; Ikram, M.A. Association of Coffee Consumption with MRI Markers and Cognitive Function: A Population-Based Study. *J. Alzheimer's Dis.* **2016**, *53*, 451–461. [CrossRef]
8. Qi, H.; Li, S. Dose-response meta-analysis on coffee, tea and caffeine consumption with risk of Parkinson's disease. *Geriatr. Gerontol. Int.* **2013**, *14*, 430–439. [CrossRef]
9. Osama, H.; Abdelrahman, M.A.; Madney, Y.M.; Harb, H.S.; Saeed, H.; Abdelrahim, M.E.A. Coffee and type 2 diabetes risk: Is the association mediated by adiponectin, leptin, c-reactive protein or Interleukin-6? A systematic review and meta-analysis. *Int. J. Clin. Pract.* **2021**, *75*, e13983. [CrossRef]
10. Dall'Lgna, O.P.; Porciúncula, L.O.; Souza, D.O.; Cunha, R.A.; Lara, D.R. Neuroprotection by caffeine and adenosine A_{2A} receptor blockade of β-amyloid neurotoxicity. *Br. J. Pharmacol.* **2003**, *138*, 1207–1209. [CrossRef]
11. Shang, F.; Li, X.; Jiang, X. Coffee consumption and risk of the metabolic syndrome: A meta-analysis. *Diabetes Metab.* **2015**, *42*, 80–87. [CrossRef]
12. Ding, M.; Bhupathiraju, S.N.; Chen, M.; van Dam, R.M.; Hu, F.B. Caffeinated and Decaffeinated Coffee Consumption and Risk of Type 2 Diabetes: A Systematic Review and a Dose-Response Meta-analysis. *Diabetes Care* **2014**, *37*, 569–586. [CrossRef]
13. Debette, S.; Markus, H.S. The clinical importance of white matter hyperintensities on brain magnetic resonance imaging: Systematic review and meta-analysis. *BMJ* **2010**, *341*, c3666. [CrossRef]
14. Georgakis, M.K.; Duering, M.; Wardlaw, J.M.; Dichgans, M. WMH and long-term outcomes in ischemic stroke: A Systematic Review and Meta-Analysis. *Neurology* **2019**, *92*, e1298–e1308. [CrossRef]
15. Wardlaw, J.M.; Smith, E.E.; Biessels, G.J.; Cordonnier, C.; Fazekas, F.; Frayne, R.; Lindley, R.I.; O'Brien, J.T.; Barkhof, F.; Benavente, O.R.; et al. Neuroimaging standards for research into small vessel disease and its contribution to ageing and neurodegeneration. *Lancet Neurol.* **2013**, *12*, 822–838. [CrossRef]
16. Dufouil, C.; de Kersaint–Gilly, A.; Besançon, V.; Levy, C.; Auffray, E.; Brunnereau, L.; Alpérovitch, A.; Tzourio, C. Longitudinal study of blood pressure and white matter hyperintensities: The EVA MRI Cohort. *Neurology* **2001**, *56*, 921–926. [CrossRef]
17. Power, M.C.; Deal, J.A.; Sharrett, A.R.; Jack, C.R.; Knopman, D.; Mosley, T.H.; Gottesman, R.F. Smoking and white matter hyperintensity progression: The ARIC-MRI Study. *Neurology* **2015**, *84*, 841–848. [CrossRef]
18. Frey, B.M.; Petersen, M.; Mayer, C.; Schulz, M.; Cheng, B.; Thomalla, G.; Frey, B.M.; Petersen, M.; Mayer, C.; Schulz, M.; et al. Characterization of White Matter Hyperintensities in Large-Scale MRI-Studies. *Front. Neurol.* **2019**, *10*, 238. [CrossRef]
19. Ritchie, K.; Artero, S.; Portet, F.; Brickman, A.; Muraskin, J.; Beanino, E.; Ancelin, M.-L.; Carrière, I. Caffeine, Cognitive Functioning, and White Matter Lesions in the Elderly: Establishing Causality from Epidemiological Evidence. *J. Alzheimer's Dis.* **2010**, *20*, S161–S166. [CrossRef]
20. Park, J.; Han, J.W.; Lee, J.R.; Byun, S.; Suh, S.W.; Kim, J.H.; Kim, K.W. Association between lifetime coffee consumption and late life cerebral white matter hyperintensities in cognitively normal elderly individuals. *Sci. Rep.* **2020**, *10*, 421. [CrossRef]
21. Pham, K.; Mulugeta, A.; Zhou, A.; O'Brien, J.T.; Llewellyn, D.J.; Hyppönen, E. High coffee consumption, brain volume and risk of dementia and stroke. *Nutr. Neurosci.* **2021**, *25*, 2111–2122. [CrossRef] [PubMed]
22. Kim, J.W.; Byun, M.S.; Yi, D.; Lee, J.-Y.; Jeon, S.Y.; Jung, G.; Lee, H.N.; Sohn, B.K.; Lee, J.Y.; KBASE Research Group; et al. Coffee intake and decreased amyloid pathology in human brain. *Transl. Psychiatry* **2019**, *9*, 27. [CrossRef] [PubMed]

23. Baykara, E.; Gesierich, B.; Adam, R.; Tuladhar, A.M.; Biesbroek, J.M.; Koek, H.L.; Ropele, S.; Jouvent, E.; Alzheimer's Disease Neuroimaging Initiative; Chabriat, H.; et al. A Novel Imaging Marker for Small Vessel Disease Based on Skeletonization of White Matter Tracts and Diffusion Histograms: Novel SVD Imaging Marker. *Ann. Neurol.* **2016**, *80*, 581–592. [CrossRef]

24. Haller, S.; Montandon, M.-L.; Rodriguez, C.; Herrmann, F.R.; Giannakopoulos, P. Impact of Coffee, Wine, and Chocolate Consumption on Cognitive Outcome and MRI Parameters in Old Age. *Nutrients* **2018**, *10*, 1391. [CrossRef] [PubMed]

25. West, R.K.; Ravona-Springer, R.; Livny, A.; Heymann, A.; Shahar, D.; Leroith, D.; Preiss, R.; Zukran, R.; Silverman, J.M.; Schnaider-Beeri, M. Age Modulates the Association of Caffeine Intake with Cognition and with Gray Matter in Elderly Diabetics. *J. Gerontol. Ser. A Biol. Sci. Med. Sci.* **2019**, *74*, 683–688. [CrossRef]

26. Perlaki, G.; Orsi, G.; Kovács, N.; Schwarcz, A.; Pap, Z.; Kalmár, Z.; Plozer, E.; Csathó, A.; Gábriel, R.; Komoly, S.; et al. Coffee consumption may influence hippocampal volume in young women. *Brain Imaging Behav.* **2011**, *5*, 274–284. [CrossRef]

27. Jagodzinski, A.; Johansen, C.; Koch-Gromus, U.; Aarabi, G.; Adam, G.; Anders, S.; Augustin, M.; der Kellen, R.B.; Beikler, T.; Behrendt, C.-A.; et al. Rationale and Design of the Hamburg City Health Study. *Eur. J. Epidemiol.* **2020**, *35*, 169–181. [CrossRef]

28. D'Agostino, R.B., Sr.; Vasan, R.S.; Pencina, M.J.; Wolf, P.A.; Cobain, M.; Massaro, J.M.; Kannel, W.B. General Cardiovascular Risk Profile for Use in Primary Care. *Circulation* **2008**, *117*, 743–753. [CrossRef]

29. Nöthlings, U.; Hoffmann, K.; Bergmann, M.M.; Boeing, H. Fitting Portion Sizes in a Self-Administered Food Frequency Questionnaire. *J. Nutr.* **2007**, *137*, 2781–2786. [CrossRef]

30. UNESCO Institute for Statistics. *International Standard Classification of Education (ISCED) 2011*; UNESCO Institute for Statistics: Montreal, QC, Canada, 2012; ISBN 978-92-9189-123-8.

31. Hebestreit, K.; Yahiaoui-Doktor, M.; Engel, C.; Vetter, W.; Siniatchkin, M.; Erickson, N.; Halle, M.; Kiechle, M.; Bischoff, S.C. Validation of the German version of the Mediterranean Diet Adherence Screener (MEDAS) questionnaire. *BMC Cancer* **2017**, *17*, 341. [CrossRef]

32. Petersen, M.; Naegele, F.L.; Mayer, C.; Schell, M.; Petersen, E.; Kuehn, S.; Gallinat, J.; Fiehler, J.; Pasternak, O.; Matschke, J.; et al. Brain Imaging and Neuropsychological Assessment of Individuals Recovered from Mild COVID-19. *BioRxiv*, 2022; *preprint*. [CrossRef]

33. Gorgolewski, K.; Burns, C.D.; Madison, C.; Clark, D.; Halchenko, Y.O.; Waskom, M.L.; Ghosh, S.S. Nipype: A Flexible, Lightweight and Extensible Neuroimaging Data Processing Framework in Python. *Front. Neuroinform.* **2011**, *5*, 13. [CrossRef]

34. Cieslak, M.; Cook, P.A.; He, X.; Yeh, F.-C.; Dhollander, T.; Adebimpe, A.; Aguirre, G.K.; Bassett, D.S.; Betzel, R.F.; Bourque, J.; et al. QSIPrep: An integrative platform for preprocessing and reconstructing diffusion MRI data. *Nat. Methods* **2021**, *18*, 775–778. [CrossRef]

35. Fischl, B.; Salat, D.H.; Busa, E.; Albert, M.; Dieterich, M.; Haselgrove, C.; van der Kouwe, A.; Killiany, R.; Kennedy, D.; Klaveness, S.; et al. Whole Brain Segmentation: Automated Labeling of Neuroanatomical Structures in the Human Brain. *Neuron* **2002**, *33*, 341–355. [CrossRef]

36. Fischl, B.; Dale, A.M. Measuring the thickness of the human cerebral cortex from magnetic resonance images. *Proc. Natl. Acad. Sci. USA* **2000**, *97*, 11050–11055. [CrossRef]

37. Sundaresan, V.; Zamboni, G.; Le Heron, C.; Rothwell, P.M.; Husain, M.; Battaglini, M.; De Stefano, N.; Jenkinson, M.; Griffanti, L. Automated lesion segmentation with BIANCA: Impact of population-level features, classification algorithm and locally adaptive thresholding. *Neuroimage* **2019**, *202*, 116056. [CrossRef]

38. Griffanti, L.; Zamboni, G.; Khan, A.; Li, L.; Bonifacio, G.; Sundaresan, V.; Schulz, U.G.; Kuker, W.; Battaglini, M.; Rothwell, P.M.; et al. BIANCA (Brain Intensity AbNormality Classification Algorithm): A new tool for automated segmentation of white matter hyperintensities. *Neuroimage* **2016**, *141*, 191–205. [CrossRef]

39. Avants, B.; Epstein, C.; Grossman, M.; Gee, J. Symmetric diffeomorphic image registration with cross-correlation: Evaluating automated labeling of elderly and neurodegenerative brain. *Med. Image Anal.* **2008**, *12*, 26–41. [CrossRef]

40. R Core Team. *R: A Language and Environment for Statistical Computing*; R Foundation for Statistical Computing: Vienna, Austria, 2018.

41. Andersen, L.F.; Jacobs, D.R.; Carlsen, M.H.; Blomhoff, R. Consumption of coffee is associated with reduced risk of death attributed to inflammatory and cardiovascular diseases in the Iowa Women's Health Study. *Am. J. Clin. Nutr.* **2006**, *83*, 1039–1046. [CrossRef]

42. Jeszka-Skowron, M.; Zgoła-Grześkowiak, A.; Grześkowiak, T. Analytical methods applied for the characterization and the determination of bioactive compounds in coffee. *Eur. Food Res. Technol.* **2014**, *240*, 19–31. [CrossRef]

43. Van Dijk, E.J.; Prins, N.D.; Vermeer, S.E.; Vrooman, H.A.; Hofman, A.; Koudstaal, P.J.; Breteler, M.M. C-Reactive Protein and Cerebral Small-Vessel Disease: The Rotterdam Scan Study. *Circulation* **2005**, *112*, 900–905. [CrossRef]

44. Satizabal, C.L.; Zhu, Y.C.; Mazoyer, B.; Dufouil, C.; Tzourio, C. Circulating IL-6 and CRP are associated with MRI findings in the elderly: The 3C-Dijon Study. *Neurology* **2012**, *78*, 720–727. [CrossRef] [PubMed]

45. Walker, K.A.; Power, M.C.; Hoogeveen, R.C.; Folsom, A.R.; Ballantyne, C.M.; Knopman, D.S.; Windham, B.G.; Selvin, E.; Jack, C.R., Jr.; Gottesman, R.F. Midlife Systemic Inflammation, Late-Life White Matter Integrity, and Cerebral Small Vessel Disease—The Atherosclerosis Risk in Communities Study. *Stroke* **2017**, *48*, 3196–3202. [CrossRef]

46. Engelhart, M.J.; Geerlings, M.I.; Meijer, J.; Kiliaan, A.; Ruitenberg, A.; van Swieten, J.C.; Stijnen, T.; Hofman, A.; Witteman, J.C.M.; Breteler, M.M.B. Inflammatory Proteins in Plasma and the Risk of Dementia: The Rotterdam Study. *Arch. Neurol.* **2004**, *61*, 668–672. [CrossRef] [PubMed]

47. Cesari, M.; Penninx, B.W.; Newman, A.B.; Kritchevsky, S.B.; Nicklas, B.J.; Sutton-Tyrrell, K.; Rubin, S.M.; Ding, J.; Simonsick, E.M.; Harris, T.B.; et al. Inflammatory Markers and Onset of Cardiovascular Events: Results From the Health ABC Study. *Circulation* **2003**, *108*, 2317–2322. [CrossRef] [PubMed]

48. Kang, J.; Jia, T.; Jiao, Z.; Shen, C.; Xie, C.; Cheng, W.; Sahakian, B.J.; Waxman, D.; Feng, J. Increased brain volume from higher cereal and lower coffee intake: Shared genetic determinants and impacts on cognition and metabolism. *Cereb. Cortex* **2022**, *32*, 5163–5174. [CrossRef] [PubMed]

49. Behan, W.M.H.; Stone, T.W. Enhanced neuronal damage by co-administration of quinolinic acid and free radicals, and protection by adenosine A$_{2A}$ receptor antagonists: Quinolinate and Free Radicals. *Br. J. Pharmacol.* **2002**, *135*, 1435–1442. [CrossRef] [PubMed]

50. Monopoli, A.; Lozza, G.; Forlani, A.; Mattavelli, A.; Ongini, E. Blockade of adenosine A2A receptors by SCH 58261 results in neuroprotective effects in cerebral ischaemia in rats. *Neuroreport* **1998**, *9*, 3955–3958. [CrossRef]

51. Chen, J.-F.; Xu, K.; Petzer, J.P.; Staal, R.; Xu, Y.-H.; Beilstein, M.; Sonsalla, P.K.; Castagnoli, K.; Castagnoli, N.; Schwarzschild, M.A. Neuroprotection by Caffeine and A$_{2A}$ Adenosine Receptor Inactivation in a Model of Parkinson's Disease. *J. Neurosci.* **2001**, *21*, RC143. [CrossRef]

52. Ding, M.; Bhupathiraju, S.N.; Satija, A.; van Dam, R.; Hu, F.B. Long-Term Coffee Consumption and Risk of Cardiovascular Disease: A systematic review and a dose-response meta-analysis of prospective cohort studies. *Circulation* **2014**, *129*, 643–659. [CrossRef]

53. Liebeskind, D.S.; Sanossian, N.; Fu, K.A.; Wang, H.-J.; Arab, L. The coffee paradox in stroke: Increased consumption linked with fewer strokes. *Nutr. Neurosci.* **2015**, *19*, 406–413. [CrossRef]

54. Taylor-Bateman, V.; Gill, D.; Georgakis, M.K.; Malik, R.; Munroe, P.; Traylor, M.; on behalf of the International Consortium of Blood Pressure (ICBP). Cardiovascular Risk Factors and MRI Markers of Cerebral Small Vessel Disease: A Mendelian Ran-domization Study. *Neurology* **2021**, *98*, e343–e351. [CrossRef]

55. Barbaresko, J.; Lellmann, A.W.; Schmidt, A.; Lehmann, A.; Amini, A.M.; Egert, S.; Schlesinger, S.; Nöthlings, U. Dietary Factors and Neurodegenerative Disorders: An Umbrella Review of Meta-Analyses of Prospective Studies. *Adv. Nutr.* **2020**, *11*, 1161–1173. [CrossRef]